ISRAEL OCEANOGRAPHIC & LIMNOLOGICAL RESEARCH LTD. חקר ימים ואגמים לישראל בע"מ
TEL SHIKMONA, P.O.B. 8030, HAIFA 31080 FAX: 04-8511911 :פקס TEL: 04-8515202 :טלפון 31080 חיפה, 8030 ת"ד שקמונה, תל

A Concise Physical, Chemical and Biological Characterization of the Eastern Mediterranean with Emphasis on the Israeli Coast

Edited by Dov S. Rosen with contributions by

Bella Galil, Barak Herut,
Dov S. Rosen and Zvi Rosentroub

IOLR Report H07/2006
February 2006

דו"חות חיא"ל

IOLR REPORTS

National Institute of Oceanography
ISRAEL OCEANOGRAPHIC & LIMNOLOGICAL RESEARCH

A concise physical, chemical and biological characterization of the Eastern Mediterranean with emphasis on the Israeli coast

Edited by Dov S. Rosen with contributions by

Bella Galil, Barak Herut,
Dov S. Rosen and Zvi Rosentroub

IOLR Report H07/2006

February 2006

Submitted to

Dr. Yosi Bar-Tov – Chief Scientist

Israel Ministry of National Infrastructures

CONTENTS

CONTENTS - continued

LIST OF TABLES

LIST OF FIGURES

LIST OF FIGURES - continued

LIST OF FIGURES - continued

CHAPTER 1

INTRODUCTION

This report was prepared at the request of Dr. Yosi Bar-Tov, Chief Scientist of the Ministry of Infrastructures to aid the Ministry bodies with various marine activities related to marine infrastructures.

The report presents a concise overview on the physical, chemical and biological characterization of the Eastern Mediterranean with emphasis on the Israeli coast. The information presented is based on investigations and measurements conducted by the Israel Oceanographic & Limnological Research as well as additional relevant published information.

The information in this report is provided as a public service. To the best knowledge of the authors the provided information is accurate and reliable. Nevertheless, it may still contain errors, despite the efforts and professional skills invested in the preparation of the report. Correspondingly, any user of this report's information is solely responsible for such use, and Israel Oceanographic and Limnological Research and the authors disclaim any responsibility for whatsoever use of the report information.

The report consists of 4 chapters (including this one). Chapter 2 covers the Physical Oceanography of the Levantine Basin and further details related to area off the coast of Israel. Chapter 3 covers the characterisation of the winds, sea levels and waves climate of the eastern Mediterranean with further emphasis on their climate at the Mediterranean coast of Israel. Finally, Chapter 4 presents an environmental evaluation of the Levantine part of the Mediterranean sea, emphasizing the chemical and biological aspects, and in particular at the Mediterranean coast of Israel.

We wish also to mention that each chapter is independent of the others in regards to the numbering of the figures, tables, drawings and references quoted.

In addition to internal IOLR data and reports, external sources and published information were included to enable a proper characterization of the area. The authors acknowledge with thanks the quoted authors for using their published information and reprinting some of the their figures.

CHAPTER 2

AN OVERVIEW OF THE PHYSICAL OCEANOGRAPHY OF THE LEVANTINE BASIN

by Zvi Rosentraub, Ph.D.

2.1 General

The Mediterranean Sea, as depicted in Fig.1, is an enclosed basin connected to the Atlantic Ocean by the narrow Strait of Gibraltar (width ~13 km, sill depth ~300 m) and connected to the Black Sea by the Dardanelles/ Marmara Sea/ Bosphorous system. It is made up of two sub-basins, the Western (WMED) and Eastern (EMED) Mediterranean, connected by the strait of Sicily (~35 km/ ~300 m). The EMED is comprised of four sub-basins: the Ionian, the Levantine, the Adriatic, and the Aegean Seas. The most eastern, the Levantine Basin, merges with the Ionian Sea through the Cretan Passage at a depth of about 1500 m between Crete and the Libyan coast and is connected, to its north, to the Aegean Sea through three relatively shallow passages (Fig. 2).

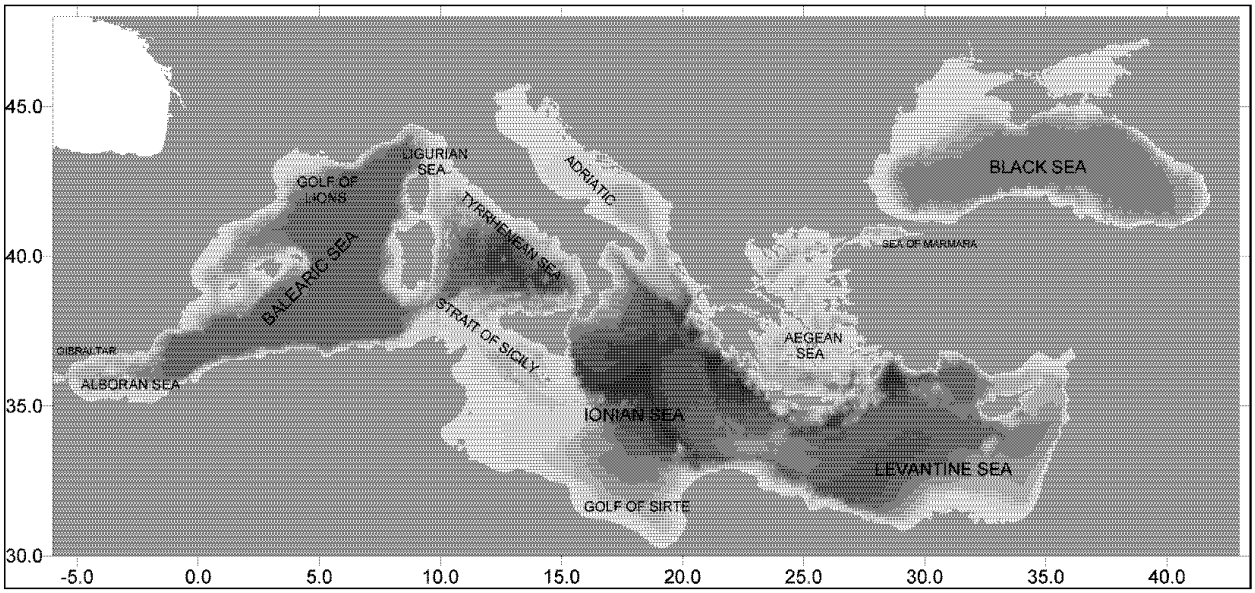

Fig. 1. The Mediterranean Sea. Geographic features.

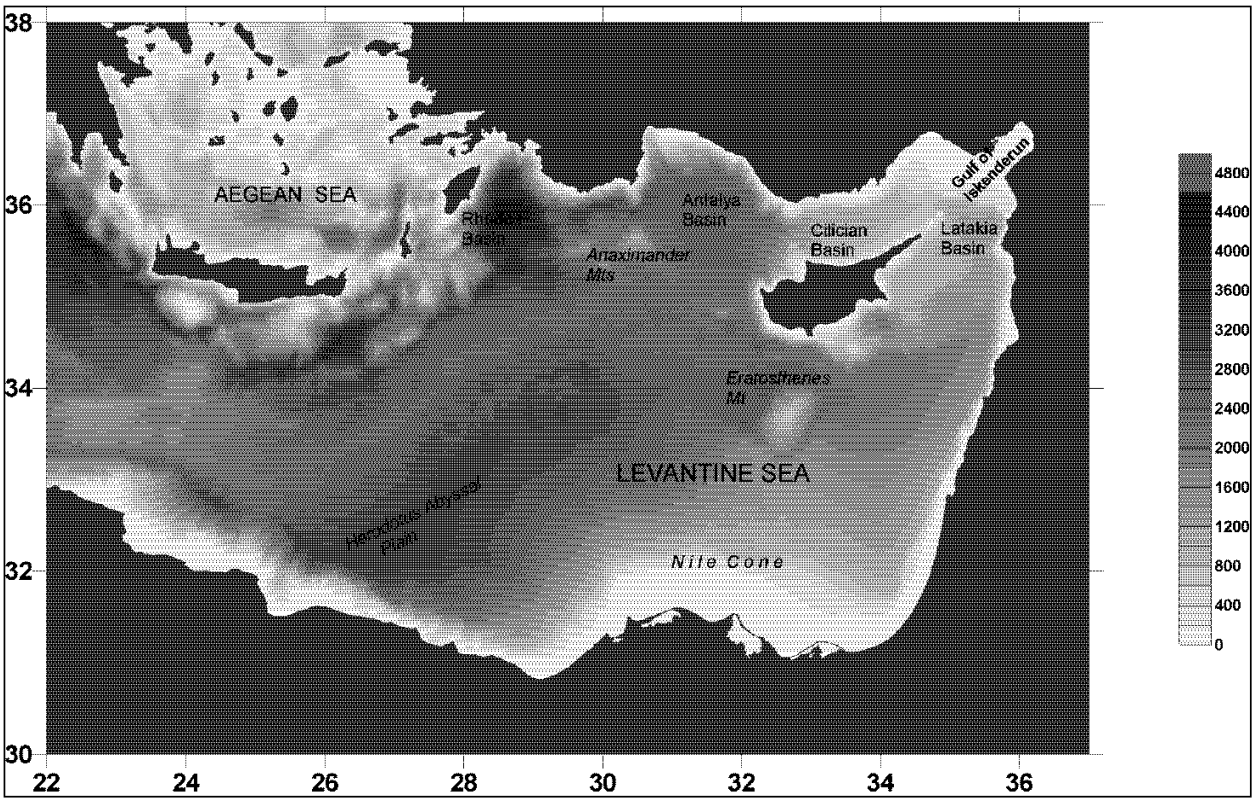

Fig. 2. Bathymetric map of the Levantine basin.

The MED has an annual negative water balance (due to the excess of evaporation (mainly in the EMED) as compared to precipitation, river runoff and Black Sea exchange) causing inflow of less saline Atlantic water through the Strait of Gibraltar. The climatological circulation of the Mediterranean basin (Fig.3) is constructed, basically, from a zonal and two meridional vertical circulation belts. The first, is an open and shallow (0-500 m) vertical circulation belt associated with the inflow of the Atlantic water at Gibraltar, which reaches the Levantine basin and is transformed there into Levantine Intermediate Water (LIW). The LIW is an important component of the flow exiting from Gibraltar into the Atlantic Ocean. The other circulation belts are meridional cells driven by deep water mass formation processes occurring in the Northern MED areas such as the Gulf of Lions or the Adriatic (Schlitzer et al., 1991), and (recently) the Aegean Sea (Roether et al., 1996) . The deep water formation in such areas which determines the abyssal waters in both the EMED and WMED basins, is affected, if not controlled, by LIW present before formation events (Wu and Haines, 1996). These cells are, thus, interconnected. The Zonal cell is thought to have a decadal timescale (Stratford and Williams, 1997), while the meridional overturning cell has a multi-decadal timescales of 70 to 120 years and ~40 years for the eastern and western basins, respectively (Stratford et al., 1998). The similarity to the North Atlantic meridional overturning circulation makes the MED an important laboratory for studying air- sea interaction and mass formation.

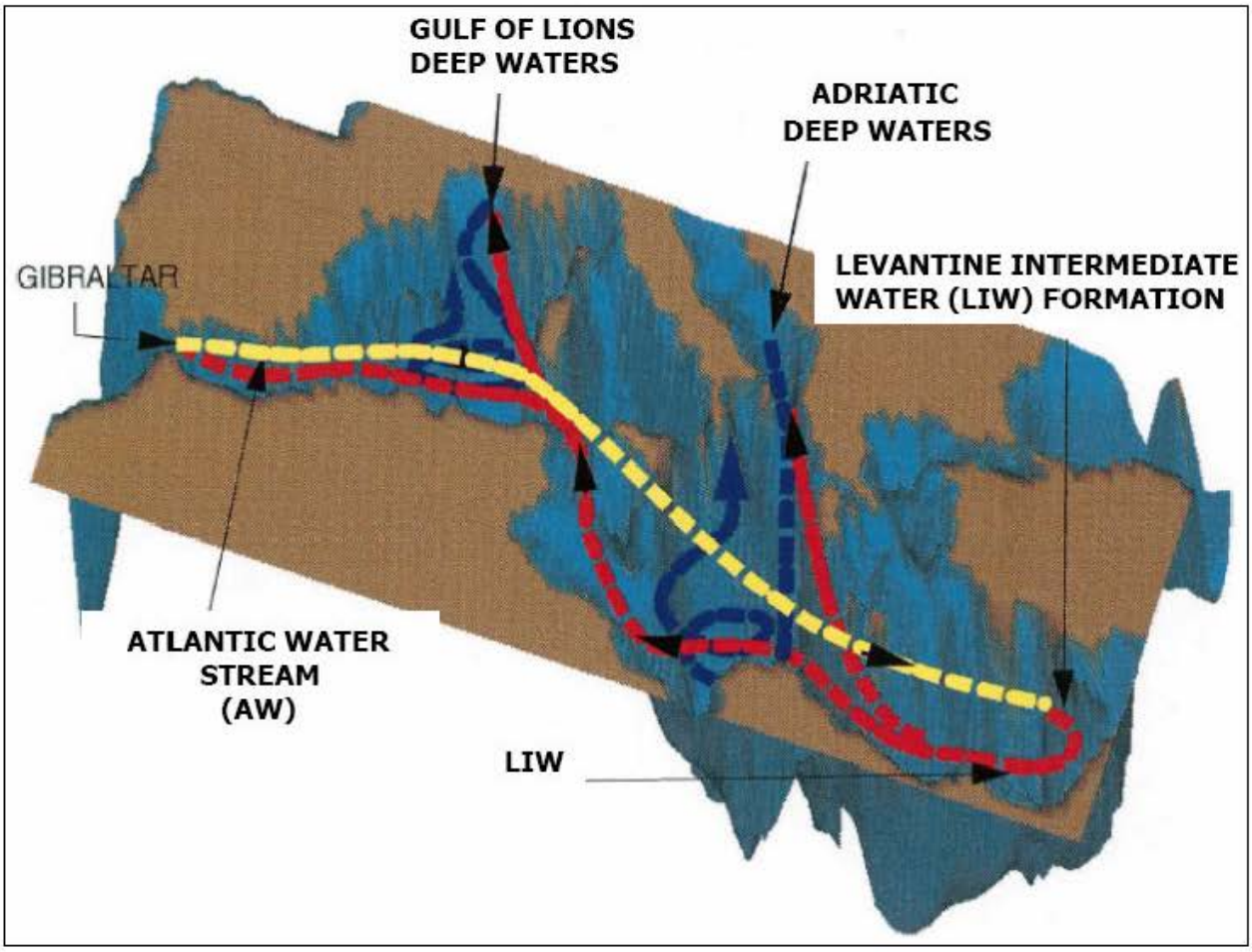

Fig 3. The schematic of the thermohaline circulation in the basin with the major conveyor belt systems indicated by dashed lines with different color. The yellow indicates the AW stream which is the surface manifestation of the zonal conveyor belt of the Mediterranean. The red indicates the mid-depth LIW recirculation branch of the zonal thermohaline circulation. The blue lines indicate the meridional cells induced by deep waters. LIW branching from the zonal conveyor belt connects meridional and zonal conveyor belts. Adapted from Pinardi and Masdetti (2000).

2.2 The Climate

The climate of the Levantine Basin is characterized by a hot and dry summer with stable atmospheric conditions, a cold and wet winter and transitional seasons in spring and autumn (Reiter, 1975). During the summer, steady westerly to northwesterly winds are dominant over the basin strengthened by the Aegean Etesian regime and superimposed by a well-developed coastal sea breeze. The climatological wind fields in winter are predominant westerlies. In contrast to summer, the winter atmospheric conditions are unstable and variable, with occasional cold and dry air outbreaks from the north and local cyclogenesis such as the Cyprus low (Ozsoy, 1981; Alpert and Reisin, 1986). Also important are the depressions moving eastward across the Mediterranean Sea (Alpert et al., 1990), which force strong southerly to south-westerly winds along the Israeli coast (or westerly winds along the southern Turkish coast) and produce

downwelling-favorable conditions. The cold and dry air outbreaks from the northern continental regions (such as the Poyraz wind along the Anatolian coast) play important roles in the oceanography of the region, leading to significant buoyancy losses and initiate the formation of the LIW.

2.3 Mean hydrographic characteristics and water masses.

2.3.1 The field measurements

Israeli contribution to the investigation of the Levantine basin dates back to 1947 and can be divided into three distinct periods. (a) The early period (1947-1979) when hydrographic cruises to collect data were based on wire mounted bottles and reversing thermometers and was confined to the upper 150 m. Most of these were part of a pioneering work to investigate the spreading of the AW throughout the basin or the appearance of the Nile floodwaters along the coast of Israel prior to the construction of the Aswan High Dam in 1964 (Oren, 1971; Oren and Hornung, 1972). (b) The Marine Climate (MC) campaign from 1979-1984 (Hecht et al., 1988), consisting of 20 cruises and using, for the first time, modern conductivity-temperature-depth (CTD) methodology and profiles, routinely sampling to 1000 m and more. The majority of the cruises covered the area south of Cyprus on a regular 0.5^0 grid. Two of the cruises also included transects to the west far as Crete (Fig.4). (c) The Physical Oceanography of the Eastern Mediterranean (POEM) (see: The POEM Group, 1992) and the Levantine basin Dynamical Studies (LBDS) open sea cruises, covering the years 1985-1992. These cruises were conducted as part of a multinational coordinated effort. Since the Levantine Basin was covered almost exclusively by the Israeli and Turkish ships (Figs 5a, 5b), several joint analyses of the Levantine data alone were conducted and published by the two teams (e.g., Ozsoy et al., 1993).

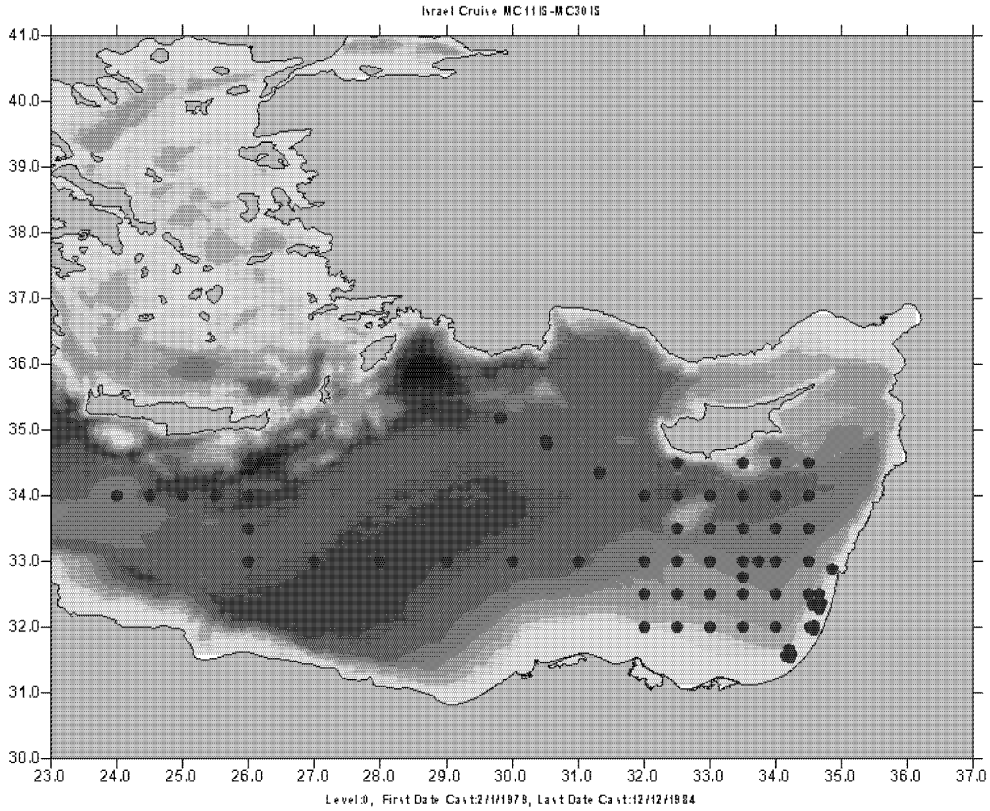

Figure 4. Station locations during the MC cruises (1979-1984)

(a)

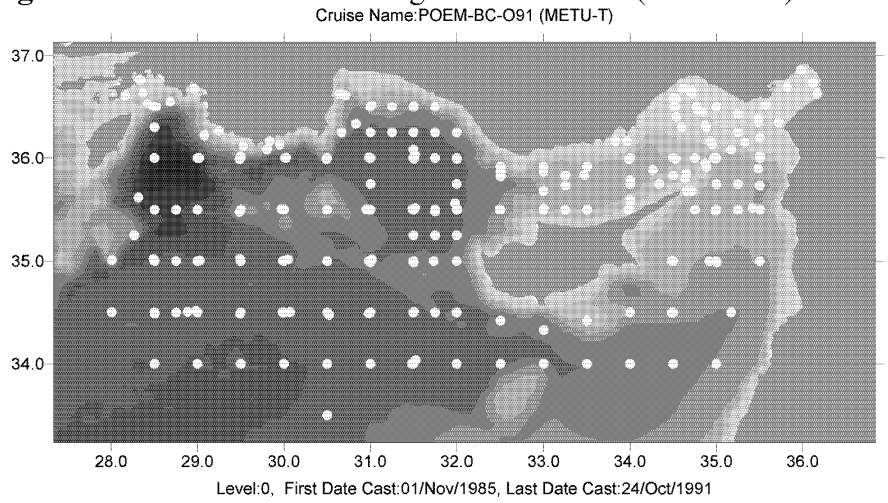

(b)

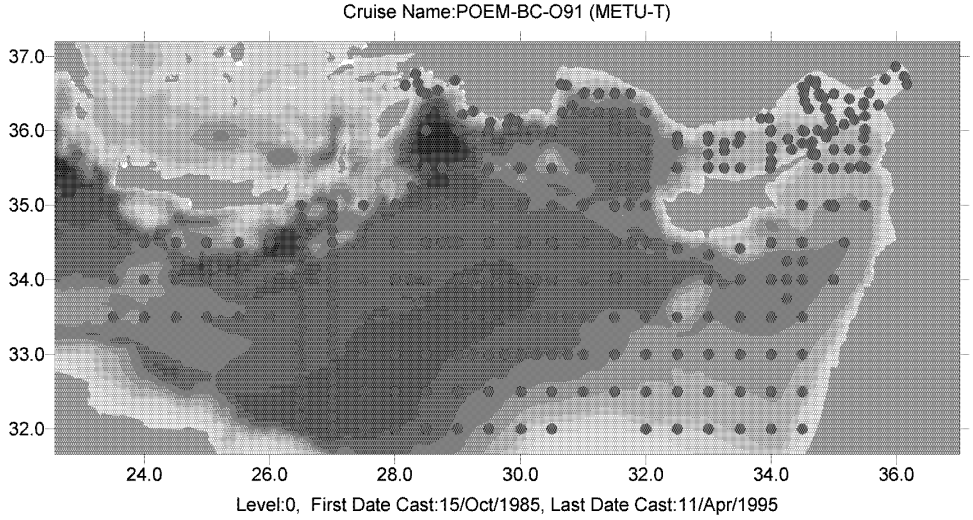

Fig 5. Station locations of the POEM Turkish (a) and Turkish+Israeli cruises(b).

2.3.2 The mass field

The MC Hydrographic measurements at the southeastern Levantine Basin (LB) show four identified water masses (Hecht et al., 1988): the warm and salty Levantine Surface Water (LSW) during the warm seasons which is very thin during the summer (Depth ~25 m, Smax=39.11, Tmax=28.2) ; the relatively fresh modified Atlantic Water (AW) below the seasonal helocline (Depth= 25-100m, S<= 38.87); the saline Levantine Intermediate Water (LIW) from 135-315 m during summer, or 75-325 m during winter (Smax=38.98); and the deep water (DW) below 700 m (S<=38.74). The temperature from 700 m to the bottom drops from 13.79^0 C to 13.35^0 C and almost doesn't change with time. It should be noted that the above values were averaged over the MC region.

The MEDAR/MEDATLAS-2 Data base archive (http://doga.ogs.Trieste.it/medar/climatologies) allows for updated (to 1998-99) climatological physical and chemical parameters for the south-east LB region (Lat <=34 35.0 N , Long >= 32 10.0 E) and north-east LB (Lat>=34 36.0 N, Long>= 32 10.0 E). The climatologically profiles for the salinity and temperature for both these regions (Figs. 6a, 6b) show clearly the various water masses, as well as the marked contrast between the winter and the summer season in temperature and salinity at the upper layer.

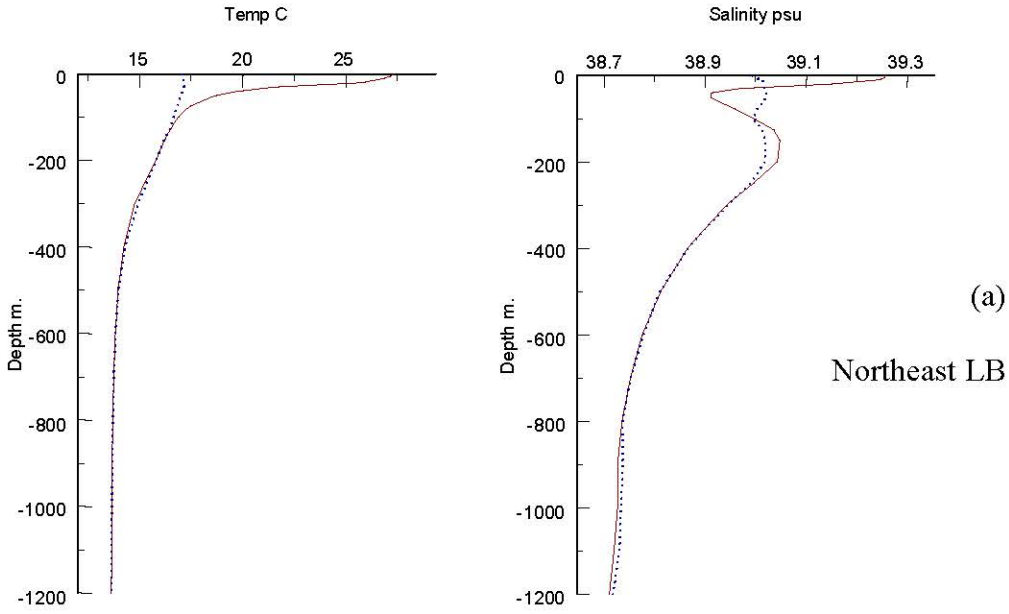

(a)

Northeast LB

(b)

Southeast LB

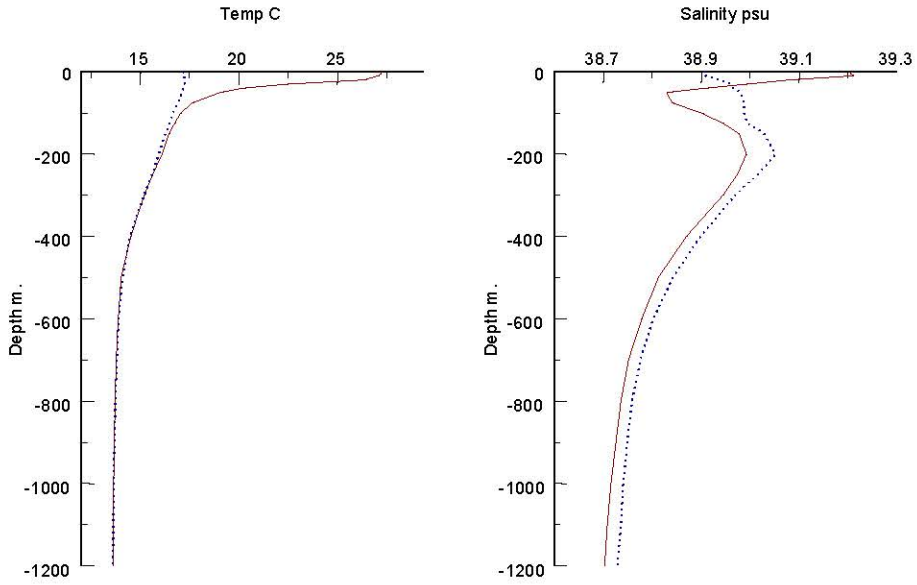

Fig 6. Averaged temperature and salinity profiles during winter (blue) and summer (red) for:
(a) northeast LB (Lat>=34 36.0 N, Long>= 32 10.0 E) and
(b) southeast LB (Lat<=34 35.0 N, Long >= 32 10.0 E).

The climatological values mask, however, the intense variability in time and in sub-basin and mesoscale length scales, found during the various cruises (Robinson et al., 1987; The Poem Group, 1992; Ozsoy et al., 1993). For example, one of the most outstanding features seen in the MC and later in the POEM data was an intense, recurrent warm-core eddy to the south of Cyprus which has since been referred to as the Shikmona or Cyprus eddy (The POEM group, 1992; Brenner et al., 1991; Brenner, 1993). Most of the information is available, at this time, on modern databases, such as the MEDAR/MEDATLAS-2, or the Israel Marine Data Center (ISRAMAR) on the IOLR web site (www.ocean.org.il) (Fig. 7 shows, as an example, the temperature and salinity vertical north-south cross sections (respectively) off the southern Turkish coast during September 1987).

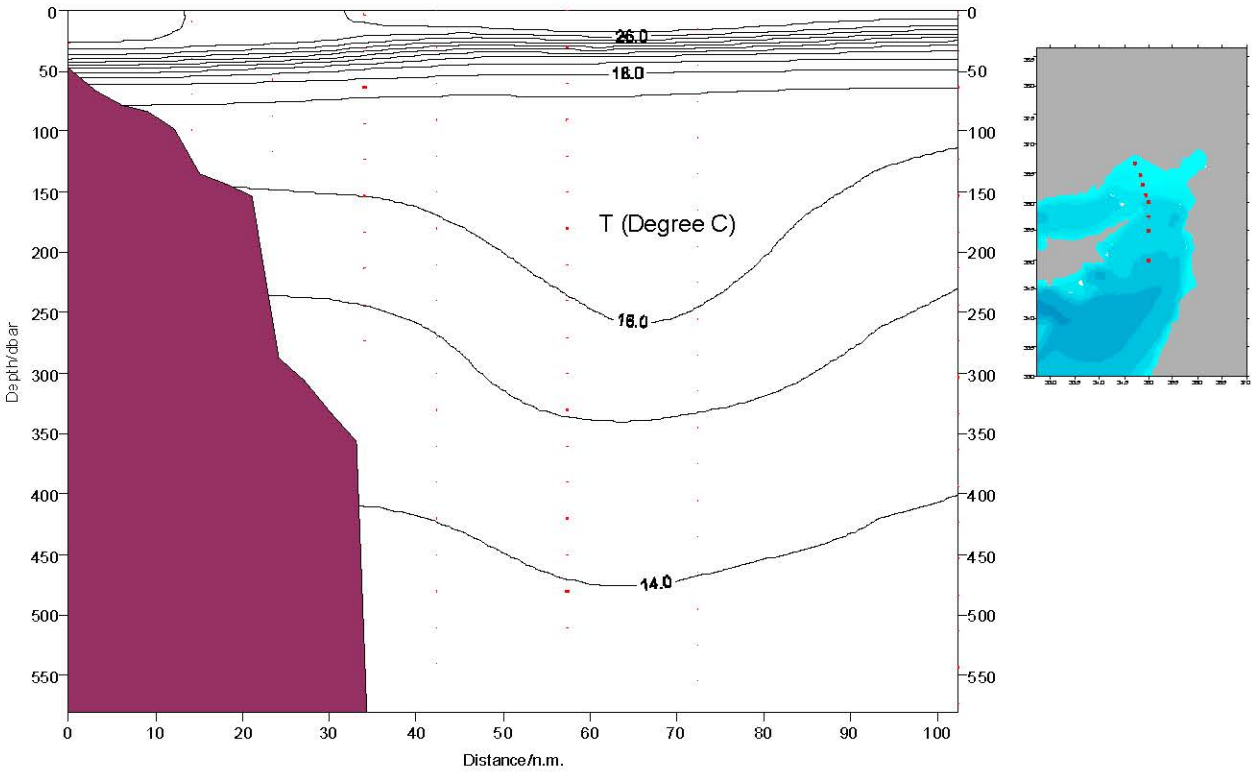

Fig 7. Cross-section of the temperature off Turkey on September 87.

Over a shelf/slope region the water temperature and salinity may differ from that of the open sea due to the shallow depth and the special flow characteristics in such a region. Off the Israeli coast the summer thermocline tilts downwards, from the deep sea, across the slope and intersects the bottom at mid- shelf (Figs 8a, 8b). The cross sections of salinity are much more complex. Noticeable, are the AW lenses off the shelf. In contrast to summer, the upper 100 m of the sea during winter becomes mixed and homogenous as seen in the temperature or salinity cross sections (Figs 9a, 9b).

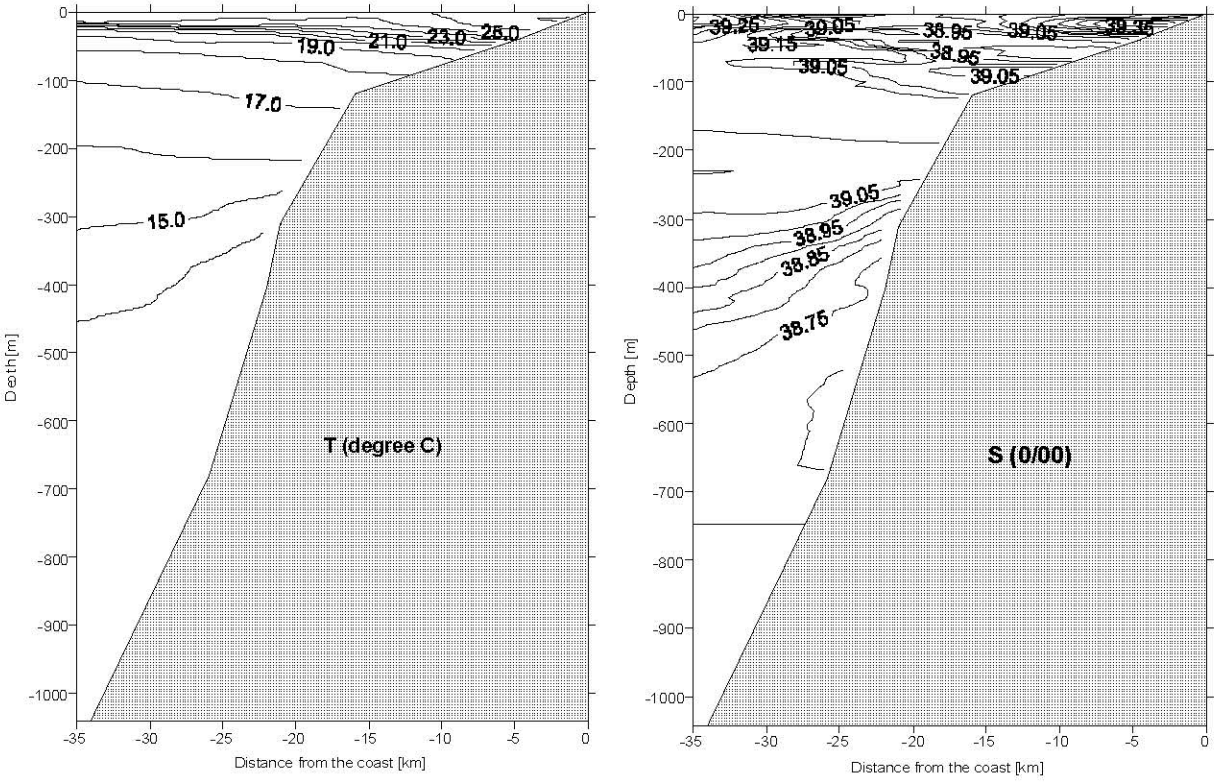

Fig. 8. Temperature and salinity cross sections off Netanya on June 25, 1996.

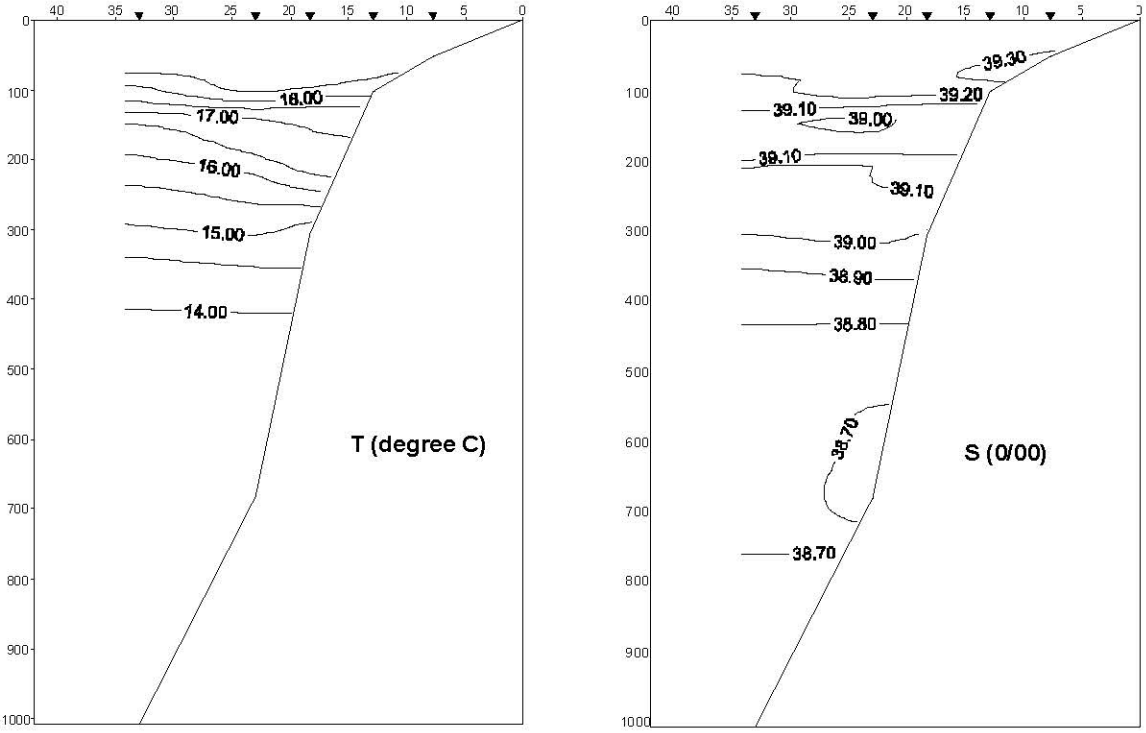

Fig. 9. Temperature and salinity cross sections off Hadera on Jan 2, 1996.

2.4 The general circulation.

The major factors, which directly drive the open sea circulation in the Levantine basin, are the wind stresses and internal horizontal pressure gradients due to varying water densities. The majority of significant currents are, generally, confined to the few uppermost hundreds of meters while depths bellow 700 to 1000 m are considered to be relatively motionless. The general circulation in the Levantine basin, as obtained from the density field measured by the above-mentioned observational programs, is shown to consist of features spanning a wide spatial and temporal range. Features include basin and sub-basin scale gyres interconnected by jets as well as the mesoscale eddies. Some of the features are permanent while others are persistent or recurrent and others are transient (The POEM Group, 1992; Ozsoy et al., 1993). Among the permanent features are the Rhodes cyclonic gyre (a place of LIW production) or the Mersa-Matruh anticyclonic gyre, or gyre system, off the African coast (~28 0 E). One new outcome of these observations is the possible presence of a Mid-Mediterranean- Jet (MMJ) at mid-basin, also affecting the circulation to the north or south of Cyprus (Robinson et al., 1992). However, in spite of the work done during the last two decades, the circulation pattern in the LB is not documented well enough and is still under debate. Among the reasons for this are the difficulties in sampling and interpreting the complex flow pattern and its strong variability in the synoptic and seasonal time scales. Another major reason is the lack of observations over the continental margins off the African and the eastern LB coasts (see Figs 4 and 5). Based on satellite remote sensing of sea surface temperature, it is argued that the surface flow of the LB is more constrained alongslope and cyclonically around the basin, (Millot and Tauppier-Letage, 2005; Hamad et al. 2005; Alhammoud et al., 2005).This circulation is dominated by mesoscale eddies but still resembles, to some extent, the traditional view of the basin- scale cyclonic pattern known in the past (Nielsen, 1912; Ovchinnikov, 1966). Pinardi et al. (2004) present an integrated view of the general circulation, which is also based on numerical simulations. This circulation is described schematically in fig. 10 (upper panel) and can be compared to the two other circulation schematics (Fig 10). According to Pinardi et al. (2004), the Atlantic-Ionian stream, containing the modified Atlantic water, enters the Cretan passage close to the African coast and bifurcates at the Mersa-Matruch Gyre system. One branch continues alone the African coast while the northern one, the MMJ, inflows at mid- basin. The coastal cyclonic circulation consists of: an eastward current off the Libyan and the Egyptian coasts known as the Southern Levantine Current; a northward current off the eastern LB coasts; and, a western current off the southern Turkish coast known as the Asia Minor Current (AMC). The MMJ flows eastward at mid basin. Southwest of Cyprus it may bifurcate. One branch flows south of Cyprus and joins

the coastal cyclonic circulation while the other branch turns northward and feeds the AMC off Antalia. The (eastern) part of the AMC, between Cyprus and Turkey, also called the Cilician Current (CC), may have special characteristics due to the depth transitions at Lattakia and the Cilicia Basin (Ozsoy, 1993) as well as the possible blocking effects of a recurrent Lattakia gyre. Robinson et al. (1992) identify the CC in their schematic (Fig. 10, lower panel) as a non-permanent current being only partly fed by the MMJ.

One of the most intense dynamic features of the open sea in the southeastern LB is the Shikmona (Cyprus) anticyclonic eddy south of Cyprus, with a typical diameter of ~ 100 Km, whose influence extends to depths of about 400m and whose current speed may reach, at its rim, 30-40 cm/s. This eddy was shown by the various filed programs (the previously mentioned MC and POEM, the Cyprus Basin Oceanography (CYBO) project in the let 90s and the EU CYCLOPS project in 2001 and 2002 (Zodiatis et al., 2005)) to be recurrent and persistent for long periods; the exact position at a particular time determining the occurrence or the direction of the MMJ south of Cyprus and affecting the circulation in the southeastern LB as well.

THE MEDITERRANEAN SEA CIRCULATION SCHEMATIC

(from Pinardi *et al.*, 2004)

1a Liguro-Provencal-Catalan current (LPC)
1b Gulf of Lyon Gyre
1c Western Corsica Current
2 Northward Tyrrhenian current and gyres:
2a Northward current and Southern Tyrrhenian Gyre
2b Northern Tyrrhenian Gyre
2c Eastern Corsica Current
3 Gibraltar-Atlantic current system
3a Alboran basin Gyres and meanders
3b Algerian current gyres, eddies and meanders
3c Tyrrhenian bifurcation/current
3d Atlantic-Ionian Stream
3e African MAW (Modified Atlantic Water) Current
3f Mid-Mediterranean Jet
3g Southern Levantine current
4 Rhodes Gyre
5 Western Cretan cyclone
6 Western Ionian cyclonic Gyre
7 Syrte Gyre
8 Anticyclonic system of the South-eastern Levantine basin
8a Mersa-Matruh Gyre system
8b Shikmona Gyre system
9 Asia Minor current
10 Iera-Petra Gyre
11 Pelops Gyre
12 Southern Adriatic cyclonic Gyre
13 Western Adriatic Coastal Current
14 Western Ionian anticyclonic Gyre

(from Millot *et* Taupier-Letage, 2005)

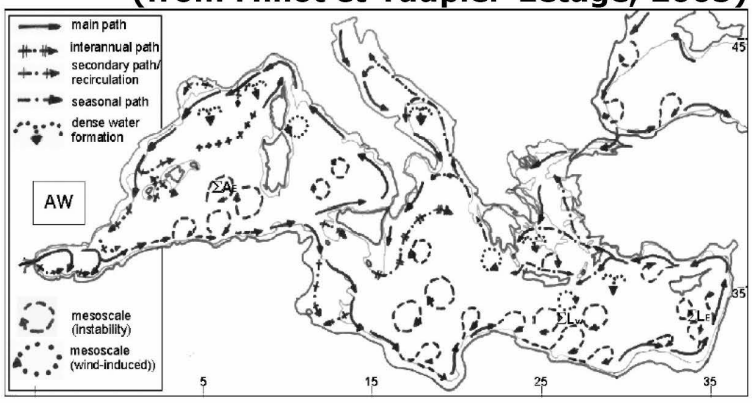

(from Robinson *et al.*, 1992)

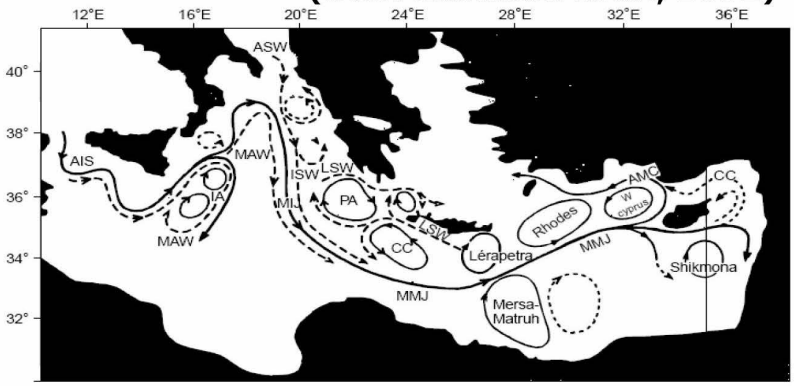

AIS = Atlantic-Ionian Stream
MIJ = Mid Ionian Jet
MAW = Modified Atlantic Water
ISW = Ionian Surface Water
IA = Ionian Anticyclones
MMJ = Mid-Mediterranean Jet
ASW = Adriatic Surface Water
LSW = Levantine Surface Water
PA = Pelops Anticyclone
CC = Cretan Cyclone
AMC = Asia Minor Current

MFSTEP Monthly Bulletin N. 13 - September 2005

Figure 10 – The Mediterranean circulation schematic

2.4.1 Numerical models.

During the past decade numerical modeling of the Mediterranean circulation in general, and of the eastern Mediterranean in particular, has advanced rapidly and significantly. The major contribution comes from ongoing multinational EU projects aiming to create operational forecasting systems for the Mediterranean Sea, started in 1998. The first project is the Mediterranean Forecasting System Pilot Project (MFSPP) which has the specific goal of designing and building a prototype ocean forecasting system consisting of near real time data acquisition, assimilation, and forecasting with a hierarchy of nested numerical circulation models (Pinardi et al., 2003). The main hydrodynamic model was the Ocean General Circulation Model (OGCM) that was implemented for the full Mediterranean Basin. Nested within are several regional models (such as the ALERMO model for the Aegean Levantine area) and also, on the now ongoing MFSTEP program, shelf models. The regional models obtain their boundary conditions from the OGCM model and provide boundary conditions to the shelf models. Among the last are the Cyprus CYCOFOS for the northeast LB, or those for the southeast LB, operational at IOLR (Brenner 2003) (another shelf model is intended for the southern Turkish coast within the framework of WP9). All of these are using the POM model (Blumberg and Mellor, 1987). Through the downscaling procedure each sub- region has a refining grid size. The grid size for the OGCM full basin model has doubled since the MFSTEP project (started in 2001) to 1/16 x 1/16 degrees. The ALERMO is at 1/20x1/20 (but 1/30, ~3.5 km, in the future), CYCOFOS at 2.5km (1.5km, in the future) and the southeastern LB model at 1.5 km. These programs provide information of the 3D circulation and the thermohaline structure at increasing resolution, which is implemented in other products and applications of the MFSTEP program. These include: Oil spill modeling, general contamination dispersion models, search and rescue, ecosystem modeling etc. The MFSTEP-OGCM runs in 1-week/10-day analyze/forecasting modes using atmospheric forcing data provided by analyses and forecasts from the European Center for Medium-Range Weather Forcing (ECMWF). The analysis is computed assimilating SST, SLA along the tracks, VOS-XBT data and ARGO floats date. This data, as well as the forecasts from the regional and shelf models, can be obtained through the Web site of the MFSTEP (www.bo.ingv.it/mfstep).

Examination of the monthly mean analyzed surface currents of the MFSTEP-OGCM model, with the refined grid size at 1/16 as published in the MSFSTEP monthly bulletins (Sep 2004- Jan 2006), shows considerable seasonality of the circulation along the eastern rim of the Levant basin. During the winter (Dec-Feb) and the summer (Jun-Aug) seasons a cyclonic circulation

along the continental margins exists, generally. During these seasons the eastward current off the Sinai coast, being the eastern part of the South Levantine Current, is strong (surface currents reaching 0.2-0.4 m/s). Similarly strong are the westward Cilician Current and the AMC off the southern Turkish coast. The cyclonic circulation differs, however, to some extent, from the schematics of fig.10, given by Pinardi et al. (2004), regarding the northward current along the eastern coasts of the Levantine Basin. According to the model outcomes, there is a separation of the current off the northern Israeli or off the Lebanese coast. This currents flows northwestwards, reaching southeast Cyprus and then tends to flow along the eastern margin of Cyprus, and specifically, along the extreme northeastern, wedged shaped, peninsula, before entering the Cilician basin. A significant outcome of the model is the occurrence of a northward, alongslope jet off the Israel coast during the winter or summer seasons. The maximal velocities in the jet in the summer are for the month of July, reaching 0.4 m/s at the sea surface. This value is comparable to those obtained during winter. In contrast to the winter and summer seasons, during the months April - May in the spring, or the months September-October, in the autumn, the currents off the Sinai coast as well as along the Israeli coast are weak (surface currents < 0.1 m/s). An important feature, divulged by the models, is a recurrent long- lived anticyclonic eddy east of Cyprus and south of the Latakia basin, having surface velocities of 0.2-0.4 m/s. It is found to exist most of the time (except during the two first months of summer 2005), resulting in southward currents close to the Syrian and the northern Lebanon coasts. More detailed information regarding the spatial and temporal variability of the circulation, obtained from the MFSTEP daily-analyzed circulation data base, point out the area off Haifa bay as the preferable point of boundary current bifurcation or separation during the winter and summer seasons (Figs 11 and 12, respectively). In addition, it is shown that during winter, the boundary current south of Haifa may, occasionally, be intensified due to the approach of a large cyclonic regional scale meander.

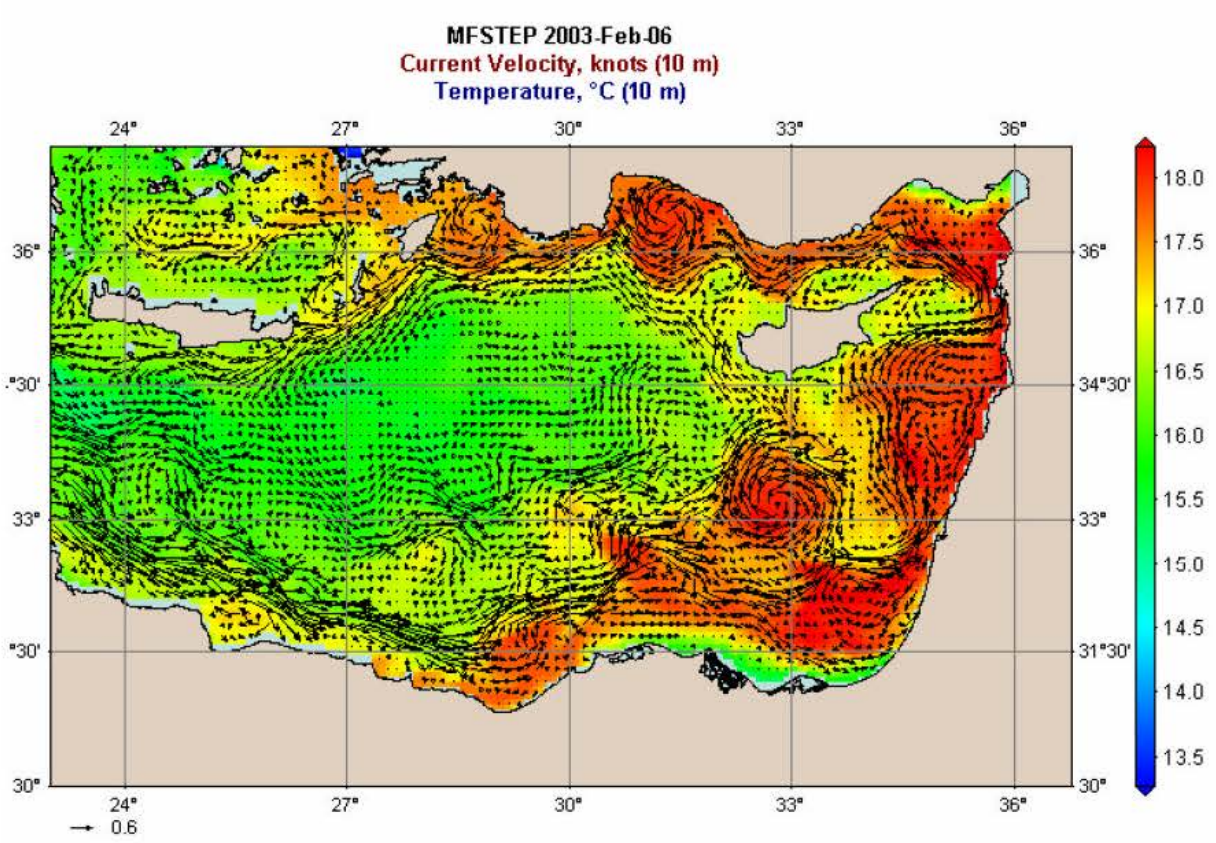

Fig. 11: Example of a daily- mean analysed near surface currents and temperature from the MFSTEP data set in winter.

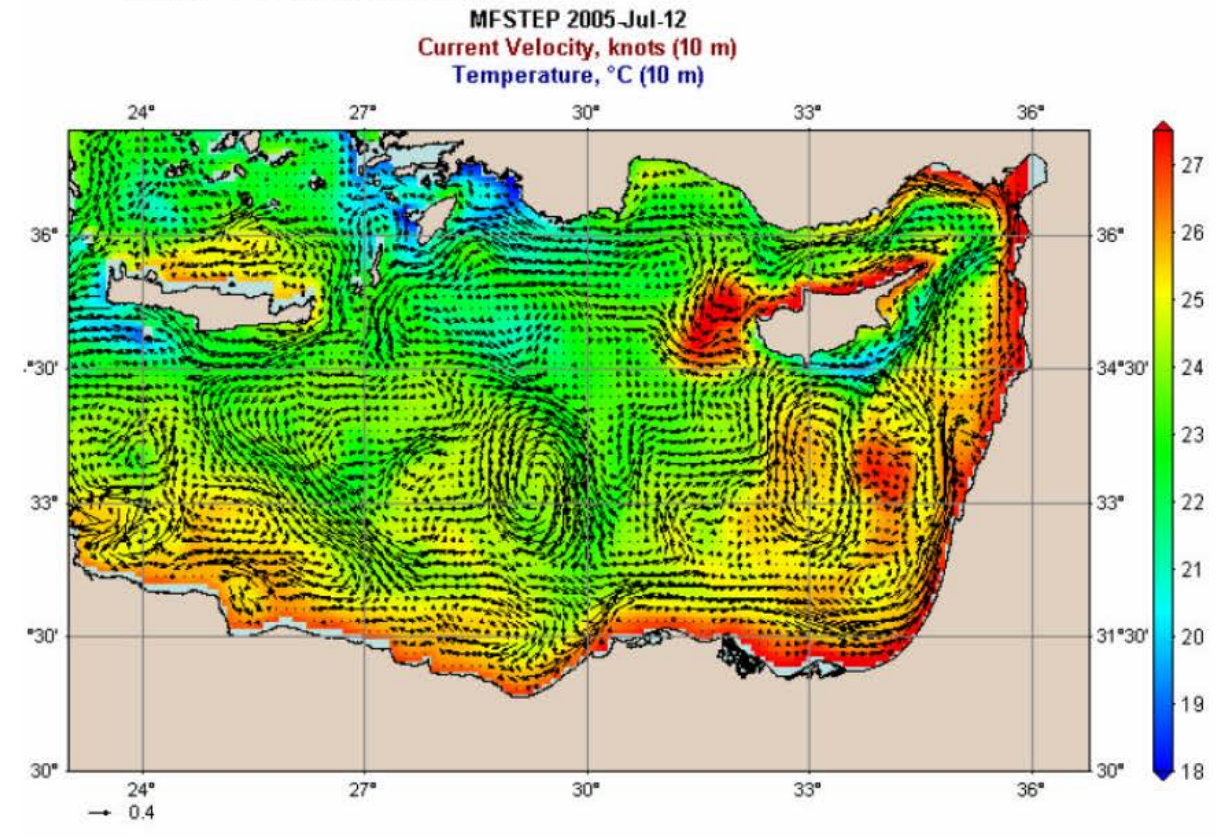

Fig. 12: Example of a daily- mean analysed near surface currents and temperature from the MFSTEP data set in summer.

2.5 On the circulation over the Israeli continental shelf and slope

Conservation of vorticity in the rotating earth system forces the geostrophic circulation (time scales from a few days to a few weeks) to follow the bottom contours. This constraint may inhibit cross slope flow due to the great changes in depth, restricting the influence of the deep sea and separating, to some extent, the flow over the shelf from the general open sea circulation. Ageostrophic conditions allow, however, the transport of water masses and constituents between the shelf and the open sea. This issue, discussed and analyzed in great detail by Huttenance (1995), is of special importance along the eastern and northeastern coasts of the LB due to the very narrow shelves and the proximity of the deep sea. There is, in this respect, some similarity in the open sea conditions off the shelf of Israel and those off Turkey, in the sense that both have an along slope or boundary current jet which may interact strongly with the shelf.

The Israeli continental shelf has a relatively simple bathymetric relief structure with isobaths roughly parallel to the coastline. The shelf width (up to the shelf edge at 100 meters of depth) at the southeastern end of the Levantine basin varies from approximately 60 km off the coast of Sinai to 20 km in southern Israel, narrowing to about 10 km in the north. In 1987 the Israeli National Institute of Oceanography started a 10-year observational study to investigate the circulation and the thermohaline structure off the Israeli coast (Rosentraub, 1990, 1994, 1995, 1996). It was conducted with subsurface current meter moorings on the shelf and at mid-slope (Fig.13) as well as with hydrographic across-shelf sections. [in recent years the field measurements have been based on bottom mounted Acoustic Doppler Current Profilers (ADCP) on the inner shelf (depths 10-25 m) (Rosentraub, 1999, 2000, 2002) , and on ADCP ship transects]. Statistical and spectral analyses of the currents over the shelf show no evidence of currents at the semidiurnal tidal frequency; however, quite a strong signal (~ 0.1 cm/s) is found at a daily period during the warming season due to the sea breeze. The most important part of the current energy is present in the synoptic and seasonal time scales. The synoptic currents over the Israeli shelf are mainly northwards and follow the bathymetry. The monthly mean along-shore current over the inner or mid-shelf has a seasonal period with a maximum northward velocity magnitude during summer and winter seasons of O(0.1 m/s) (Fig. 14).

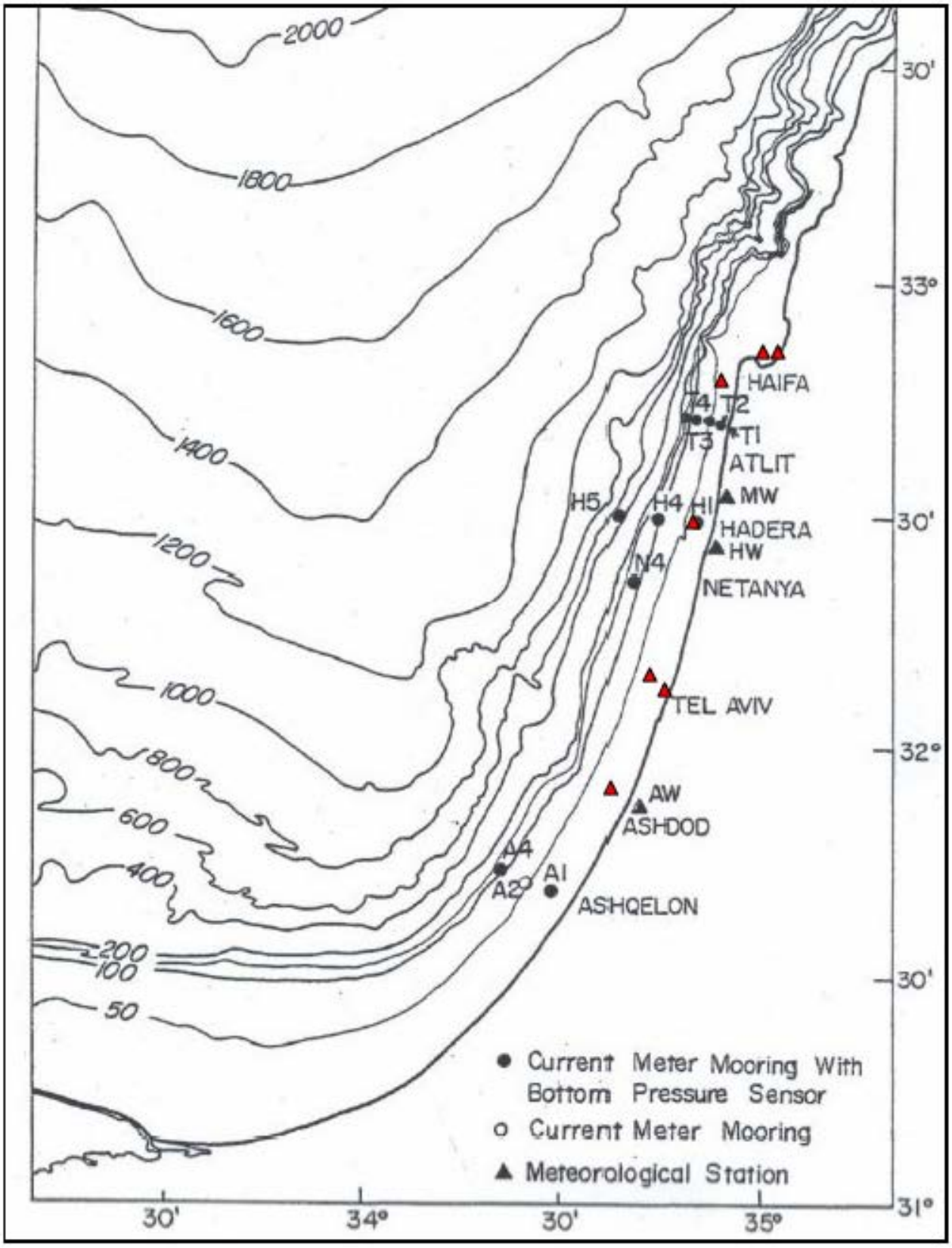

Fig. 13. Current meter station locations during the years 1987-1996 and the ADCP stations during the recent years (marked by ▲)

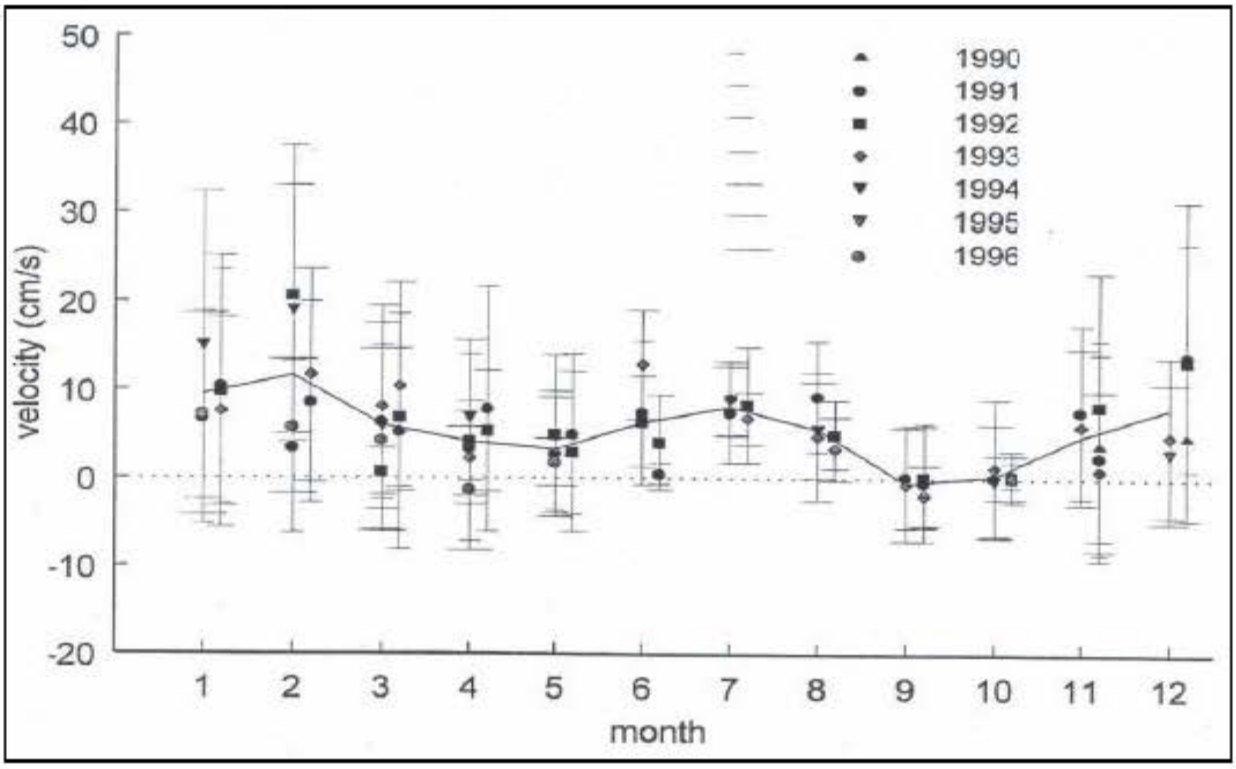

Fig 14. The monthly mean and standard deviation of the alongshore 40-hour low pass filtered velocity component at shallow stations H1 and A1 (right shifted) during years: 1990-1996. Positive indicates northward velocity.

During the stratified summer season, both the monthly mean currents and synoptic velocity along-shore fluctuations decrease with depth below the surface mixed layer. The decrease of the mean velocity is in agreement with the strong stratification and sloping isopycnals over the shelf, resulting in low velocities of only a few cm/s near the bottom at the outer shelf (Fig. 15). Characteristic for this season is an offshore increase in the northward seasonal current within the upper water layer as shown e.g. for the sites off Atlit (Fig. 15). The recent basin scale and regional modeling simulation support the idea that this current is associated with a cyclonic boundary current jet or a large cyclonic meander in the Southeastern Levantine basin. Indication of such a jet may be inferred from the ADCP transect off Haifa carried out during the early spring of 2004 (Fig. 16).

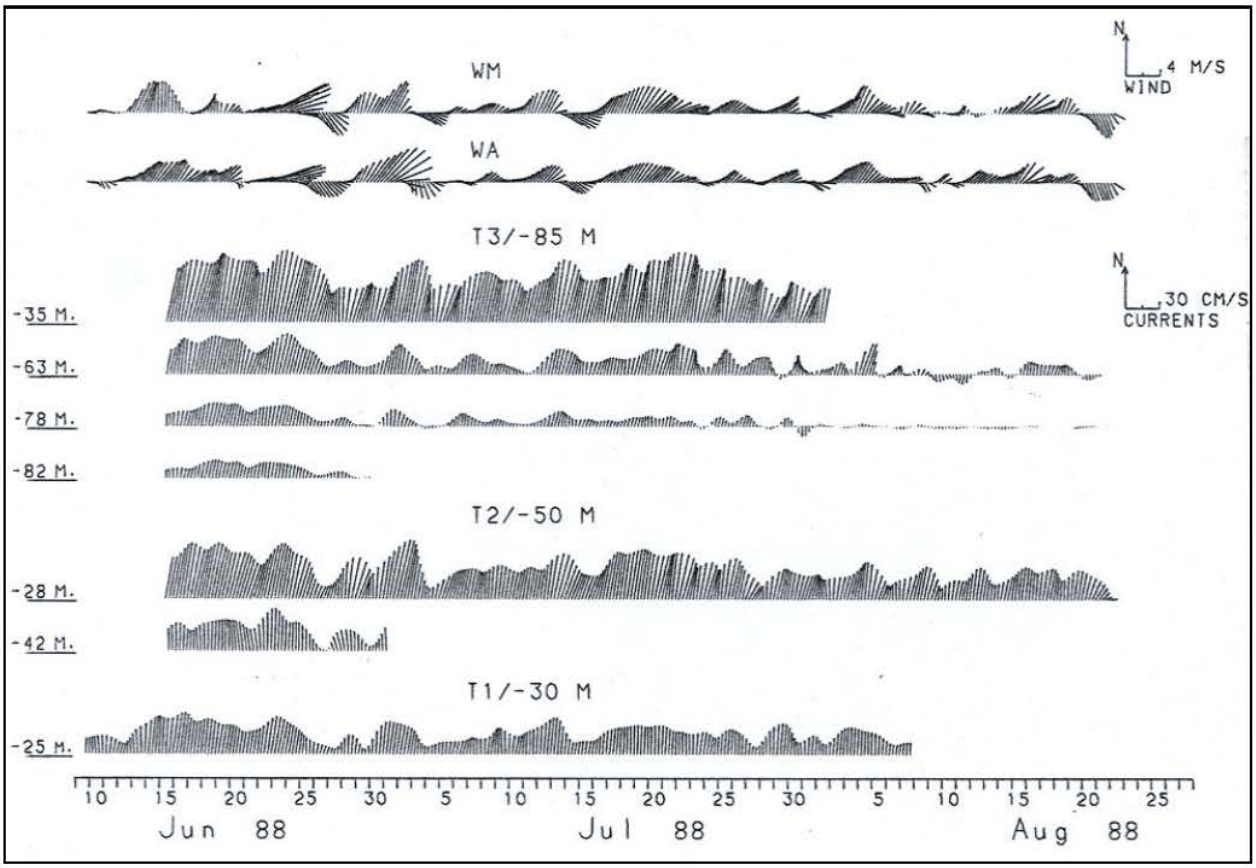

Fig 15: Summer 40h-low pass filtered current vector time series at station T1, T2 and T3 off Atlit. Wind from coastal station is shown in the top panel.

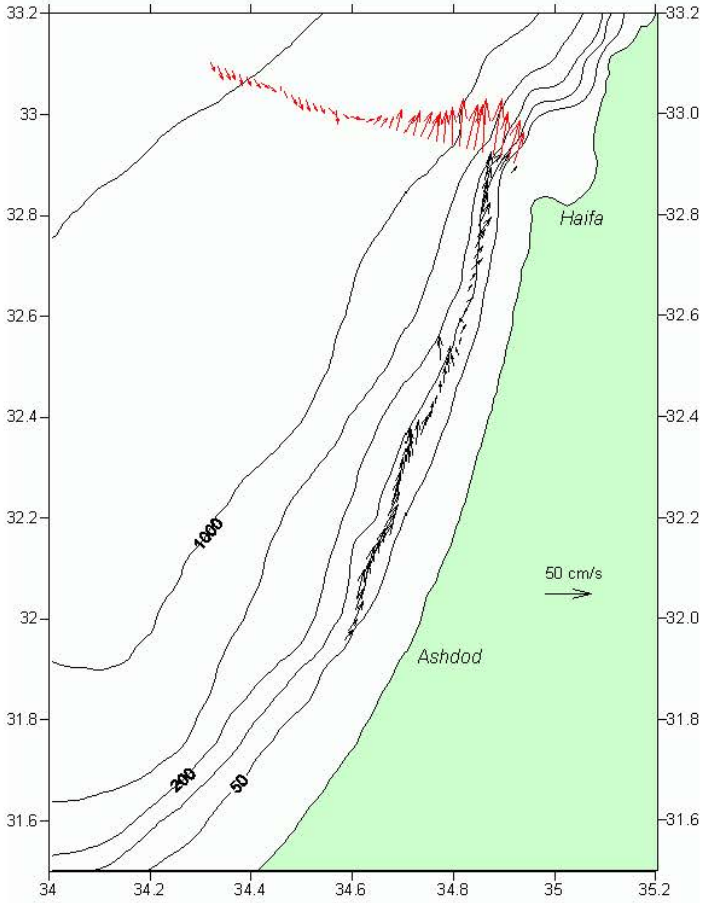

Fig. 16. BB-ADCP (75kHz) velocity vectors at 16 meters below the sea surface along the shelf (May 19-20, 2004) and along a transect off Haifa (September 7, 2004).

During winter the water over much of the shelf is homogenous and the synoptic currents are highly coherent and vertically uniform (Fig. 17). Although occasional southward currents have been observed, the winter season is characterized, mainly, by strong northward currents (O(0.6 m/s)) during the winter cyclonic storms which exhibit a strong along-shore wind stress component. These currents also imply, in addition to a large along-shore transport, strong bottom friction and vertical mixing. The magnitude of the along-shelf synoptic velocity component depends mainly upon the along-shelf wind stress and pressure gradients. The direct response to the wind is mostly confined to the inner and mid-shelf, whereas the shelf edge sites show open sea influence (Rosentraub, 1995). The cross-shelf circulation is characterized by onshore surface Ekman transport that is compensated for by a seaward (downwelling) flow in the bottom boundary layer. At the shelf break sites the seaward flow is also accompanied by an intensification of the northward current. Current measurements, as well as hydrographic cross sections, indicate the possibility that part of this transport is also due to gravitational advection and downslope cascading of dense shelf water, induced by winter cooling and evaporation.

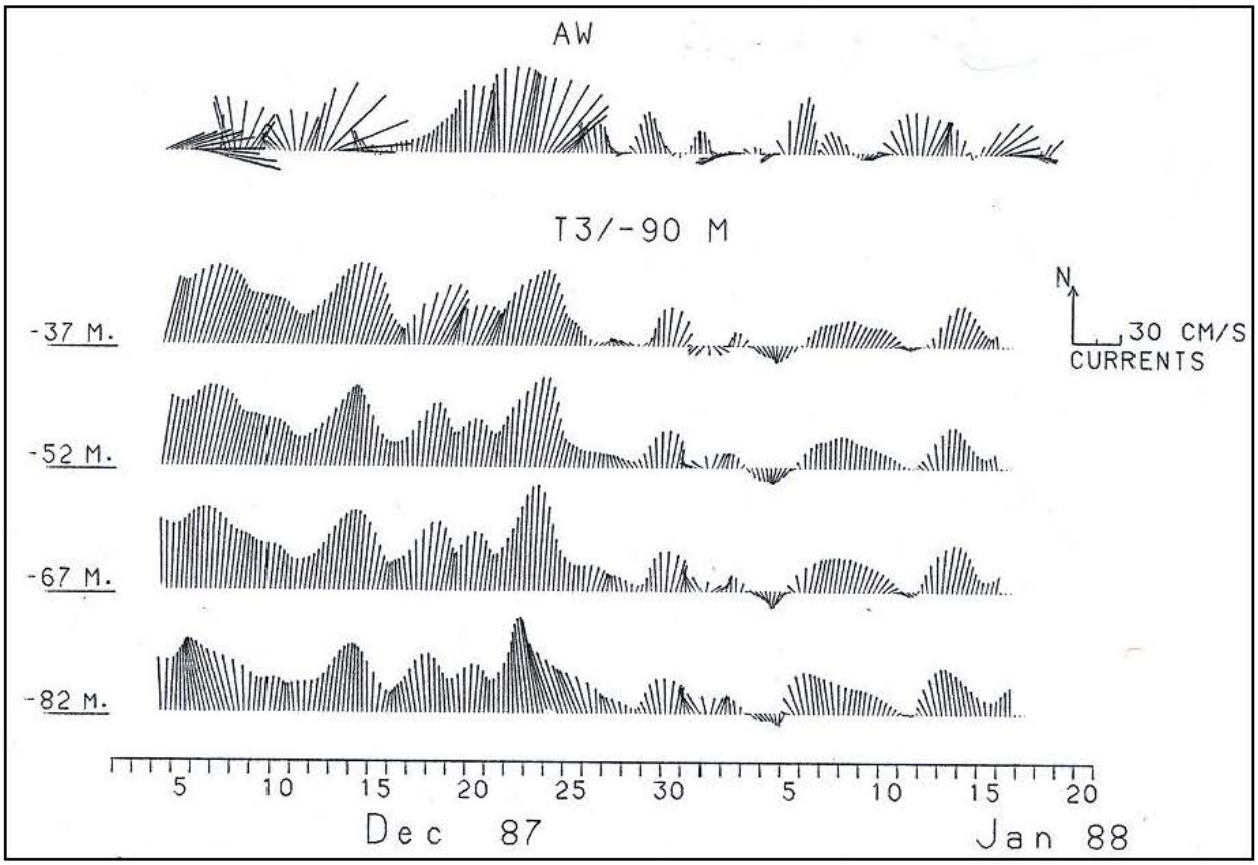

Fig 17: Winter 40h-low pass filtered current vector time series at station T3 (bottom depth: 90m) off Atlit. Wind from coastal station is shown in the top panel.

Currents on the continental slope

Current measurements from a single mooring on the continental slope off Hadera (water depth of 500 m) reveal, occasionally, during summer and winter, the existence of a strong northward along-slope baroclinic jet confined to the upper 50-200 meters (respectively) with monthly mean velocities of 0.2-0.4 m/s. During winter storms the hourly velocities at the upper layers of the jet may reach a magnitude of 0.9 m/sec (Fig. 18) or be, as high as 0.3 m/s near the bottom, at the end of the winter mixing season. This jet seems to have an impact on the outer and mid-shelf circulation.

The presence of a strong current on the slope can be explained by the steering effect of the topography (Huttenance, 1995; Gjevik et al., 2002; Xing et al., 2002), shown also in the MFSTEP numerical models. It is worthy, however, to note that the jet was not found in all of the winters records, supporting some results of the numerical models, suggesting that the jet found is part of an open deep sea meander. The ADCP transect shown in Fig. 16 hinting that its width may occupy the whole continental margin. Certainly, many more measurement efforts are needed in order to study the rate of incidence and the structure of the eddy off the Israeli coast, and in particular, its role in the shelf/deep sea mass and momentum exchange.

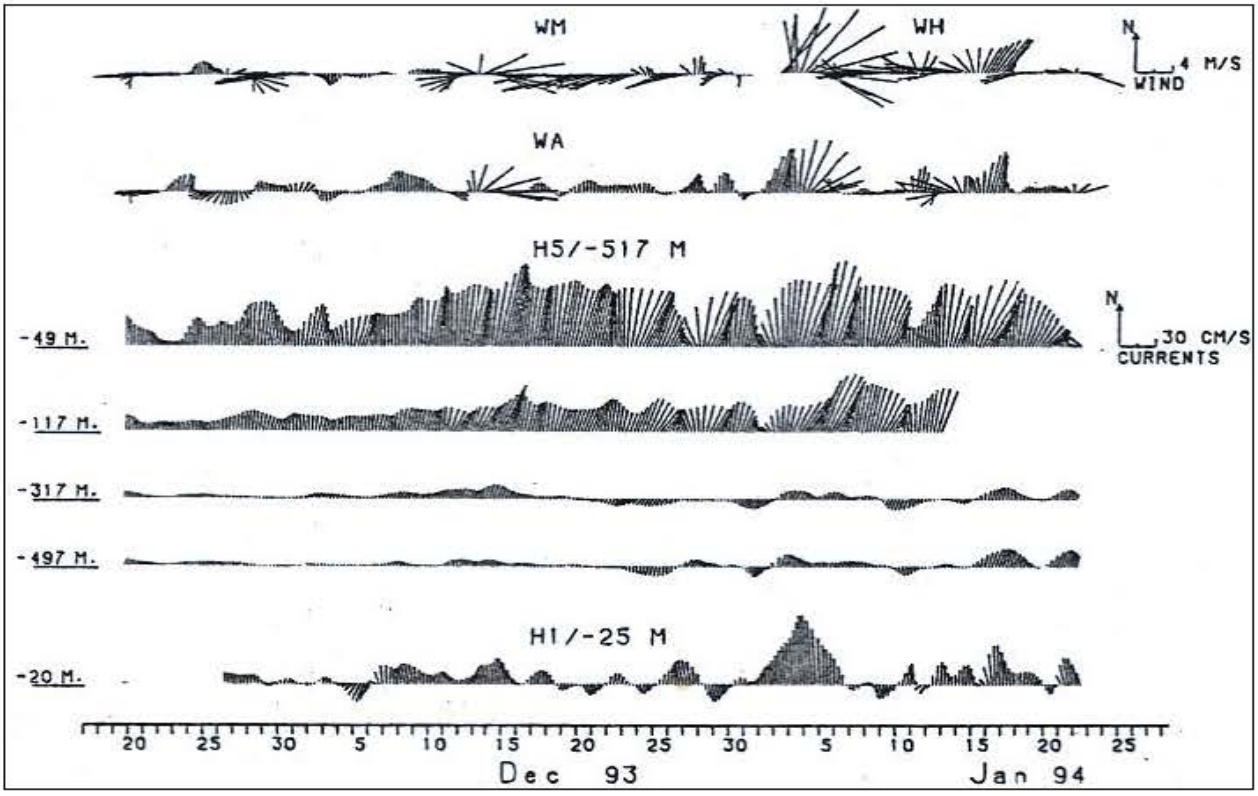

(a)

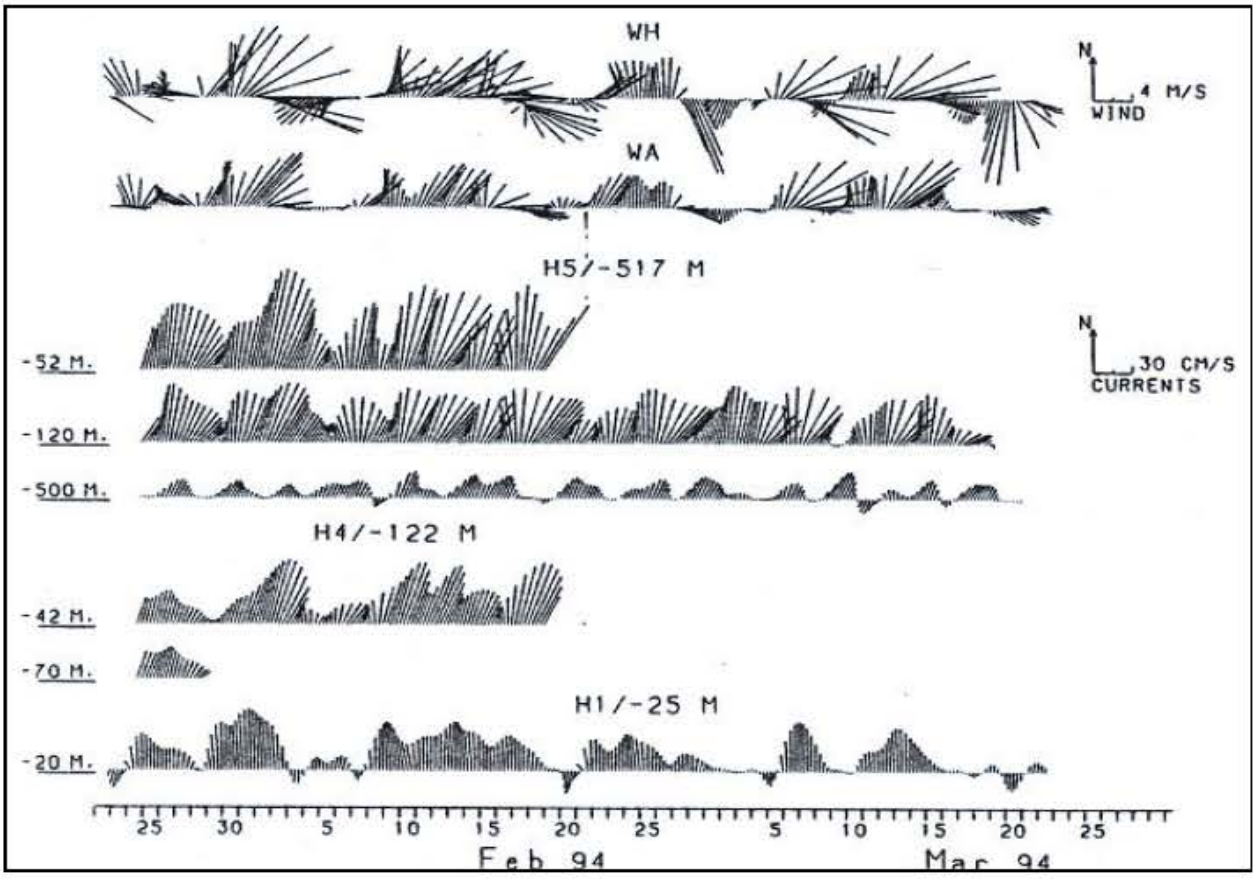

(b)

Fig 18: Winter 40h-low pass filtered current vector time series on the shelf and on the slope (Station H5) during relative calm (a) and stormy (b) weather conditions. Included are wind time series from the coastal stations.

2.6 References of Chapter 2

Alhammoud , B. Beranger, K., Mortier, L., Crepon, M, and I. Dekeyser., 2005. Surface circulation of the Levantine Basin: comparison of model results with observations. *Progress in Oceanography*, doi:10.1016/j.pocean.2004.07.015.

Alpert, P., and T. Reisin, 1986. An early winter polar air mass penetration to the Eastern Mediterranean, *Mon. Wea. Rev.*, **114**, 1411-1418.

Alpert, P., B. U. Neeman, and Y. Shay-El, 1990. Intermonthly variability of cyclone tracks in the Mediterranean, *J. Climate* , **3**, 1474-1478.

Blumberg, A.F. and G.L. Mellor, 1987 A description of a three dimensional coastal ocean circulation model. In: Coastal Ocean Circulation Models, N. Heaps, editor, American Geophysical Union, Washington DC, pp. 1-16.

Brenner, S., Z. Rozentroub, M. Krom, and Y. Bishop, 1991. The mixed layer / thermocline cycle of a persistent warm core eddy in the eastern Mediterranean. *Dyn. Atmos. Oceans*, **15**, 457-476.

Brenner, S., 1993. Long term evolution and dynamics of a persistent warm core eddy in the eastern Mediterranean. *Deep Sea Res. II*, **40**, 1193-1206.

Brenner, S., 2003. High-resolution nested model simulations of the climatological circulation in the southeastern Mediterranean Sea. *Annal. Geophys.*, **21**, 267-280.

Gjevik, B., H. Moe and A. Ommundsen (2002) Idealized model simulations of barotropic flow on the Catalan shelf. *Continental Shelf Research*, **22**, 173-198

Hamad N., Millot C.,and I. Taupier-Letage, 2005. A new hypothesis about the surface circulation in the eastern Mediterranean Sea. *Progress in Oceanography* **66**, 287-298.

Hecht, A., N. Pinardi, and A.R. Robinson, 1988. Currents, water masses, eddies and jets in the Mediterranean Levantine Basin. *J. Phys. Oceanogr.*, **18**, 1320-1353.

Huthnance, J. M., 1995. Circulation, exchange and water masses at the ocean margin: the role of physical processes at the shelf edge, *Prog. Oceanog.*, **35**, 353-431.

Millot C. and Tauppier I., 2005. Circulation in the Mediterranean Sea. Handbook of Environmental Chemistry, Vol 1 (The Natural Environment and the Biological Cycle), Springer-Verlag Editor, in press.

Nielsen, J. N., 1912. Hydrography of the Mediterranean and adjacent waters. Report of the Danish Oceanographic Expedition 1908-1910 to the Mediterranean and the adjacent waters, **1**, 77-192.

Oren, O.H., 1971. The Atlantic water in the Levant Basin and on the shores of Israel. *Cah. Oceanogr.* **23**, 291-297.

Oren, O.H. and H. Hornug, 1972. Temperatures and salinities off the Israel Mediterranean coast. *State of Israel, Ministry of Agriculture, Sea Fisheries Research Station Bulletin,* **59**, 17-31.

Ovchinnikov, I. M., 1966. Circulation in the surface and intermediate Layers of the Mediterranean. *Oceanology*, **6**, 48-59.

Ozsoy E, 1981. On the atmospheric factors affecting the Levantine Sea. ECMWF Tech. Rep. No. 25, 30 pp.

Ozsoy, E., A. Hecht, U. Unluata, S. Brenner, H.I. Sur, J. Bishop, M.A. Latif, Z. Rosentraub, and T. Oguz, 1993. A synthesis of the Levantine Basin circulation and hydrography, 1985-1990. *Deep-Sea Res. II*, **40**, 1075-1119.

Pinardi, N. and E. Masdetti, 2000. Variability of the large scale general circulation of the Mediterranean Sea from observations and modeling: a review. *Palaeogeography, Palaeoclimatology, Palaeogecology* **158**, 153-173.

Pinardi, N., I. Allen, E. Demirov, et al., 2003. The Mediterranean Ocean Forecasting System: First phase of implementation (1998-2001). *Annal. Geophys.*, **21**, 3-20.

Pinardi, N., Arneri E., Crise A., Ravaioli M., and M., Zavatarelli, 2004. The physical and ecological structure and variability of shelf areas in the Mediterranean Sea, "*The Sea*", Vol. **14**, chapter 32, in press.

The POEM Group, 1992. General circulation of the eastern Mediterranean. *Earth-Sci Rev.*, **32**, 285-309.

Reiter, E. R., 1975. Handbook for the forecasters in the Mediterranean, Environmental Prediction Research Facility, Naval Postgraduate School, Monterey CA, Tech. Pap. No. 5-75, 344 pp.

Robinson, A.R., A. Hecht, N. Pinardi, Y. Bishop, W.G. Leslie, Z. Rosentraub, A.J. Mariano, and S. Brenner, 1987. Small-scale synoptic/mesoscale eddies: The energetic variability of the Eastern Levantine Basin. *Nature,* **327**, 131-134.

Robinson A., Malanotte-Rizzoli P., Hecht A., Michelato A., Roethen W., Theocharis A., Unluata U. pinardi N., and POEM Group. 1992. General circulation of the Eastern Mediterranean. *Earth Sciences Reviews.* 285-309.

Roether, W., Manca, B., Klein, B. Bregant, D., Georgolpoulos, D., Beitzel, V., Kovacevic, V., and A. Lucchetta , 1996. Recent changes in Eastern Mediterranean deep waters. *Science* **271**, 333-335.

Rosentraub, Z. (1990). Study of the circulation on the continental shelf of Israel. Sponsored by the Ministry of Energy and Infrastructure . Publication No. ES-25-90. IOLR Rep. H18/90.

Rosentraub, Z. (1994). Study of the circulation on the continental slope of Israel. Sponsored by the Ministry of Energy and Infrastructure . Publication No. ES-30-94. IOLR Rep. H19/94.

Rosentraub, Z. (1995). Winter currents on the continental shelf of Israel. Dsc Thesis, Technion-Israel Institute of Technology.

Rosentraub, Z. and Gertman, I. (1996). Hydrographic survey to investigate the thermohalin structure and circulation on Israeli continental margin. Final report for year 1996. Ministry of Energy and infrastructure, Rep. ES-65-96, IOLR Rep. H28/96.

Rosentraub, Z., J. Bishop, and Brenner S. (1999). Current measurements in Haifa Bay: Final Rep and summary 17 February 1998-12 May 1999. Submitted to Haifa Port Expansion P Environmental Impact Assessment, Rep. 28. IOLR Rep. H18/99.

Rosentraub, Z. (2000). New current measurements off Tel Aviv-Herzlia coast . Yearly summary Rep. 1999-2000, In: Assessment of marine environmental impacts due to construction of artificial islands. Israel land management administration, Progress Rep. No. 8. IOLR Rep. H34/00.

Rosentraub, Z., Y. Bishop, and S. Brenner (2002). Current measurements off Ashdod Port. Final Rep. : First year of measurements: march 2001-March 2002. IOLR rep. H22/2002, 37 pp.

Schlitzer, R., Roether, W. Oster, H., Junghaus, H.-G., Hausm,ann, M., Johannesen, J., and A. Michelato, 1991. Chlorofluoro methane and oxygen in the Eastern Mediterranean *Deep Sea Research* **38**, 1531-1551.

Stratford, K., and RG., Williams, 1997. A tracer study of the formation, dispersal, and renewal of Levantine Intermediate Water. *Journal of Geophysical Research.* Oceans., Vol. **102**, no C6, 12,539-12,549.

Stratford, K. Williams, RG., and PG., Drakopoulos, 1998. Estimating climatological age from model-derived oxygen-age relationship in the Mediterranean. *Journal of Marine Systems*. Vol. **18**, no. 1-3, 215-226.

Wu, P., and K., Haines, 1996. Modeling the dispersal of Levantine Intermediate Water and its role in Mediterranean deep water formation. *Journal of Geophysical Research* ,**101**, 6591-6607.

Xing J. and A. M. Davies (2002) Influence of shelf topography upon along shelf flow and across shelf exchange in the region of the Ebro Delta. *Continental Shelf Research*, **22**, 1447-1477.

Zodiatis G., Drakopoulos P., Brenner S., and S. Groom. Variability of the Cyprus warm core Eddy during the CYCLOPS project. *Deep-Sea Res.* Part 2: Topical studies in oceanography. Vol. **52**, 2897-2910.

CHAPTER 3

A WINDS, SEA LEVELS AND WAVES CHARACTERISATION OF THE EASTERN MEDITERRANEAN, EMPHASISING THE ISRAELI COAST

by Eng. Dov. S. ROSEN, M. Sc.

3.0 General

The summary of winds, sea levels and waves climate specified below was prepared at the request of the Ministry of Infrastructures. Part of the wave characteristics presented here are based on older measurements, gathered via visual and afterwards wave rider buoy off Ashdod. These were updated in recent years with data from newer and more modern directional wave equipment.

3.1 The wind climate

3.1.1 General

The coast of Israel, is located at the eastern boundary of the Mediterranean. The shore line orientation is generally S-N, with the coast line orientation changing from about 30 degrees azimuth at Ashkelon to 0 degrees at Haifa.

The climate of the region is subtropical, with warm and dry summers and rainy and windy winter seasons. Usually, summer season includes the months May through December, winter season includes the months December through March and months April and November represent short spring and autumn seasons.

3.1.2 The summer season

The average meteorological conditions during summer season are related to the almost permanent low pressure region SE of Cyprus with increasing pressures toward the west (Fig. 1). These conditions are induced by the frequent presence of a "high" center in the eastern Atlantic and a "low" center located in the northwestern India.

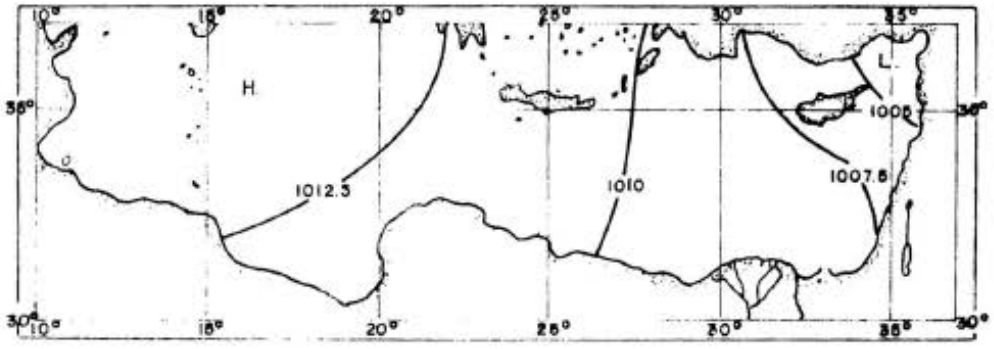

Fig. 1 - Atmospheric pressure at mean sea level
July. (Mediterranean Pilot, Volume V, 1961)

These atmospheric pressure conditions in the summer time induce in the offshore region of the eastern part of the Mediterranean prevailing wind directions from the sector SW to NW (Fig. 2). However, predominant wind directions are from W and NW. During this season another characteristic meteorological phenomenon taking place is the local breeze.

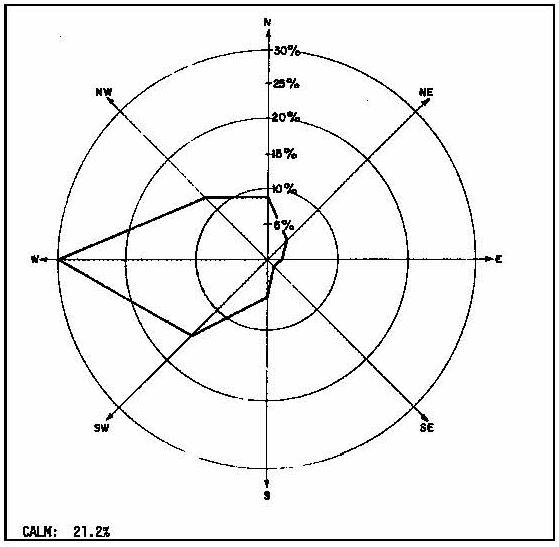

Fig. 2 – Offshore wind frequency, Summer (directional intervals of 45 deg)
(Sea and Swell, U.S. Naval Oceanographic Office)

The breeze is induced by the quicker warming of the land relative to the sea during the day and by the quicker cooling of the land at night relative to the sea. Consequently the wind blows offshore during the night and onshore during the day.
However, due to the added effect of the almost constant barometric depression towards India, the breeze is weaker at night then during the day. The breeze direction usually changes in a clockwise direction from day to night starting in the morning from S-SW, from W at noon, the from N-NW in the afternoon, from E-SE after midnight and finally from S-SE in the early morning hours

3.1.3 The winter season

The weather during the winter season is dominated by cyclones passing in the easterly directions (Fig. 3).

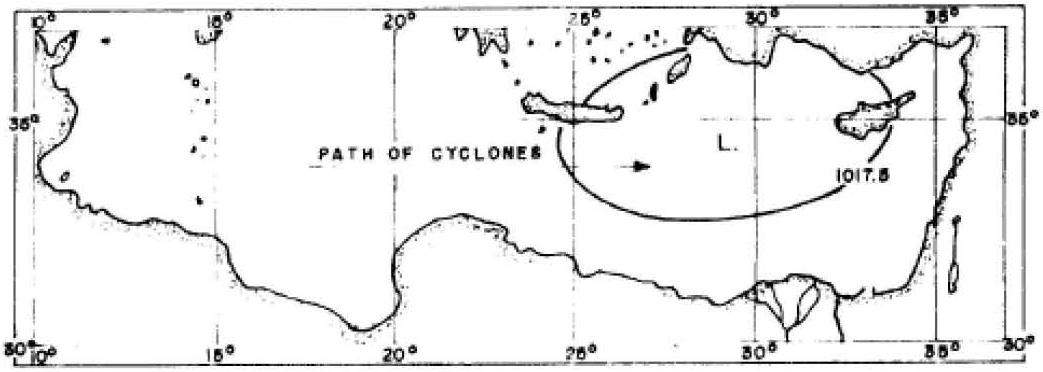

Fig. 3 - Atmospheric pressure at mean sea level, January.
(Mediterranean Pilot, Volume V, 1961)

The passage of cyclones leads to unstable conditions, with prevailing winds occurring from directions between south west and north-east (through north-west). Wind frequencies for the eastern Mediterranean during the winter season are presented in Fig. 4.

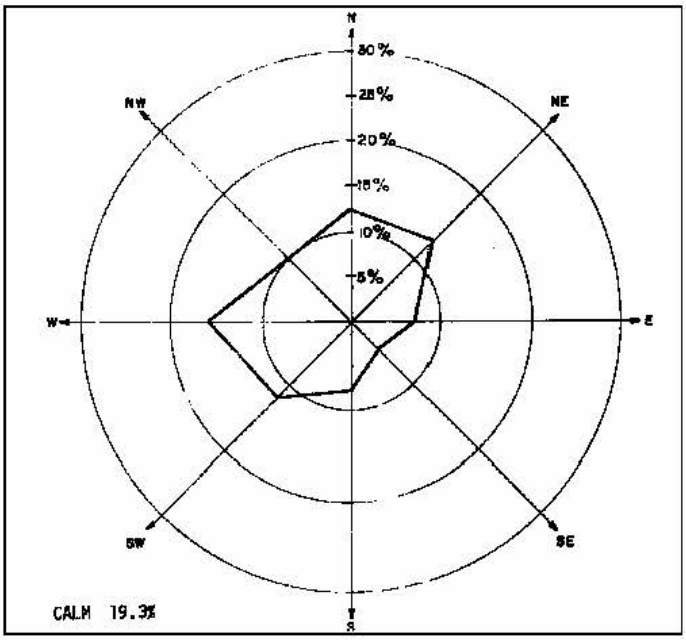

Fig. 4 - Offshore wind frequency, Winter (directional intervals of 45deg)
(Sea and Swell, U.S. Naval Oceanographic Office)

Although the depressions in the Mediterranean are of higher latitudes, they are liable to develop rapidly strong or gale force winds. The cyclones move usually rather slowly, using a few days to travel over the eastern part of the Mediterranean. Sometimes they even remain stationary for a day or two near Cyprus. Such situations result in stationary winds from westerly directions, which may generate high waves on the sea off the coast of Israel. Such a condition occurred on 13th January 1968, when wind speeds of 18 m/sec were measured (See Fig. 5 below)

.

Fig. 5 - Map of isobars over eastern Mediterranean on 13 Jan. 1968

3.1.4 Spring and autumn seasons

Cyclones pass over the region also during spring and autumn. However, the number and intensity of depressions decrease in the spring progressively from winter conditions towards summer conditions, and vice versa in the autumn. The duration of these transitional seasons is

shorter, usually one month (April and November respectively). They are characterized by easterly and south-easterly winds developing from low pressure centers located on the north-eastern part of Africa or in the Sinai peninsula.

3.1.5 Local wind measurements

Winds have been routinely measured by the Israel Meteorological Service (IMS) as well as sometimes by other bodies, such as PRA , Israel Electric Company(IEC), IOLR and the air force. When dealing with winds above sea area, the only IMS available relevant records are from those gathered onshore at Ashdod port and at the Tel-Aviv Dov airport and at Hadera port. Relatively recently, IOLR has been gathering wind data at the GLOSS station number 80 at Hadera, 2.1km offshore. The wind data at Ashdod were processed and reported in yearly reports for the period 1958-1971 by the Coast Study Division of PRA (dislocated since 1985). They were further analyzed for extreme statistics by Rosen and Vajda (1978) in regards to the Hadera offshore terminal construction. Additional wind data were received from the IMS, regarding those available from Tel-Aviv Dov Airport station (on the shore) since 1971. These data were gathered by the Israel Meteorological service at 3 hour intervals. The offshore wind data from the Hadera GLOSS station of IOLR, 2km offshore at 10m above sea-level, are available since 1995. However, the Tel-Aviv data are available only as instantaneous readings taken every 3 hours, because the recorded data were not digitized (and processed) by the IMS due to budget difficulties. This however reduces their reliability, but since they cover such a long period, it was decided to use them and verify their applicability by contrasting them against parallel hourly averaged wind data from Hadera.

The hourly wind data from Hadera and Ashdod, and 3 hourly instantaneous data from Tel-Aviv were statistically processed to result contingency tables of wind speed versus direction as well as yearly stick bar diagrams. The results are summarized below in Table 3-1

Table 3-1 Summary of wind statistics at Israel coast

General Average Year Intensity Distribution:	
Ashdod at shore (1958-1971)	
light winds (less than 10 knots)	**~ 81.4 percent of time**
fresh winds (11 to 21 knots)	**18.3 percent of time**
strong winds (22 to 33 knots)	**1.2 percent of time**
winds above 33 knots	**< 0.1 percent of time**
Ashdod at shore (1992-1995)	
light winds (less than 10 knots)	**~ 84.3 percent of time**
fresh winds (11 to 21 knots)	**~15.3 percent of time**
strong winds (22 to 33 knots)	**0.45 percent of time**
winds above 33 knots	**< 0.1 percent of time**
Tel – Aviv at shore (1971-1997)	
light winds (less than 10 knots)	**~ 79.6 percent of time**
fresh winds (11 to 21 knots)	**~18.9 percent of time**
strong winds (22 to 33 knots)	**0.36 percent of time**
winds above 33 knots	**< 0.1 percent of time**
Hadera offshore (1995-1997)	
Light winds (less than 10 knots)	**~ 69.8 percent of time**
Fresh winds (11 to 21 knots)	**~28.2 percent of time**
Strong winds (22 to 33 knots)	**1.93 percent of time**
Winds above 33 knots	**< 0.1 percent of time**

Table 3-1 Summary of wind statistics at Israel coast - continued

General Average Year Directional Distribution:
Ashdod (1958-1971)
~77% of the **fresh** winds blowed from directions W to N through NW.
~77% of the **strong** winds blowed from directions SW to W trough WSW.
Ashdod (1992-1995)
~52% of the **fresh** winds blow from directions W to N through NW.
~49% of the **strong** winds blow from directions SW to W trough WSW.
Tel-Aviv (1971-1997)
~39% of the **fresh** winds blow from directions W to N through NW.
~47% of the **strong** winds blow from directions SW to W trough WSW.
Hadera offshore (1995-1997)
~30% of the **fresh** winds blow from directions W to N through NW.
~16% of the **strong** winds blow from directions SW to W trough WSW.
General Average Seasonal Distribution based on Ashdod (1958-1971):
~94% of the **strong** winds occur between November and March, and
~60% of the **strong** winds occur in January and February.

Table 3-2 presents the recurrence of high wind velocities as estimated using Weibull distribution:

Table 3-2 Average recurrence of high wind velocities at Israel coast

Average recurrence	**Wind speed (average of 10 highest minutes in 1 hour)**	
once/year	23.6 m/sec	46 knots
once/50 years	31.5 m/sec	61 knots
once/100 years	32.6 m/sec	63 knots

These values are in good agreement with those evaluated by Elbashan (reference 5), who quotes a value of 60 knots for an average recurrence interval of 50 years.
The influence of the winds on the behavior of vessels and on marine structures is partly indirect, through generation of waves and water level set-up, and partly direct (wind loads).

This direct effect is very significant, especially in the case of vessels in ballast loading, causing relatively high dynamic loads due to variation of wind intensity. It practically varies in semi-cycles of about 20 seconds from one gust to another, with gust durations of about 2-3 seconds (Davenport, reference 4). According to Elbashan (reference 5), the average ration between the maximum wind speed, averaged over 1 minute and the upper gust is about 0.81 (when measured in open field, 10 m above ground).

The ration between maximum wind speed averaged over the 10 highest minutes and the maximum wind speed averaged over the highest 1 minute is about 0.84. Therefore, the ratio between the maximum wind speed averaged over the 10 highest minutes of 1 hour and the wind speed of the upper gust is about 0.68. Combining these values with the recurrence of high winds quoted previously, it can be estimated, that wind velocities corresponding to the upper gust may be expected to be those presented in Table 3-3 below:

Table 3-3 Average recurrence of extreme wind gust velocities at Israel coast

Average recurrence	**Upper gust wind speed**	
once/year	34.7 m/sec	67 knots
once/50 years	46.3 m/sec	90 knots
once/100 years	47.9 m/sec	93 knots

These compare fairly well to a gust speed of 86 knots estimated by Elbashan for a 50 years average recurrence.

3.2 Sea levels climate

The tidal (astronomic) range on the Mediterranean coast of Israel is characteristic of the low-tide range of the Eastern-Mediterranean basin, being induced by the combined effect of the attraction forces of the moon and of the sun, and by the location of this area on the globe.

Analyses of the local constituent contributions conducted by the author have shown however that the latter are only of very minor importance, and thus the Ashdod, Jaffa, Hadera and Haifa sea-levels are in general very similar (see Figures 2, 3 and 4). The tide usually varies between 0.40m during spring tides (occurring in spring and autumn), and 0.15m during neap tides (occurring in winter and summer). The tide contribution exhibits the usual semi-diurnal periodicity (twice a day highs and lows) and fortnight (14 days) periodicity.

Extreme sea levels may occur in combination with extreme meteorological conditions. However these may differ from site to site along the coast of Israel. During spring and particularly in November – December months, offshore directed easterly winds occurring at Haifa, lower sea-levels in Haifa port and bay area, while that effect is not detected at other locations further south along the Israeli coast.

Low sea-levels occur in winter during February-March months, while high sea-levels occur in August-September, with a second maximum in December. The high levels are coincident to the warm and cold seasons (steric effect of water volume change due to temperature).

According to the results of Blank (1998) at Ashdod (1958-1984 period), the MLW is 6.5 cm below the ILSD, while the MSL is 8.1 cm above ILSD and MHW is 23.2 cm above ILSD.

According to McCarthy et al. (2001) the assessed average global sea-level rise due to global warming induced by the so called "greenhouse effect", for year 2025 is between 3 and 14cm, for 2050 between 5 and 35 cm and for 2100 between 9 and 88 cm, for a business as usual scenario.

However, it is agreed by the professional bodies involved with this assessment that regional sea-level rise can differ from the above depending to the location on the globe. A regional change may significantly differ from the above assessment due to local plate tectonic movements, land rebound due to groundwater withdrawal, etc. As the warming is expected to accelerate only in the next century, the signs of sea-level rise are presently difficult to detect, being masked by other factors like seasonal warming and cooling of the sea-water (steric effect), wind induced sea-level rise during storms (wind surge), wave induced sea-level set-up in the surf zone, atmospheric loading by passing high and low atmospheric systems. Nevertheless, the importance of continuous long-term sea-level monitoring is obvious for using as reference regarding long-term sea-level changes.

The daily mean sea levels at Ashdod port, at the Mediterranean coast of Israel and the corresponding maximum deep water significant heights above 4m (during 1968-1971) are shown below in Fig. 6, to indicate the possible relationship between extreme sea levels and high sea states.

Although it was not possible to found a definite correlation, it has been concluded that extreme wave heights are associated with increased sea levels and that low sea levels are associated with moderate wave heights.

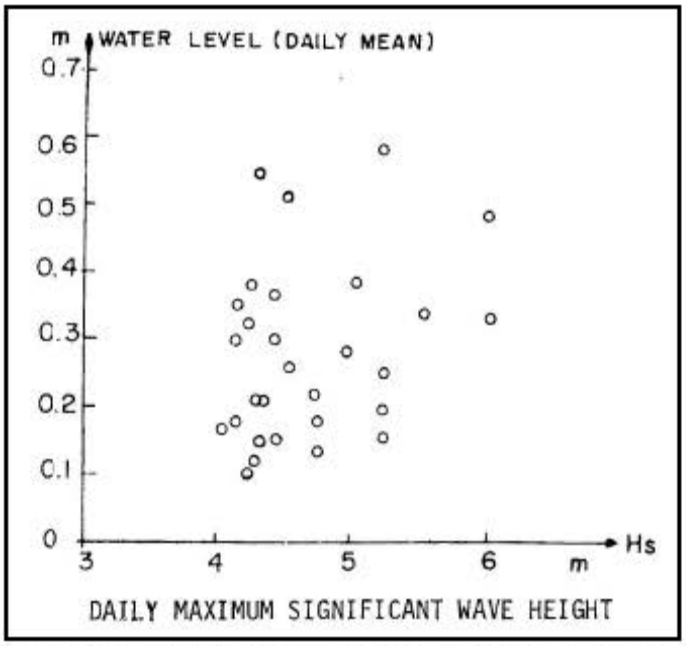

Fig. 6 Relationship between sea levels and high waves offshore Israel coast

Extreme sea levels may occur in combination with extreme meteorological conditions. Based on 30 years of data, the following average return periods presented in Table 3-4 were assessed:

Table 3-4 Average recurrence of extreme wind gust velocities at Israel coast

Average Return Period	Low Sea Level	High Sea Level
[years]	[m]	[m]
1	-0.38	0.64
50	-0.74	1.04
100	-0.87	1.10

The above values do not include the expected sea-level rise due to the "greenhouse effect", for which the assessed values for 2100, range between 0.1 m and 0.9 m. This value is a world wide average rise, while the relative regional value may differ significantly due to additional various factors, such as plate tectonics. Sea level measurements carried out at Hadera GLOSS station since 1992 as well as satellite altimetry measurements of the sea level indicate that the sea levels in the Eastern Mediterranean rose at a rate of about 1cm/year in the last 13 years, while a lowering has been measured in the Ionian sea. These changes seem to be due not only to the global warming effect but also due to fluctuations in the formation and circulation of the deep Levantine water between the Adriatic and the Aegean (see chapter 2) during this period.

Figure 7 taken from Fenoglio-Marc (2001) shows the sea level rate of change in the mentioned period over the Mediterranean and Figure 8 shows the sea level changes measured at the Hadera GLOSS station since 1992. The meteorological contribution to the sea-level has been recently assessed for the last 40 years in the Mediterranean within the HIPOCAS project (Gomis et al, 2005) and is shown in Figure 9.

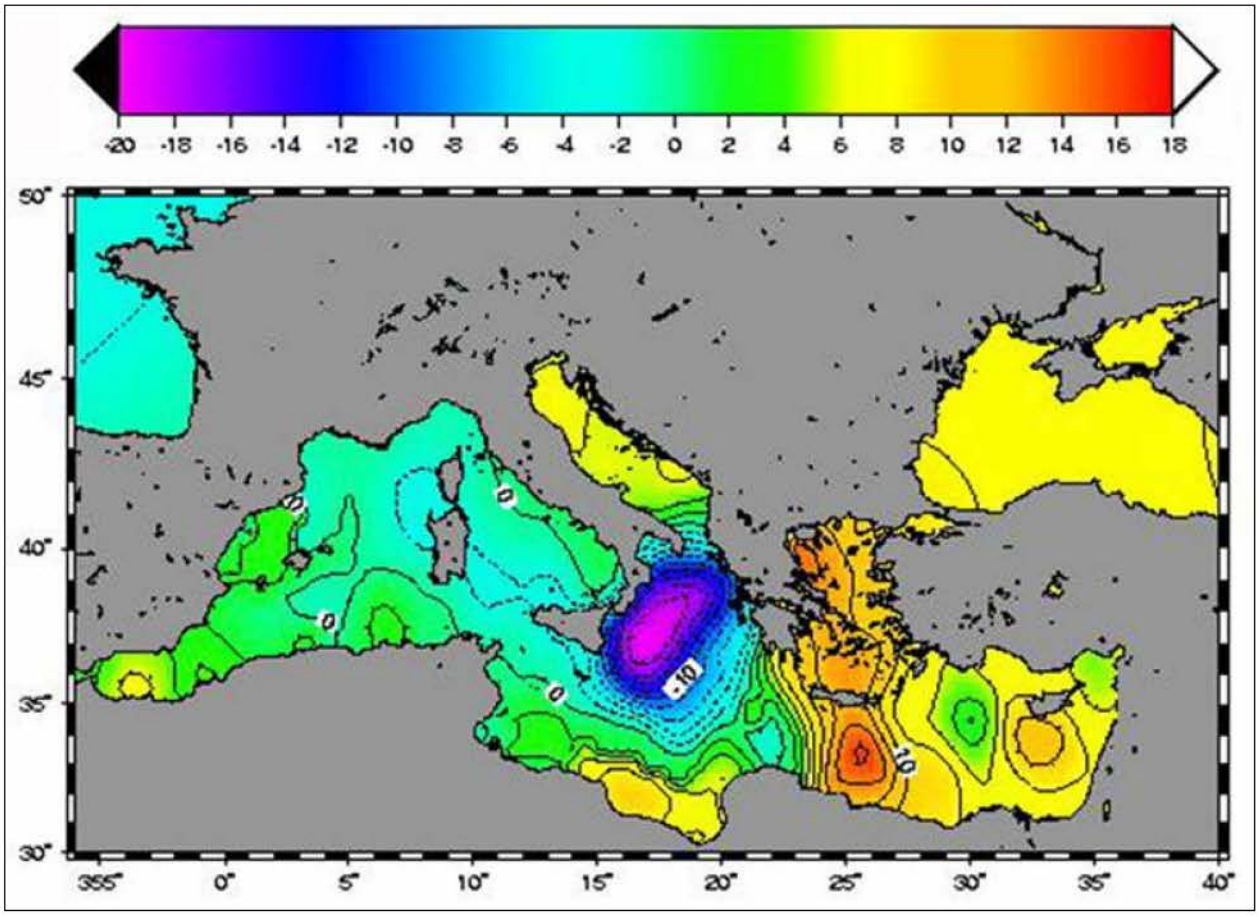

Figure 7 –Sea level changes 1992-2000 based on Topex-Poseidon satellite altimetry (from Fenoglio-Marc, 2001)

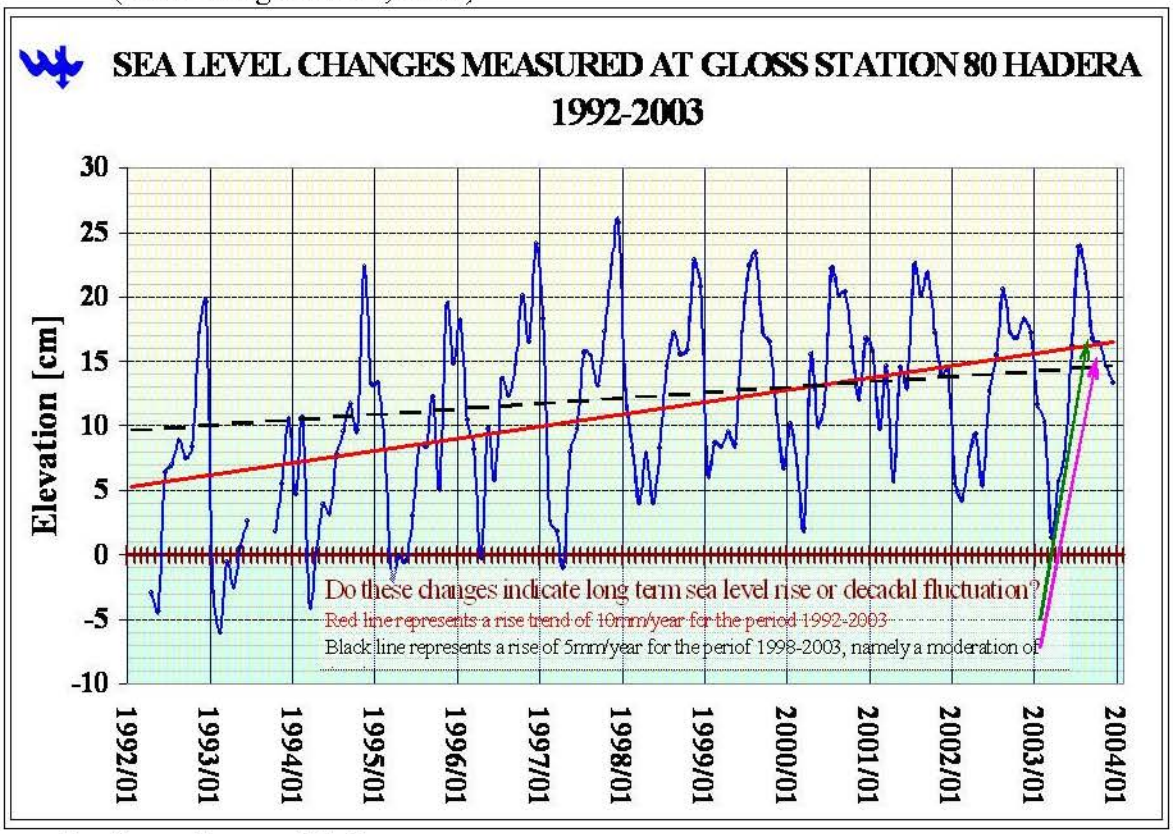

Figure 8 – (from Rosen, 2004)

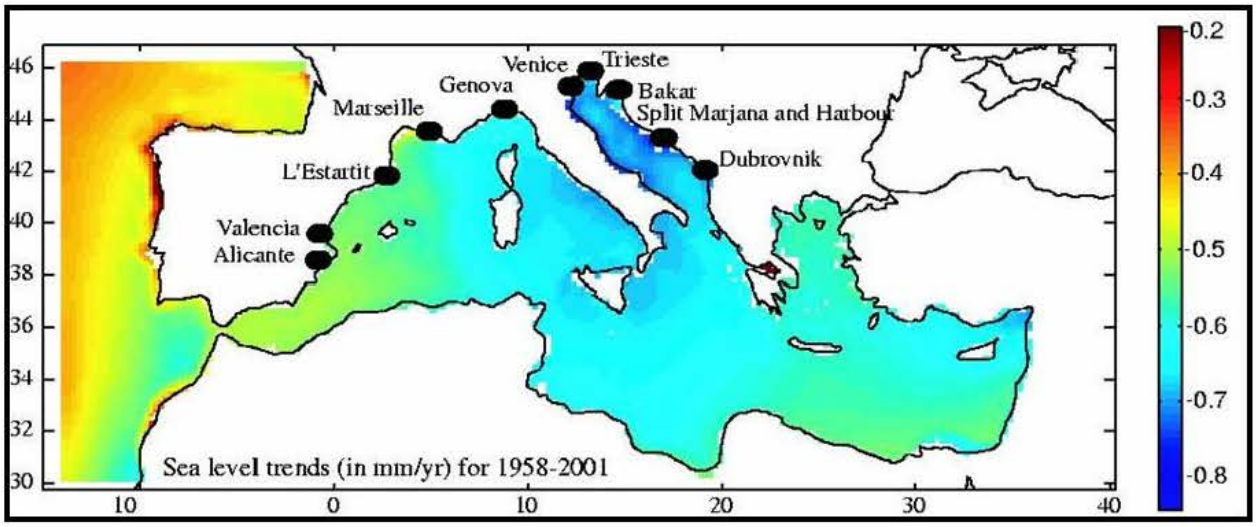

Figure 9 - Local sea level trends caused by variations in the atmospheric forcing for the period 1958 – 2001 (Gomis et al., 2005)

3.3. The wave climate

3.3.1 Wave seasons

The characteristics of the deep water wave climate of the Mediterranean coast of Israel allows to divide the year in four seasons with distinct different climates. The division follows the above described way to characterize the weather seasons, namely:

a. winter season ranging from December through March (4months)

b. spring season ranging over April (1 month)

c. summer season ranging from May through October "(6 months)

d. autumn season ranging over November (1 months)

For a multi-yearly division however, we decided that the most correct division is not according to the Gregorian year but to a meteo-marine year, starting in April and ending in March of the following year. By this, the winter is not split in two years whereas the meteo-marine conditions may be dependent in the short time range.

Alternatively, the year may also be divided in only two wave seasons with a transitional type beginning and end. In such a case the following division is obtained

a) extended winter season ranging from mid November through mid April (5 months);
b) extended-summer season ranging from mid April through mid November (7 months).

3.3.2 The winter season

In this season the wave climate is characterized by alternating periods of high sea states (storms) and low sea states (calms). The storms are in general induced by cyclones passing slowly over the Mediterranean from West to East.

The strongest storms usually occur in the period between mid December through the first week of March. Lower sea states occur at the beginning and at the end of that season. The prevailing wave direction is WNW, but the predominant wave direction is W, corresponding to the longest wind fetch.

3.3.3 The summer season

During this season the wave climate is characterised by relatively calm seas with waves induced by the weak local winds (mainly by the breeze). Therefore, the waves are usually of "sea" type, whose direction usually varies during the day in a clockwise direction from WSW in the early morning to WNW at noon and to N-NW in the afternoon.

The change of direction is induced by the breeze, which also affects the wave heights (onshore winds are stronger than offshore winds).

The prevailing wave direction is WNW (perpendicular to the shoreline). The predominant wave direction is variable:

WNW in May and June, W in July and August, WNW in September and October. The highest summer waves occur usually by the end of July through mid August. The sea is most calm in May, June and October.

3.3.4 The spring and the autumn seasons

These wave climate seasons are characterized by a transition from the winter climate to the summer climate (in April) and back to winter climate (in November). The prevailing directions during these transitional seasons is also WNW, but the predominant direction is W.

3.3.6 Short term distribution of the waves

Instrumental wave measurements consisting of 20 minutes records taken at 3 hours intervals were separately statistically analysed, to find highest waves, average wave heights and average wave periods. Power spectra estimates were obtained by means of spectral analyses using fast Fourier transforms (FFT) for each wave record having the significant height larger than 1 m. The results obtained for the period April 1979 - March 1980 were reported by Kit et al (reference 8). The following main results were obtained:

a) A good correlation has been found between the various theoretical wave height parameters and the Rayleigh distribution, confirming that this distribution is also applicable to wave heights at the Israeli coast.

b) The shape of spectra, derived from actual wave measurements differed considerably from any smooth theoretical curve. The variability of wave spectra, obtained even for a single storm showed, that it is necessary to measure and analyse waves for a long period in order to adequately determine wave characteristics and predominant spectral shapes at a certain location.

   The spectral shapes of the wave records were more similar to the average JONSWAP spectrum than to the Pierson-Moscovitz spectrum. A considerable number of spectra contained two or even three peaks.

c) The following relations were found to give fairly good approximations to the characteristics of wave spectra at the Mediterranean coast of Israel:

$H_{max} = 1.61\ H_{mo}$ (20 minutes record !)

$T_p = 1.21\ T_z$

$H_{mo} = 4\sigma = 1.56\ \overline{H}$

$T_{max} = T_{1/3} = 1.15\ T_z$

$T_p = 1.05\ T_{1/3}$

Where:

H_{mo} = characteristic wave height ; $\overline{H}$ = average wave height

H_{max} = maximum wave height in a wave record

T_z = average zero down crossing wave period; T_p = peak period ;

$T_{1/3}$ = significant wave period; σ = root mean square i.e. square root of the variance

3.3.7 Long term distribution of the waves

The analyses of waves measured at 3 stations on the Mediterranean coast of Israel lead to the results presented in **Table 3-5**.

Table 3-5 Deep water significant wave height statistics at the Mediterranean coast of Israel

Average Year Deep Water Characteristic Wave Height Distribution (Ashdod 1958-1975):	
low sea states (less than 1 m)	50.0 percent of time
moderate sea states (between 1 m and 2 m)	25.0 percent of time
strong sea states (between 2 m and 4 m)	20.0 percent of time
high sea states (above 4 m)	5.0 percent of time
Average Year Deep Water Characteristic Wave Height Distribution (Ashdod 1992-1998):	
low sea states (less than 1 m)	50.0 percent of time
moderate sea states (between 1 m and 2 m)	25.0 percent of time
strong sea states (between 2 m and 4 m)	20.0 percent of time
high sea states (above 4 m)	5.0 percent of time
Average Year Deep Water Characteristic Wave Height Distribution (Hadera 1992-1998):	
low sea states (less than 1 m)	~76.4 percent of time
moderate sea states (between 1 m and 2 m)	17.3 percent of time
strong sea states (between 2 m and 4 m)	~5.6 percent of time
high sea states (above 4 m)	~0.6 percent of time
Average Year Deep Water Characteristic Wave Height Distribution (Haifa 1994-1998):	
low sea states (less than 1 m)	~70.9 percent of time
moderate sea states (between 1 m and 2 m)	22.1 percent of time
strong sea states (between 2 m and 4 m)	~6.4 percent of time
high sea states (above 4 m)	~0.9 percent of time

During moderately high sea-states (up to about 6m characteristic height at Ashdod) there is a uniform growth in deepwater wave height from Ashdod to Haifa, due to increased fetches and the masking effect of the Libyan and Egyptian coasts to certain wave directional wave components (see Figure No.1).

Average Year Directional Wave Distribution:
All moderate and higher sea states come from WSW to NNW through W
66% of all waves approach from W trough WNW directions.
The highest sea states approach from W direction, but storm development occurs by veering from WSW to NW through W directions.

A major element of the directional climate in the study sector is the fact that the wave directions in deep water are not identical, but usually a shift in the wave direction occurs, with waves becoming more westerly towards the northern end of the coastal sector. The difference between Ashdod, located just 10 km south of the study area, and Hadera, located some 15 km north of the study area can be about 10 degrees, while at Haifa, some 50 km north to Hadera it may reach 15 to 17 degrees.

Peak Wave Periods:
Peak wave periods range between 3 and 15 seconds. During high sea states they range usually between 10 and 13 seconds, and very high sea states have peak periods between 12 and 15 seconds.

Table 3-6 Average Yearly Number of Storms and Their Average Duration

Sea State of the Storm Crossing the Specified Level

Sea State Exceeded Hmo>=	Average No. of Storms	Average Duration of the Sea State per Storm	Standard Deviation of the Storm Duration
[m]	[-]	[hours]	[hours]
0.5	79.34	90.5	127.31
1.0	59.63	39.7	44.15
1.5	33.56	35.2	35.33
2.0	24.90	29.2	29.26
3.0	9.90	24.4	20.00
4.0	5.10	16.2	13.43
5.0	1.25	12.2	9.40
6.0	0.25	5.3	4.76

Sea State of Storm Crossing Specified Level & one 1 m Higher

Sea State Exceeded Hmo>=	Average No. of Storms	Average Duration of the Sea State per Storm	Standard Deviation of the Storm Duration
[m]	[-]	[hours]	[hours]
1.0	19.69	78.35	44.29
1.5	12.50	62.77	37.26
2.0	8.94	54.36	30.49
3.0	4.44	39.90	19.22
4.0	1.25	31.99	9.78
5.0	0.25	23.65	12.36

Sea State of Storm Crossing Specified Level & one 2 m Higher

Sea State Exceeded Hmo>=	Average No. of Storms	Average Duration of the Sea State per Storm	Standard Deviation of the Storm Duration
[m]	[-]	[hours]	[hours]
1.0	7.94	100.88	51.18
1.5	5.63	79.64	41.04
2.0	4.19	70.28	32.61
3.0	1.19	54.38	20.26
4.0	0.25	40.00	14.59

Sea State of Storm Crossing Specified Level & one 3 m Higher

Sea State Exceeded Hmo>=	Average No. of Storms	Average Duration of the Sea State per Storm	Standard Deviation of the Storm Duration
[m]	[-]	[hours]	[hours]
1.0	3.94	119.70	108.77
1.5	2.50	96.91	48.13
2.0	1.19	80.84	28.68
3.0	0.25	68.10	32.83

The joint probability distribution of deep water significant waves and peak periods has been analysed by Rosen and Kit (1981) and it is presented for visual and for instrumental measurements in Figure 10 a and b below.

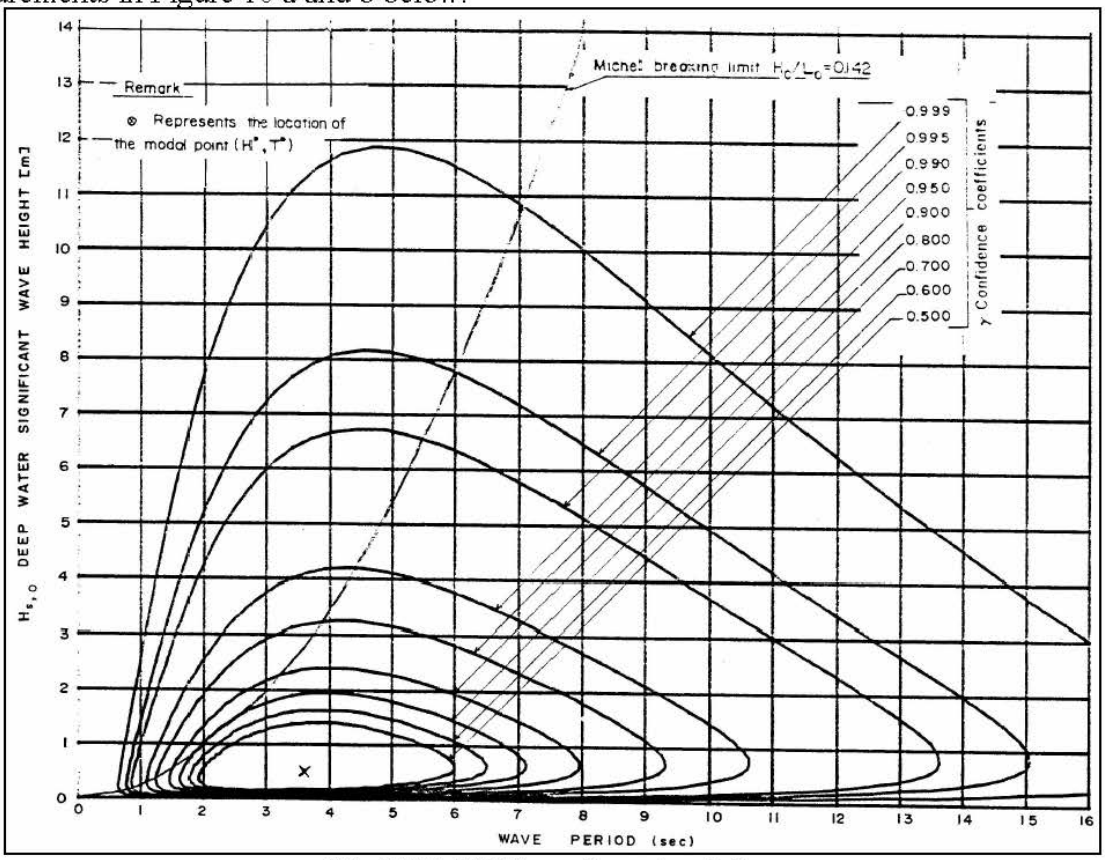

(a) 1957-1980 based on visual data

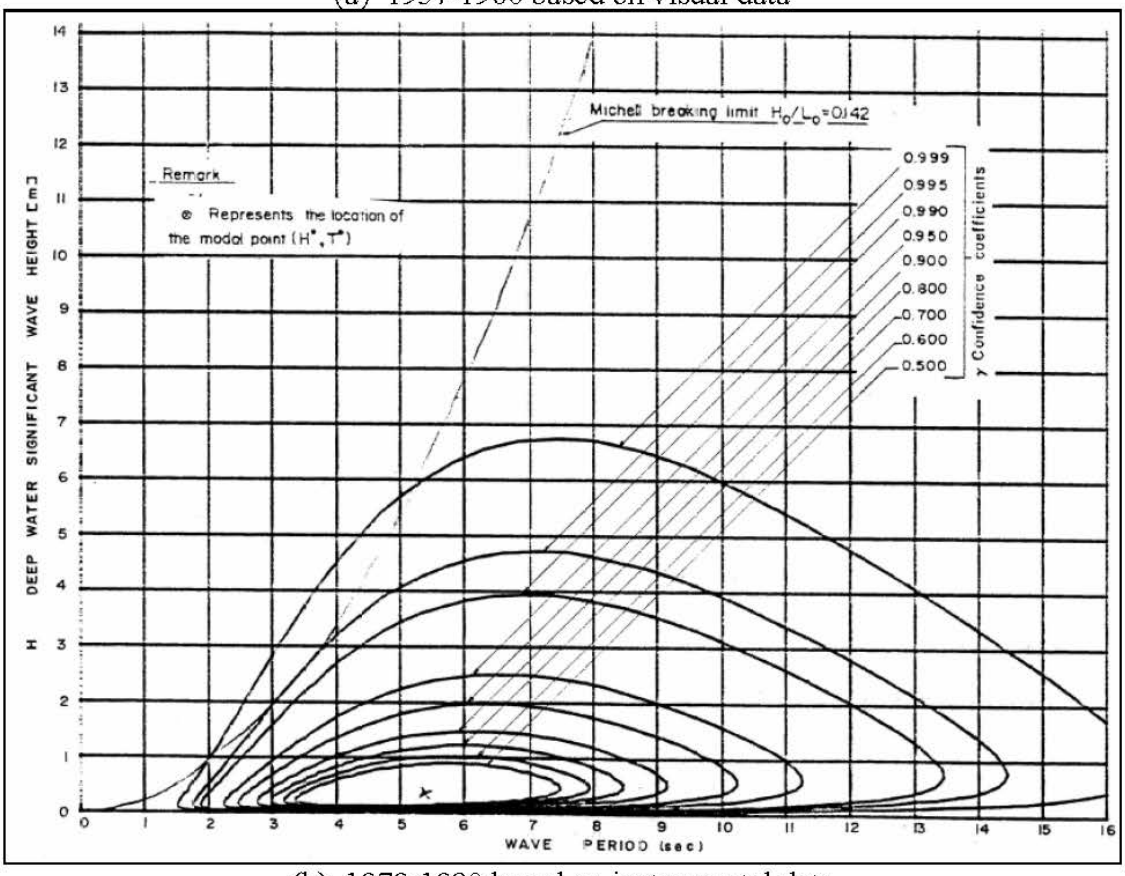

(b) 1979-1980 based on instrumental data

Figure 10 – Domains of significant wave heights and peak wave periods for various confidence coefficients (from Rosen and Kit, 1981).

3.3.8 Extreme distribution of the waves

Extreme Sea States and Average Return Periods are presented in Table 3-7 below:

Table 3-7 Recurrence of extreme deep water significant wave heights at Israel coast

Average Return Period [years]	Deep Water Characteristic Wave Height [meters]
2	5.15
4	5.95
5	6.15
6	6.25
8	6.60
10	6.80
15	7.15
20	7.40
50	8.20
100	8.70
500	10.15

Estimated extreme relationship between maximum and characteristic wave height in a given sea-state:

$$H_{\max} = 2 \cdot H_{m_o}$$

The design deep water significant wave height versus encounter risk and economical lifetime of a marine structure/project is given in Table 3-8. It should be pointed out that for structures located in transient water depths or in shallow water, the deep water wave statistics may not be appropriate and the transient or shallow location wave statistics must be determined via proper wave refraction and diffraction computations and true bathymetry.

Table 3-8 Design deep water significant wave height versus encounter risk and economical lifetime of the marine structure/project

Risk to Encounter Design Wave	Economical Life Time of Structure (years)						
[percentages]	2	4	6	8	10	15	20
	Average Return Period to be Used						
1	200	398	597	796	995	--	--
5	39	78	117	156	195	293	390
10	19	38	57	76	95	143	190
20	10	18	27	36	45	68	90
50	4	6	9	12	15	22	29
64	2	4	6	8	10	15	20

3.3.9 Wave induced currents

These currents prevail and are predominant within the surf zone. Longshore currents are induced by waves approaching obliquely to the contour lines, and flow parallel to the shore line. Rip currents are generated by perpendicular waves or edge waves, and flow from the shore offshore, almost perpendicular to shore line to a distance of up to about 3 times the surf zone width, within which they decay completely. The former may attain during storms speeds of 4 knots and even more, The latter may also attain 1 to 2 knots, but also in calmer sea states. During extreme sea states, some nearshore structures which are normally outside the surf zone may be within or at the edge of the surf zone developing under such states. Under such conditions, longshore currents of 4 knots or more may be encountered.

3.4 Long term statistics of winds and waves and in the eastern Mediterranean

The long term wind and wave statistics in the Mediterranean basin (including the Levantine basin) have been determined in the past by Bales et al. (1981). The statistics for the Levantine basin are reproduced in figures B0 to B9 and B31-1 to B31-5 in the following pages.

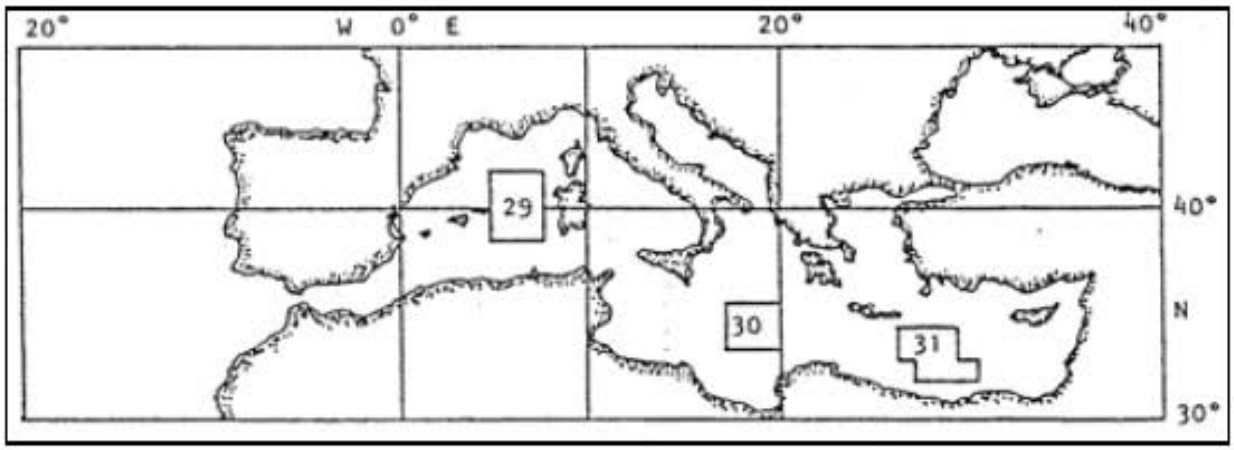

Fig. B0 – Definition of Representative Areas in the Mediterranean

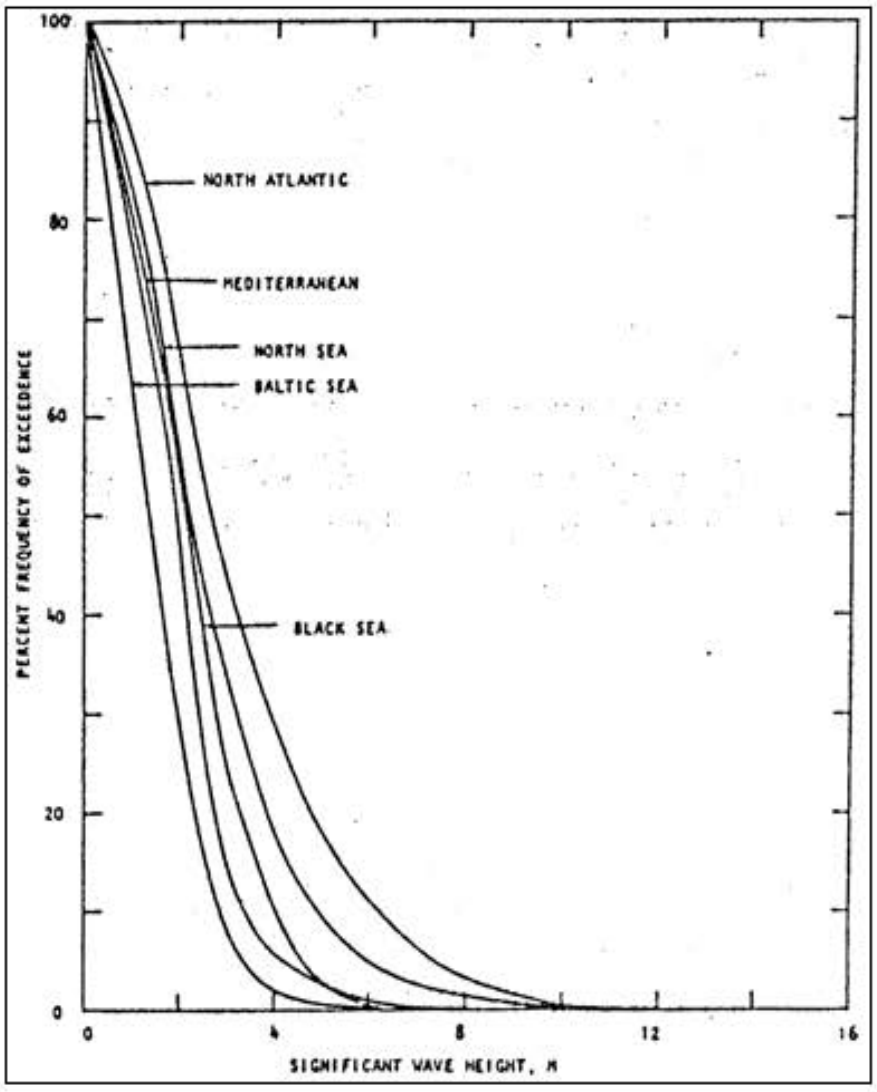

Fig. B1a – Comparison of worst season wave height exceedences at all world locations

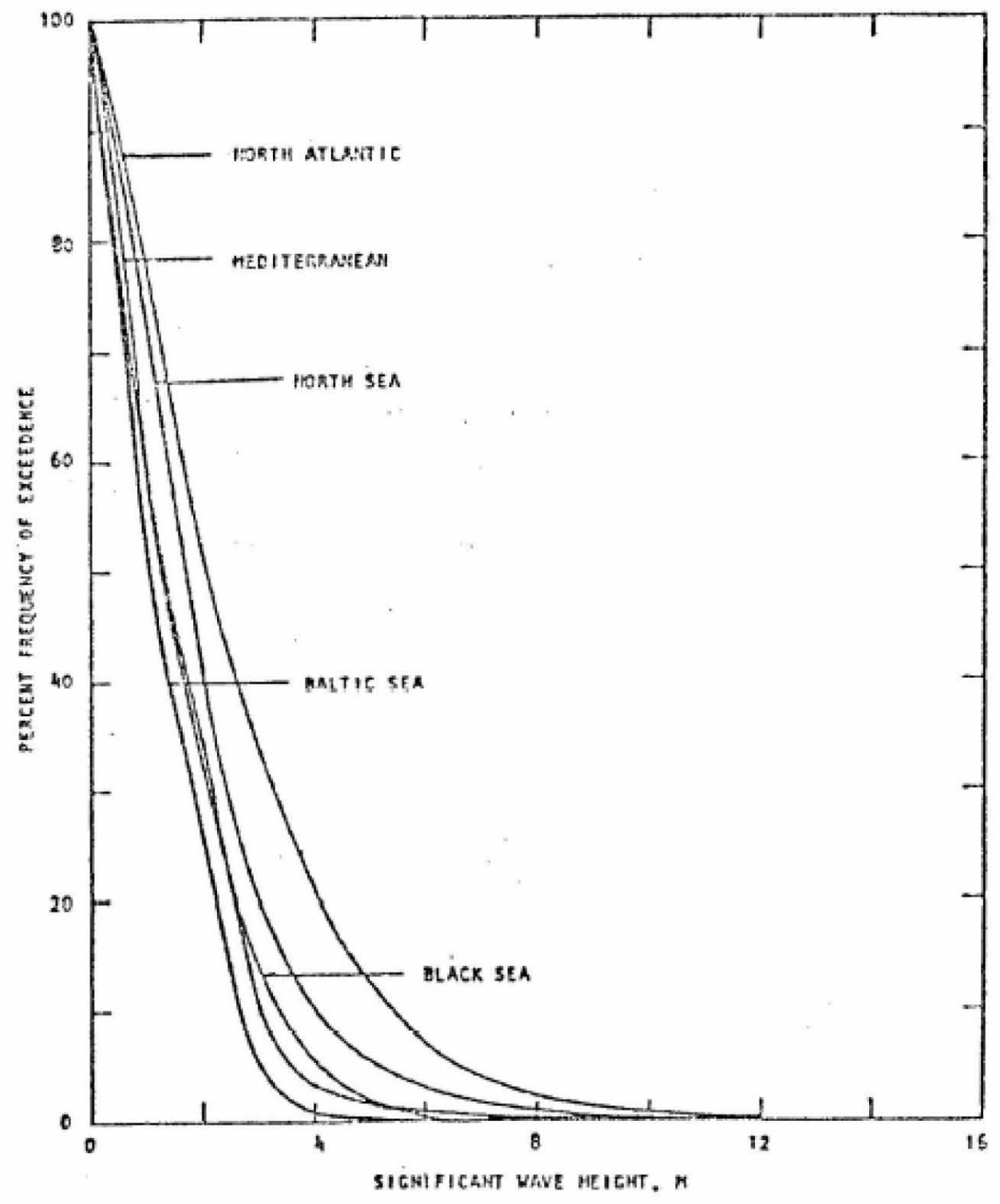

Fig. B1b – Comparison of annual deep water significant wave height exceedences at all locations

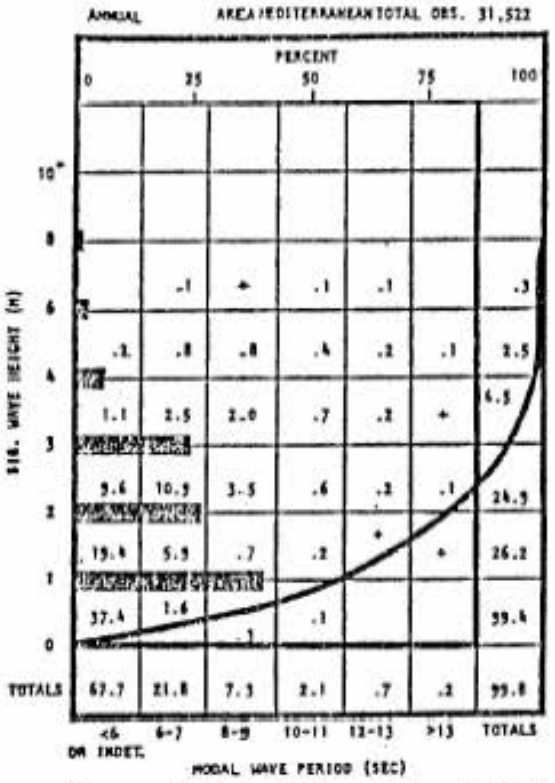

Figure B-2 Significant Wave Height by Modal Wave Period

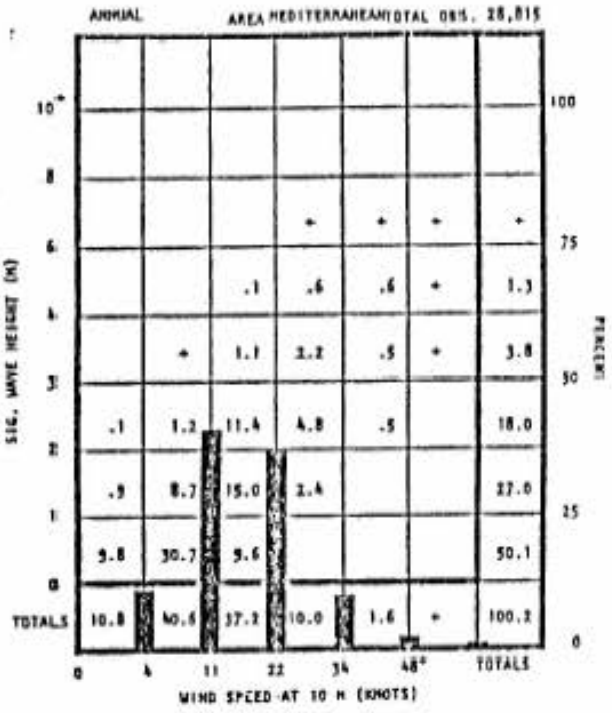

Figure B-3 Significant Wave Height by Wind Speed

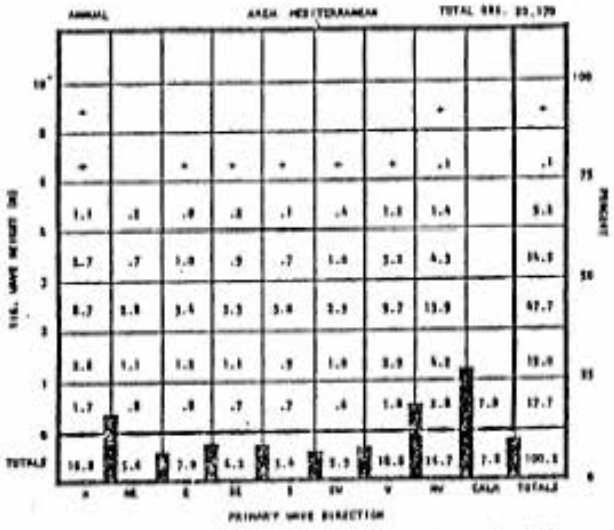

Figure B-4 Significant Wave Height by Wave Direction

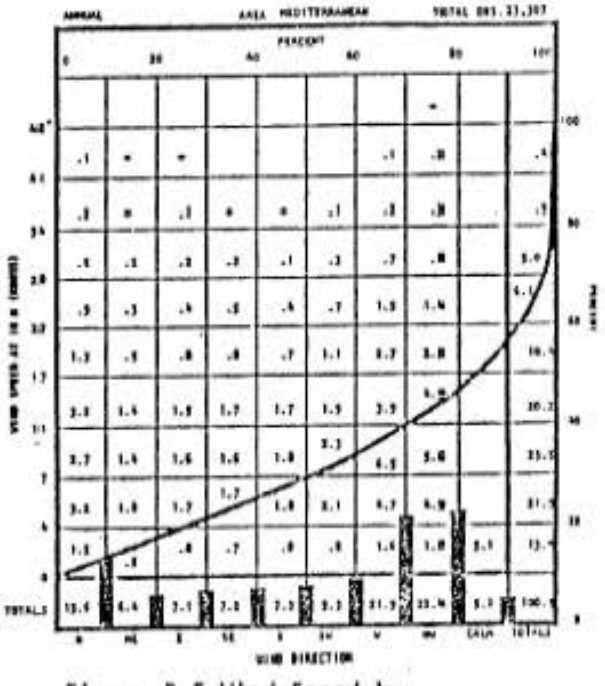

Figure B-5 Wind Speed by Wind Direction

ALL MEDITERRANEAN

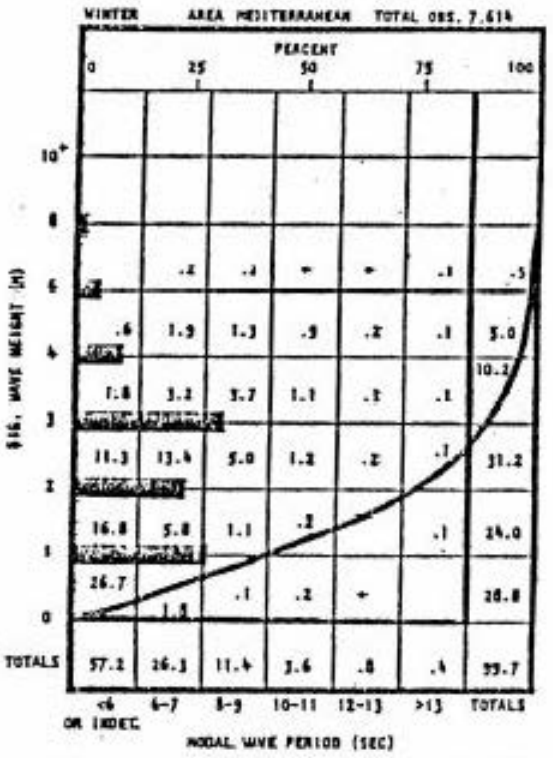

Figure B-6 Significant Wave Height by Modal Wave Period

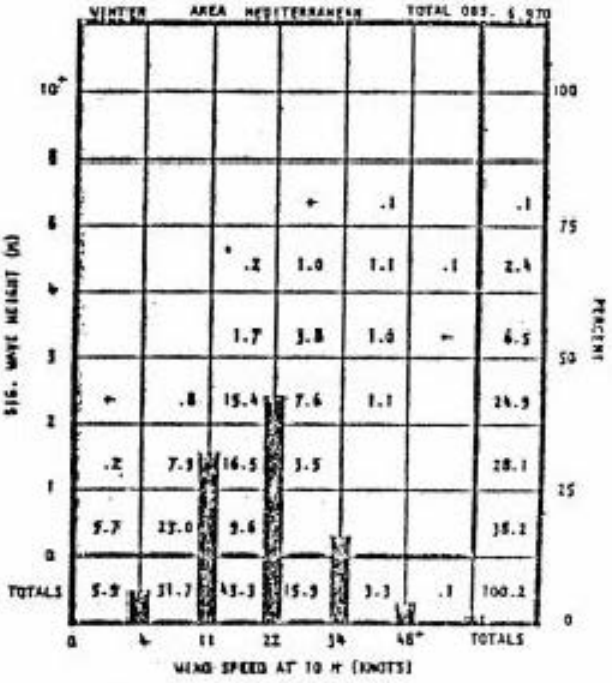

Figure B-7 Significant Wave Height by Wind Speed

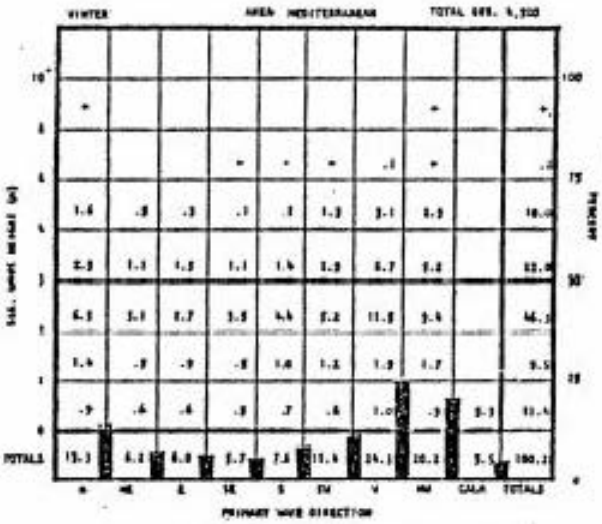

Figure B-8 Significant Wave Height by Wave Direction

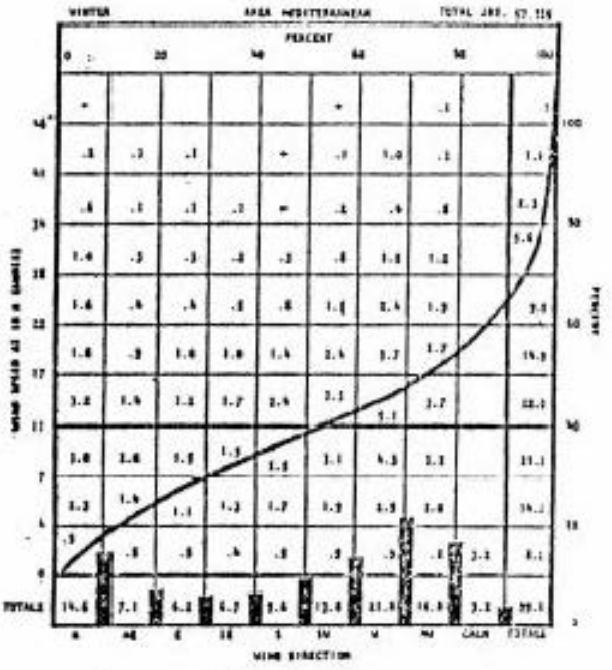

Figure B-9 Wind Speed by Wind Direction

ALL MEDITERRANNEAN

TABLE B-31-1-1 - SURFACE NATURAL ENVIRONMENT SUMMARY

Season: Annual; Location: Eastern Mediterranean Sea, 32° - 34° N, 29.5° - 30.5° E

Natural Environment	Minimum (5 Percentile)	Median (50 Percentile)	Maximum (95 Percentile)	Mean	Most Probable
Sea Surface					
Sig. Wave Height, m.	.5	2	3.5	1.5	1.5
Wave Period, sec	2.5	5	9	5	5
Direction	-	-	-	-	W - NW
Winds					
Speed, knots	2	11	25	12	11
Corresponding Mean Sig. Wave Height, m.	.5	1.5	3	1.5	1.5
Direction	-	-	-	-	W - NW
Visibility, nautical miles	7	15	25	13	15
Cloud Cover					
Total clouds, in eighths of sky obscured	1	2	8	2.5	1
Low clouds, in eighths of sky obscured	Nil	1.5	7	2	Nil
Precipitation (Occurrence)	All precipitation = 2.8% of the time				
Relative Humidity, %	59	75	95	75.5	75
Air Temperature, °C	12.5	20	27	20	-
Surface Water Temperature, °C	18.5	20.5	22.5	-	-
Sea Level Pressure, millibars	1,007	1,016	1,023	1,016	1,014
Ice	None				
Refractivity					
Mean Surface Refractivity	-	-	-	319	-
Sub-Refraction (1 km, Annual)	-	-	-	-	15% of the time
Super-Refraction or Ducting (1 km, Annual)	-	-	-	-	2% of the time

EASTERN MEDITERRANEAN

Figure B10 – Table B31-1-Eastern Mediterranean surface natural environment summary

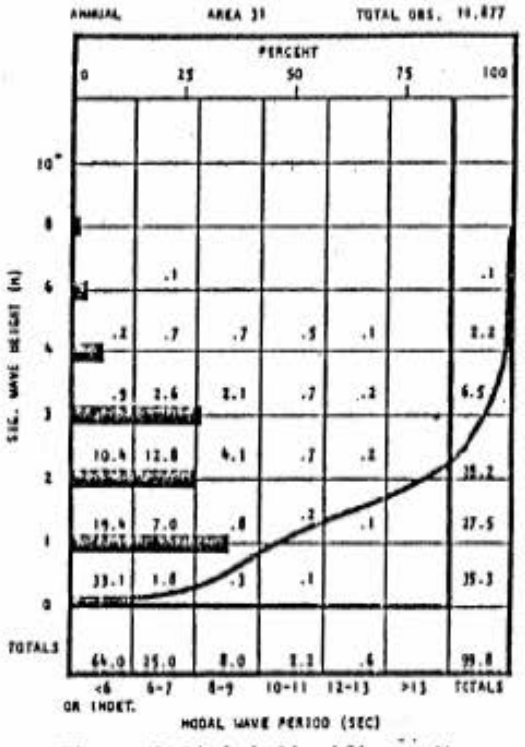

Figure B-31-1-1 Significant Wave Height by Modal Wave Period

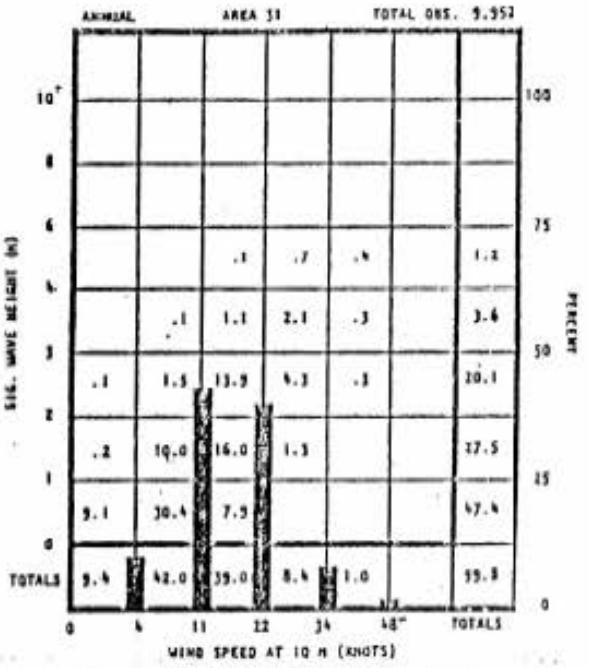

Figure B-31-1-2 Significant Wave Height by Wind Speed

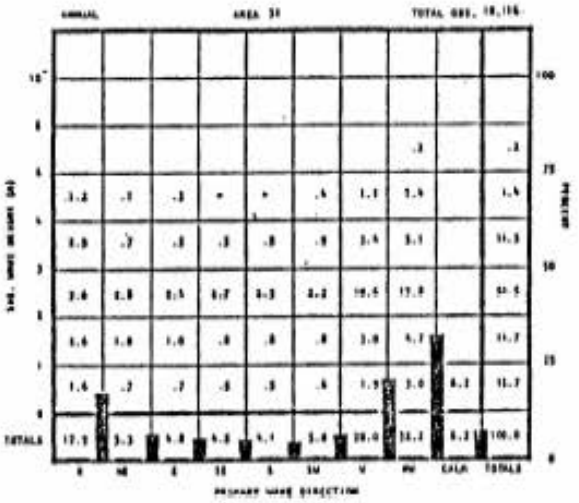

Figure B-31-1-3 Significant Wave Height by Wave Direction

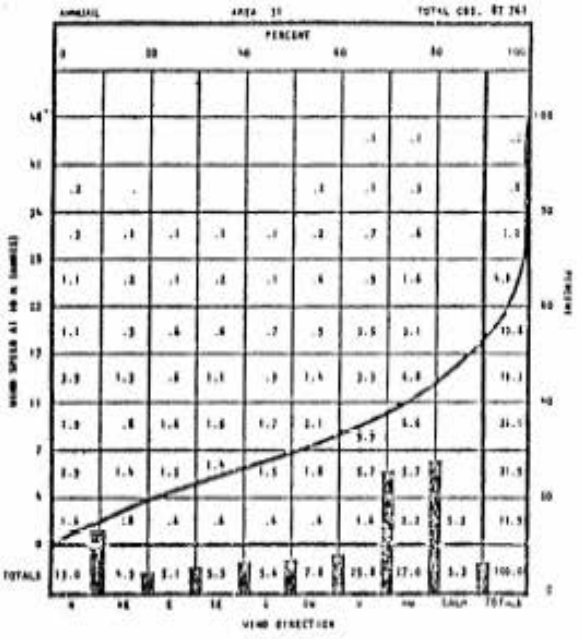

Figure B-31-1-4 Wind Speed by Wind Direction

EASTERN MEDITERRANEAN

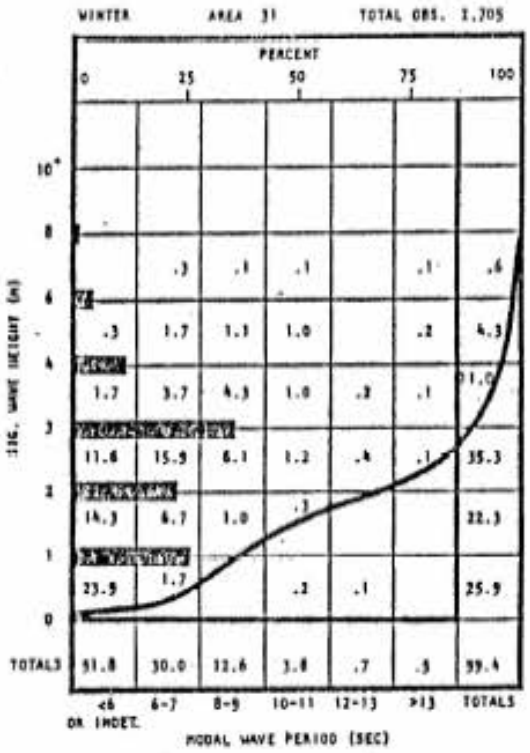

Figure B-31-2-1 Significant Wave Height by Modal Wave Period

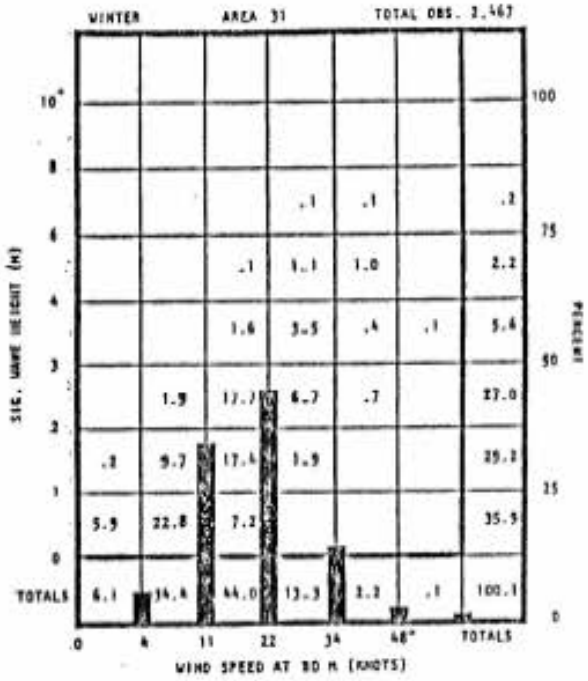

Figure B-31-2-2 Significant Wave Height by Wind Speed

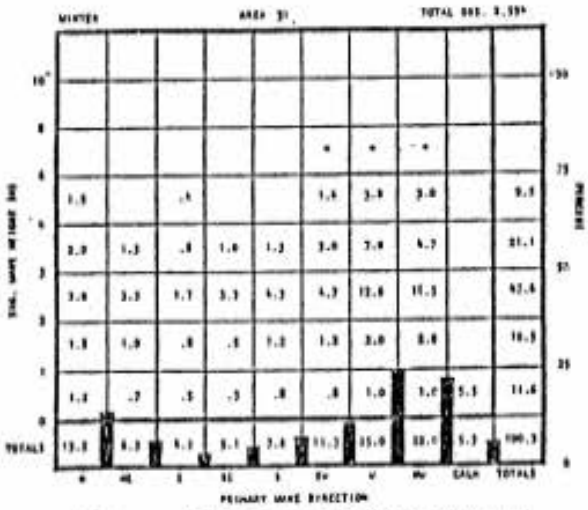

Figure B-31-2-3 Significant Wave Height by Wave Direction

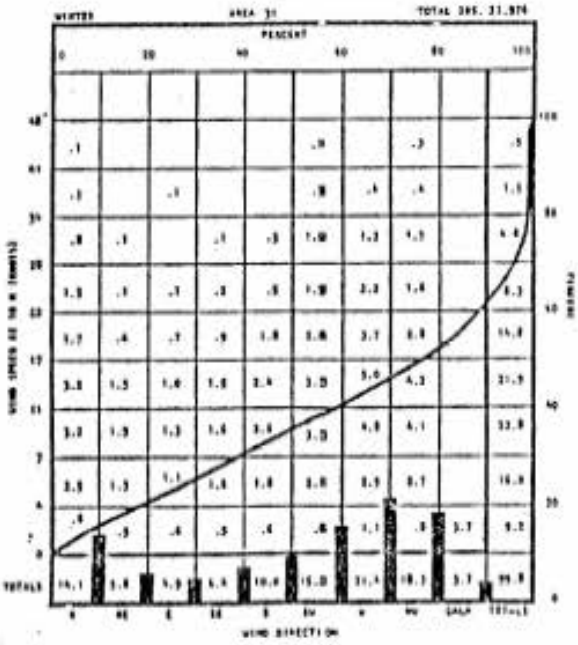

Figure B-31-2-4 Wind Speed by Wind Direction

EASTERN MEDITERRANEAN

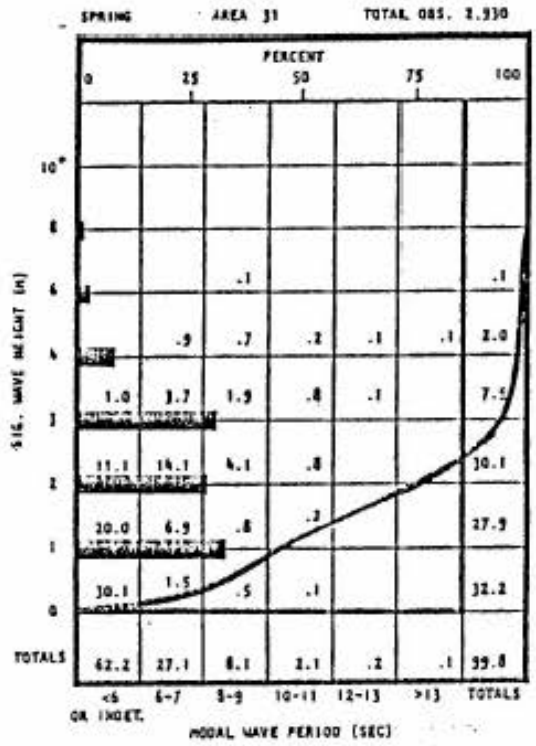

Figure B-31-3-1 Significant Wave Height by Modal Wave Period

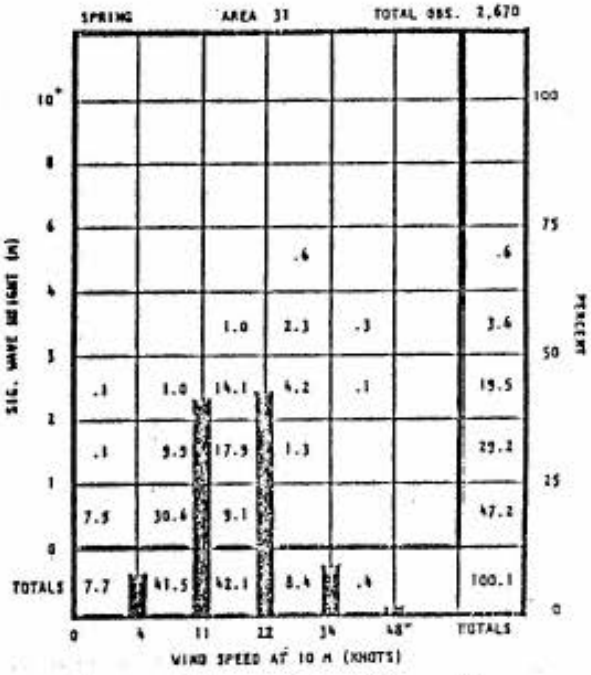

Figure B-31-3-2 Significant Wave Height by Wind Speed

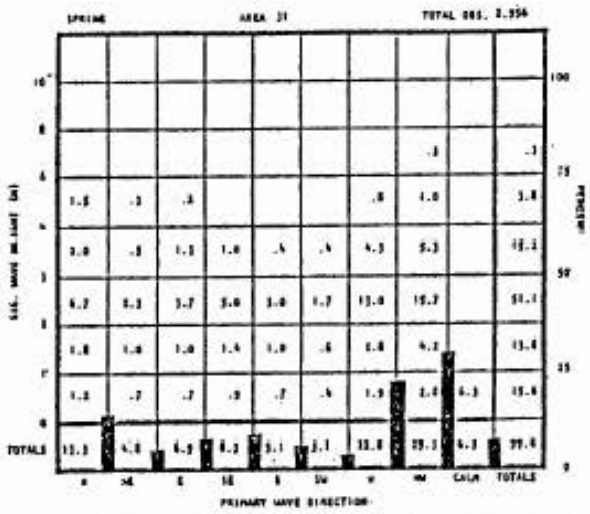

Figure B-31-3-3 Significant Wave Height by Wave Direction

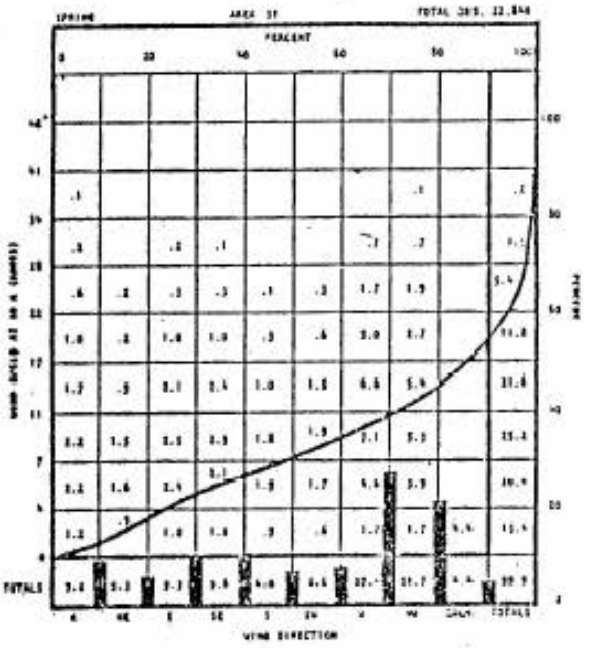

Figure B-31-3-4 Wind Speed by Wind Direction

EASTERN MEDITERRANEAN

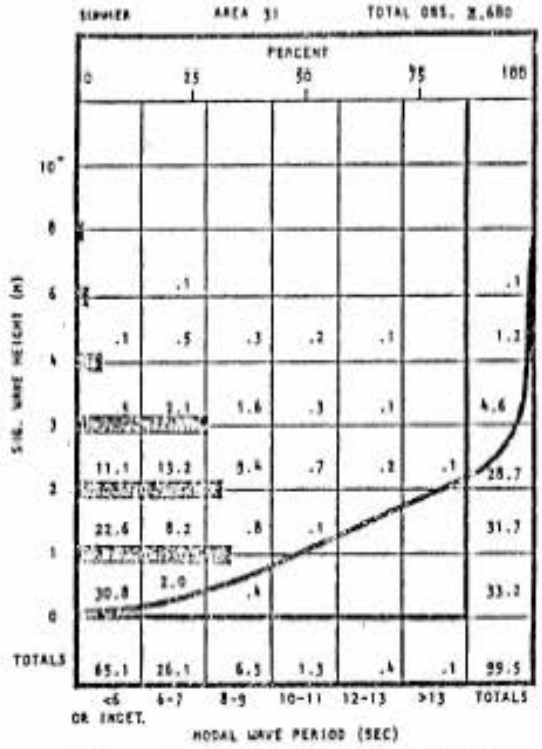

Figure B-31-4-1 Significant Wave Height by Modal Wave Period

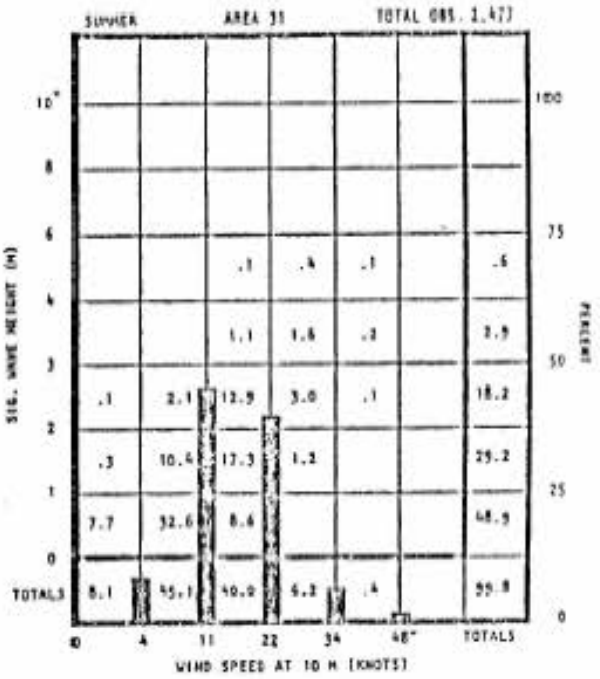

Figure B-31-4-2 Significant Wave Height by Wind Speed

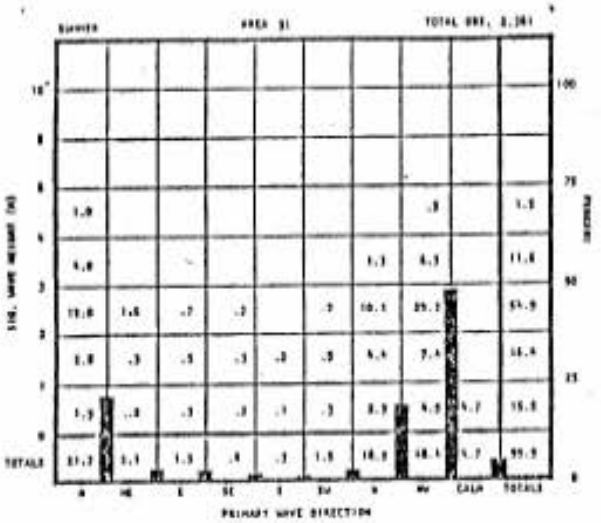

Figure B-31-4-3 Significant Wave Height by Wave Direction

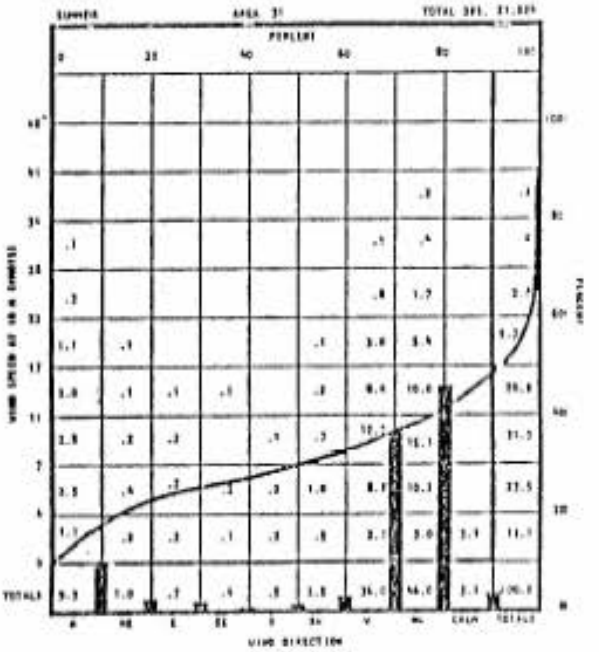

Figure B-31-4-4 Wind Speed Wind Direction

EASTERN MEDITERRANEAN

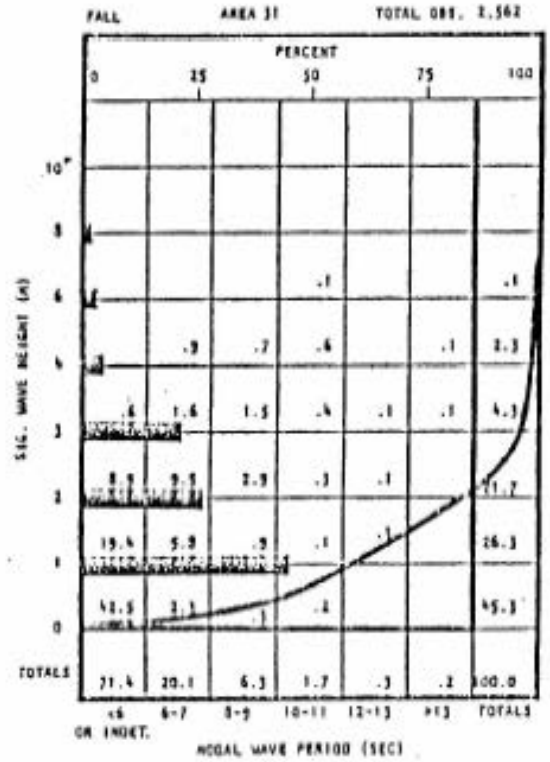

Figure B-31-5-1 Significant Wave Height by Modal Wave Period

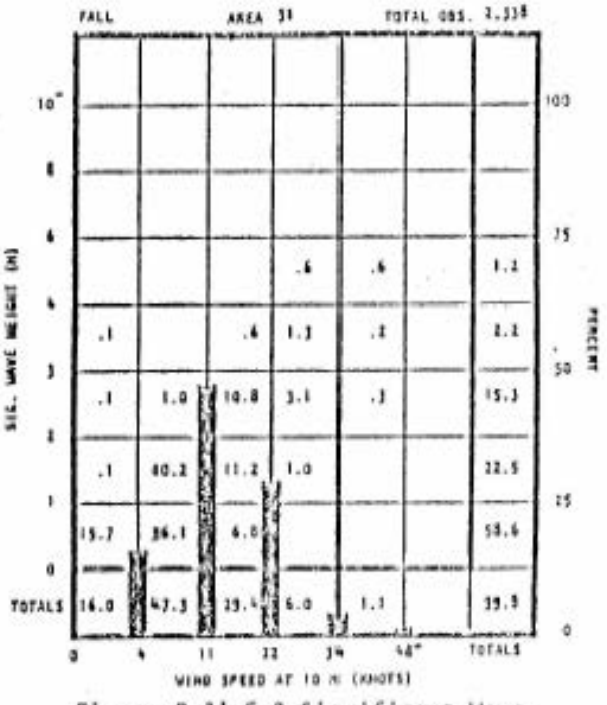

Figure B-31-5-2 Significant Wave Height by Wind Speed

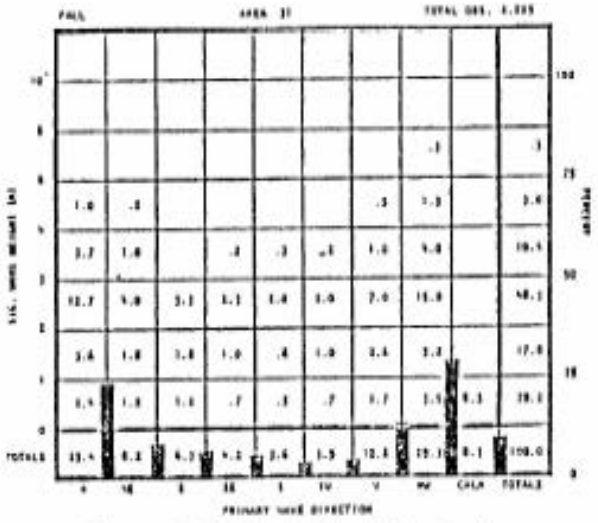

Figure B-31-5-3 Significant Wave Height by Wave Direction

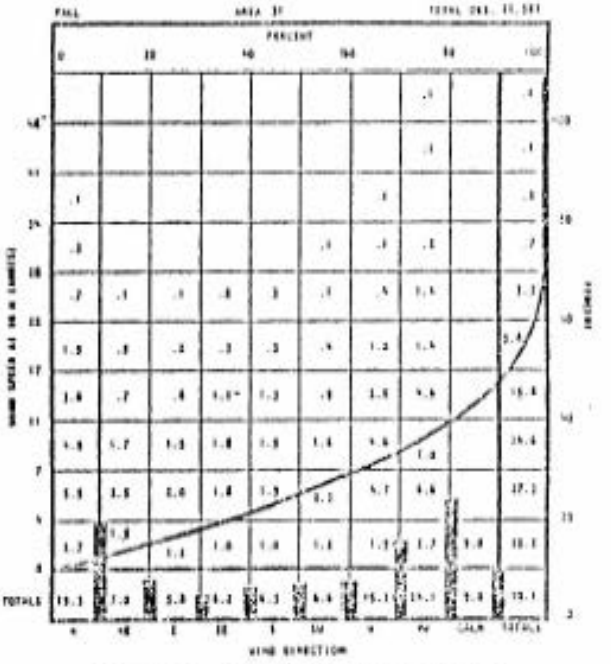

Figure B-31-5-4 Wind Speed by Wind Direction

EASTERN MEDITERRANEAN

3.5. References of Chapter 3

1. Bales S., Lee T.W., Voelker J.M., (1981), "Standardized Wave and Wind Environments for NATO Operational Area", U.S. Dept. of Commerce, David Taylor Naval Ship R&D Center, Bethesda rep. AD/A-105 414.
2. Goldsmith V., Sofer S., (1983), "Wave Climatology of the Southeastern Mediterranean", Israel Journal of Earth-Sciences, Vol.. 32, pp 1-51.
3. Blanc Y. and Rosen D.S., (1998), "An epoch analysis of the sea-level fluctuations at the Mediterranean coast of Israel and the astronomical and environmental contributions to it", Abstr. 10th Symposium on the Study of the Mediterranean Shelf of Israel, Haifa, June1998.
4. Gomis D., M.N. Tsimplis, B. Martín-Míguez, A.W. Ratsimandresy, J. García-Lafuente, S.A. Josey, (2005), Mediterranean Sea level and barotropic flow through the Strait of Gibraltar for the period 1958-2001 and since 1659, Abst. ESEAS-RI Workshop on Sea Level Variations Towards an Operational European Sea Level Service, Split, Croatia, 5-6 October 2005.
5. Fenoglio–Marc L., (2001), Analysis and representation of regional sea–level variability from altimetry and atmospheric-oceanic data, Geoph. Journal International, Vol. 145, pp.1-18.
6. Komar P.D., and Gaughan M.N., (1972), "Airy Wave Theory and Breaker Height Prediction", 13th Intl.. Coastal Engrng. Conf., A.S.C.E., New York, pp 405-418.
7. McCarthy J.J., Canziani O.F., Leary N.A., Dokken D.J., and White K.S., Ed. (2001), "Climate Change 2001, Impacts, Adaptation, and Vulnerability", IPCC TAR Working Group II, Cambridge Univ. Press.
8. Rosen, D. S., Kit E., (1981), "Evaluation of the Wave Characteristics at the Mediterranean Coast of Israel", Israel Journal of Earth-Sciences, Vol. 30, pp 120-134.
9. Rosen D.S., 1998, Assessment of the marine environmental impacts due to the construction of artificial islands on the coast of Israel, Characterisation of the meteoceanographic climate in the study sector, Progress report No.4, , I.O.L.R. Report No. H16/98, Haifa, May 1998.
10. Rosen D.S., (2004), Assessment of the impact due to sea level rise and wave climate change on the state of the Israeli beaches, in view of the monitoring activities performed by Israel Oceanographic & Limnological Research in Israel and abroad, Beaches 2004, Yearly Journal of the Israel Society for the Protection of Nature, June 2004, 6p, (in Hebrew)
11. Rosen D.S., Rosentraub Z., Raskin L., (2005), Bridging research for assessing the feasibility of constructing artificial islands, Measurements, processing and analysis of wave and current measurements off Tel-Baruch in the period 10/2002-01/2004, assessment of the wave climate at the central part of Israel by collecting, processing and analysis of wave data from Haifa, Hadera, Ashdod and Ashkelon for the period 04/2002-03/2004, IOLR report H23/2005, Haifa, May 2005 (in Hebrew).
12. Veritech Inc. and U.S. Army Corps of Engineers, Coastal Engineering Research Center, (2004), "Coastal Engineering Manual, Professional Edition", Ver.2, Vicksburg, U.S.A.
13. Vik.I., Houmb G., (1976), "Wave Statistics at Utsira with Special Reference to Duration and Frequency of Storms" Div. of Port and Ocean Engrg., Trondheim Univ., Norway.

CHAPTER 4

ENVIRONMENTAL EVALUATION OF THE LEVANTINE BASIN

by Prof. Bella Galil and Prof. Barak Herut

Source: **Herut B.** and Galil B. (2000), Environmental evaluation of the marine system along the coast of Israel (SE Mediterranean). Chapter 17, in: *Seas at the Millennium: an Environmental Evaluation* (C. Sheppard, ed.). Elsevier, England, 253-265.

4.0 Abstract

The Levantine Basin occupies the easternmost Mediterranean, east of the line connecting Rhodes and the coast of Cyrenaica. It is isolated from the deep Atlantic waters by the topographical and hydrological barriers posed by the shallow Gibraltar Straits and the Siculo-Tunisian sill. The Levantine deep water mass is distinguished by salinity and temperature values that are higher than in the rest of the Mediterranean ($T < 13.8^{o}C$, $S < 38.74$, below 700 m). The Levantine Basin is ultra-oligotrophic: Chlorophyll-a concentrations are as low as 0.4 $\mu g\ l^{-1}$ nearshore, and decrease offshore to 0.05 $\mu g\ l^{-1}$. The completion of the high dam at Aswan in the mid 1960's deprived the Levant of its influx of freshwater, nutrients and sediments, contributing to the diminishing sediment transport and negatively impacting fisheries. The opening of the Suez Canal in 1864, that linked the Red Sea with the Mediterranean, allowed hundreds of Erythrean species to settle along the Levantine coasts. Some abundant invaders are exploited commercially, others constitute a nuisance or economic burden, and yet others outcompete native species. However, the meager number and extent of the faunal explorations prompted Fredj and Laubier (1985), in their review on the deep Mediterranean benthos, to declare that " the southern part of the Levant Sea have practically never been studied".

The rapid increase in population density along the Israeli coastal plain in past half-century and its consequent urbanization generated land reclamation schemes. Sand mining in the past and the existing marine structures along the coast have depleted sand reserves and increased coastal erosion.

Effluents, such as sewage, agricultural run-off or industrial wastes may locally increase nutrient loading, most notably in Haifa Bay and in some lower reaches of the coastal streams. In such nutrient-enhanced sites, appropriate ambient physical conditions may cause the development of toxic algal blooms. Yet, overall, levels of toxic contaminants are low, but for Haifa Bay with its concentration of heavy industries.

Protective measures and monitoring activities are implemented by several legislative/administrative systems, evacuating and abating land-base pollution sources. A

modified National Plan for the Israeli Mediterranean coast, including 14 marine reserves, is in the process of affirmation and should provide a tool for an integrated sustainable coastal zone management.

4.1 Locale

The easternmost Mediterranean, from Rhodes to Cyreneica, is the Levant basin (Fig. 1).

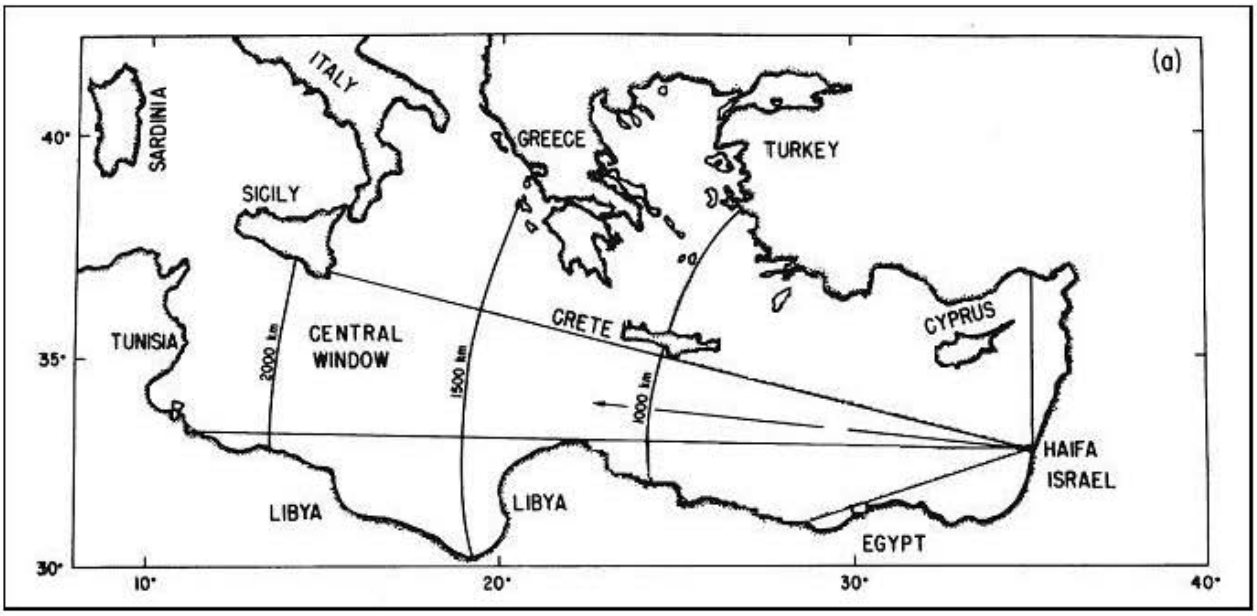

Fig. 1: Map of the East Mediterranean Basin. The fetch distances facing the Mediterranean coast of Israel are included (reprinted from Carmel et al., 1985).

The Israeli coast, at the southeastern corner of the basin, describes a slightly curved line, 180 kms long, with Haifa Bay the sole embayment (Fig. 2). The shelf narrows gradually toward the North, extending to a distance of 10-20 km from the coast (Fig. 2). Haifa, about 11 km long and 6 km wide at its southern end, is bordered in the west by three submerged sandstone ridges parallel to the coast. South of the bay the Israeli littoral is mostly sandy, with isolated sandstone outcrops. North of the bay, rocky shores predominate (Emery and Neev, 1960), but only in few places a continuous rocky substrate from the upper to the sublittoral zone is present and the occurrence of vermetid reefs is rarer still (Safriel, 1966).

Thirteen streams (Fig. 3) traverse the coastal plain, of which two, the Kishon and Naaman, flow into Haifa Bay.

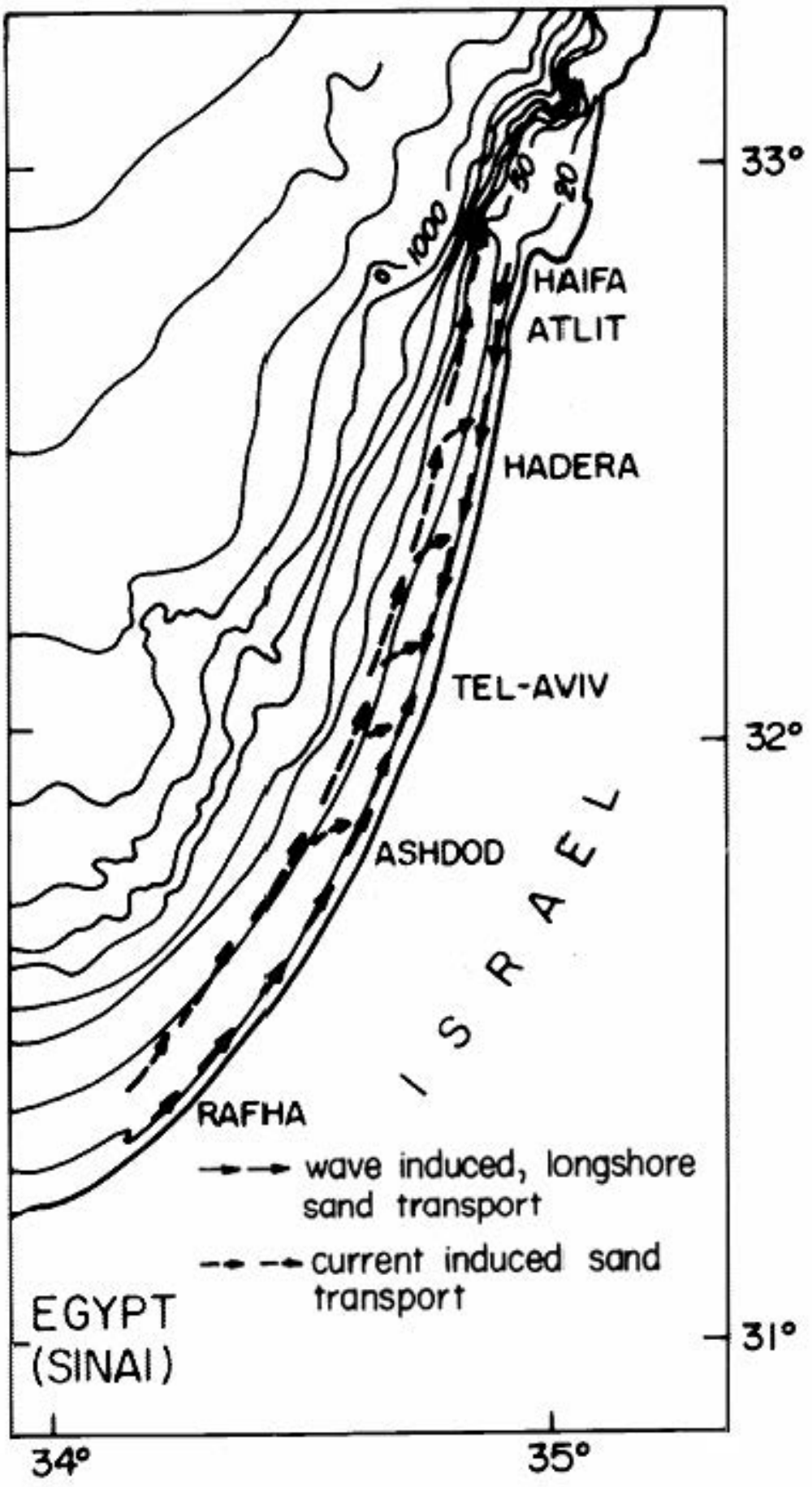

Fig. 2: Bathymetric map of the shelf off the Israeli coastline, including the sediment transport pattern according to Emery and Neev (1960).

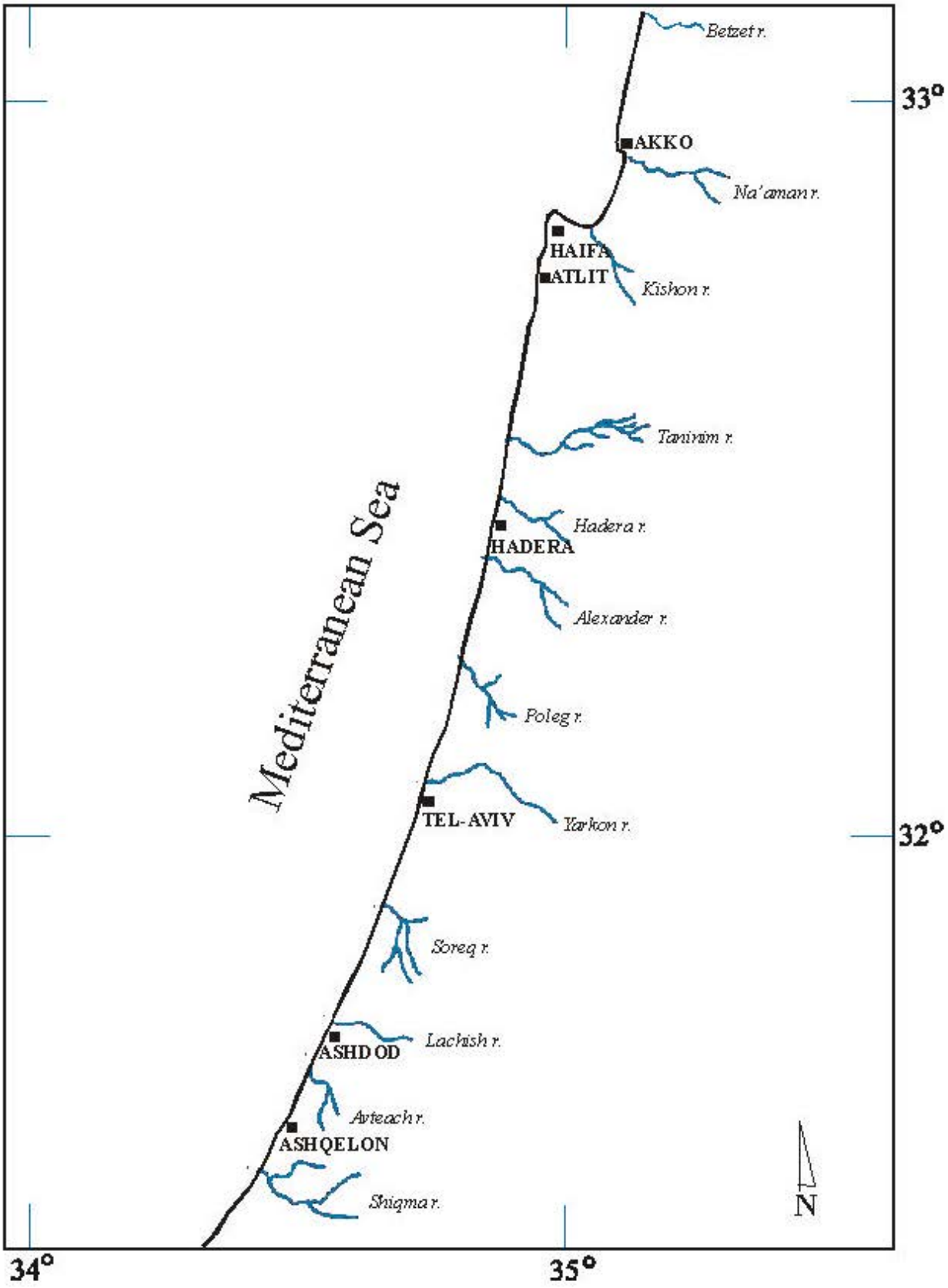

Fig. 3: Location map showing the coastal orientation, Haifa Bay (depth contours in meters) and the main coastal streams which drain into the sea.

4.2 Natural characteristics

The vertical profiles of temperature and salinity in the southeastern Levantine waters reveal four water masses (Hecht et al., 1988): Levantine Surface Water (LSW - S□38.95, 0-40 m), Atlantic Water (AW - S□38.87, 65-95 m), Levantine Intermediate Water (LIW- S□38.94, 200-310 m) and Deep Water (DW - T<13.8 ^{0}C and S<38.74, below 700 m). The formation of these water masses and their circulation in the eastern Mediterranean has been studied extensively (POEM, 1992). The two upper water masses are the most affected by seasonality. Surface water temperatures show high seasonal variations and range from ~16 °C during winter to ~28 °C in summer. The upper 50 m are well mixed in most winters and become stratified during the rest of the year with an upper mixed layer of about 25 m and a sharp halocline and thermocline below. The bottom of the seasonal thermocline is at about 100m (Hecht et al., 1988).

The offshore waters are oligotrophic, with extremely low nutrient values most of the year (Berman et al., 1984; Krom et al., 1991; Yacobi et al., 1995). The concentration of phosphate in surface waters is close or below the detection limit (0.01 □M), increasing to about 0.28 □M in deep waters (> 700 m depth). Nitrate concentrations show a similar trend with values between detection limit and approximately 6 □M, and silicic acid concentrations range between 1 to 12 □M. A typical vertical nutrient profile show low concentrations in the upper 150 m (< 0.05 and < 1 □M phosphate and nitrate, respectively), a nutricline development between 150-200 m and increasing concentrations down to 600 m. Silicic acid, however, continuously increases with depth. Near surface chlorophyll-a (chl-a) concentrations vary from 0.4 □g/l near shore and decreases westward to 0.05 at 20 km off shore (Berman et al., 1986; Gitelson et al., 1996; Yacobi et al., 1995). The seaward gradient is seasonal and higher in summer as compared to winter and early spring (Berman et al., 1986). The depth distribution of chl-a concentrations typically shows a deep chlorophyll maximum (DCM) between 75 to 130 m. The Levantine oligotrophy is attributed to the eastward surface flow of nutrient-depleted waters, further diluted by the nutrient depleted LIW; the arid and semi-arid climate with low terrigeneous runoff of nutrient- rich waters; the relatively narrow continental shelf off Israel and northward, allowing little benthic-pelagic coupling for nutrient recycling (Berman et al., 1984). In addition, the construction of the Aswan Dam arrested the flow of the major terrigeneous nutrients source (Azov, 1991).

The circulation on the shelf, dominated by the geostrophic current and shelf waves, is mostly northward (Rosentraub, 1995). Thus, the currents are mostly parallel to the coast, along depth contours, and effect particle transport along the shelf. The current fluctuations occur on both the daily (mainly sea breeze controlled) and synoptic (3-14 days) time scales. The strongest currents,

predominately northward, occur in winter and summer, while in spring and autumn, currents are weaker and alternate from north to south (Rosentraub, 1995). In the stratified summer the relatively strong currents and fluctuations are confined to the upper layer and increases towards the continental slope to mean speeds of 40 cm s^{-1}. In the mixed winter the currents distribution is uniform throughout the water column.

The coast is fanned by light winds (<10 knots) during 80% of the year, fresh winds (11-21 knots) for 18%, and by strong winds (>22 knots) only 2% (Rosen, 1998). In winter and early spring the winds are mostly from SW direction attributed to eastward moving depressions across the Levantine Basin. In summer and autumn the area is controlled by NW winds system on top of the local breeze. The wind transports sand particles from the beach inland, where gaps in the coastal cliff exists, forming sand dunes which extend to a distance of up to 10 km from shore. The highest, longest waves are westerly, due to the longer fetch (2400 km) (Fig. 1, Carmel et al., 1985). Wave height distribution allows for low waves (<1 m) nearly half the time, moderate waves (1-2 m), 25% of the time, high waves (2-4 m) 20%, and storm waves (>4 m) only 5% of the time, mostly from W direction (Rosen, 1998). The angle between the wave direction and the coastline orientation (beach normal) is the main factor that determines transport of sand by the wave-induced longshore currents (Emery and Neev, 1960). The tidal currents are weak, about 0.05 cm s^{-1}, and have but minor effect on sediments flow. The extremely low natural flow in the coastal streams, except for occasional storm runoff, and their lower reaches bathymetry, permits the penetration of seawater inland.

The quartz sands making up the shelf, beaches and inland dunes of Israel originate in the Nile river and delta (Pomerancblum, 1966) and constitute a part of the Nile littoral cell which extends from the Nile delta to Akko (Inman and Jenkins, 1984). The Nile sediments are transported northward by currents on the upper continental shelf, and by the wave-induced longshore currents (Emery and Neev, 1960) (Fig. 2). The magnitude of the longshore sediment transport is estimated at 170000-540000 m^3 y^{-1}, decreasing northwards (Golik, 1997). However, the pattern of sand movement along the coast, and particularly along its northern part (from south of Hadera to Haifa) is not entirely clear, and may be either northward or southward (Golik, 1993, 1997). The contribution of local streams to the sand budget is negligible as their drainage basins are dominated by carbonate rocks.

The geomorphology of the beaches is diverse: from Gaza to Tel-Aviv wide (30-50 m), sandy beaches backed by large dune fields are prevalent; from Tel-Aviv to Hadera, the beaches are

narrower (0-30 m), bordered by a calcareous cliff; from Hadera to Haifa the narrow beach lacks the cliff; Haifa Bay is bordered by a sandy beach; and from Akko to the Lebanese border the beach is mostly rocky. Ridges of eolianite sandstone (locally called "Kurkar") extend parallel to the coastline on the coastal plain and on the upper shelf.

4.3 The shallow marine habitats, the Red Sea invaders

Community studies of the continental shelf of Israel have been conducted for nearly half a century. The earlier studies were mainly fishery research (Wirszubski, 1953; Gilat-Gottlieb, 1959), and it was only in the 1960's that an extensive program was undertaken by Gilat (1964) to describe the macrobenthal communities off the Israeli coast. Gilat, and later Galil and Lewinsohn (1981), and Tom and Galil (1990) recognized parallel dominant species with other parts of the Mediterranean. However, Galil and Lewinsohn (1981) noted that the sandy-mud associations at depths of 20-50 m have no known parallel outside the Levant.
Vermetid reefs occur in the narrow zone of the infralittoral fringe, on exposed rocky shores under high energy conditions. The rimmed reef platforms are formed by the gregarious sessile gastropod *Dendropoma petraeum* (Monterosato) and *Vermetus triqueter* (Bivona), endemic to the Mediterranean. The porous structure of the vermetid reef and the underlining aeoleanithic sandstone allows for a rich community of endoliths. The resulting local organic enrichment coupled with structural complexity of the edifice, have led to the establishment of an extraordinarily dense ichthyofauna of great diversity - probably the most diverse ecosystem in the Mediterranean coast of Israel.

The total annual catch of the Mediterranean fisheries of Israel is estimated at 3000 tons. The fishery is divided into three categories according to the methods employed: inshore, employing trammel nets and hook-and-line, purse seine, and trawl fishery. Red Sea immigrants constitute 50% of the trawl catch.

The opening of the Suez Canal that joined the Red Sea and the Mediterranean initiated a remarkable faunal movement. Despite physical and hydrological impediments, hundreds of Erythrean species settled in the Mediterranean, forming thriving populations along the Levantine coasts - this extraordinary movement is considered "the most important biogeographic phenomenon witnessed in the contemporary oceans" (Por, 1989).
Many alien species have become ubiquitous, but by no means, all. In fact, three modes of population gain can be discerned: persevering, exploding and ubiquitous. Many, if not most, of the Erythrean aliens, have established small, but stable populations off the Levantine coast.

Rather more attention has been given to those instances of explosive population gain followed by sharp decline. In the late 1940's the immigrant goldband goatfish, *Upeneus moluccensis*, made up 10-15% of the total mullid catches. Following the exceptionally warm winter of 1954-55, its percentage in the catch increased to 83% (Oren, 1957). Its share has since been reduced to 30% of the catch (Ben Tuvia, 1973). Following that same winter, the brushtooth lizardfish, *Saurida undosquamis*, became commercially important and its proportion in trawl fisheries catches rose to 20% in the late 1950's. The population then diminished and catches stabilized at about 5% of the total trawl catch (Ben Yami and Glazer, 1974). Similarly, the gastropod *Rhinoklavis kochi*, first reported in Haifa Bay in the mid-1960's, spread rapidly to become, by the late 1970's, one of the dominant species on sandy-mud bottoms between 20-60 m (Galil and Lewinsohn, 1981; Tom and Galil, 1990). Samples taken a decade later consisted mostly of empty shells (Galil, 1993). And then, there are immigrants that are common and abundant. Alien fish now constitute nearly half of total fish biomass in commercial trawl catches along the Israeli coast (Golani and Ben Tuvia, 1995). *Strombus decorus persicus*, littering the shallow sandy littoral: "one can speak of an invasion... hundreds of dead shells on the beaches and shoals of live Strombus, of all sizes, colors and patterns, feeding on the sea floor up to 20 meters depth" (Curini- Galleti, 1988). Another Eryhtrean alien that proliferated in astonishingly short span of time is the nomadic jellyfish, *Rhopilema nomadica* (Galil et al., 1990). It was first collected in the Mediterranean in 1977; by the mid-1980's huge swarms would appear each summer along the southeastern Levant coast, and by 1995 also off the southeastern coast of Turkey (Kideys and Gucu, 1995) and Cyprus. The massive swarms, the sizable biomass of these voracious planktotrophs must play havoc with the meagre resources of this oligotrophic sea, and when those shoals draw nearer shore, they impact fisheries, coastal installations and tourism.

Invasion is often followed by competition for resources or direct interference between native and invading species; the former outcompeted wholly, or in part, of their habitat space. Por (1978) maintained that "Other than the case of *Asterina gibbosa* there is no known case in which a lessepsian migrant species has completely replaced a local one". Indeed, the decimation of the indigenous sea star, *A. gibbosa*, populations from the Israeli coast paralleled the rapid advent of its Red Sea congener *A. wega* (Achituv, 1973). But it is far from singular: there are other documented instances of an extreme change in abundance that can be attributed to the new competition. A native penaeid prawn, *Penaeus kerathurus*, was "very commonly caught by trawlers on Israel coastal shelf especially on sandy or sandy mud bottoms" according to Holthuis and Gottlieb (1958), and supported a commercial fishery throughout the 1950's. It has since nearly disappeared and its habitat overrun by the Red Sea penaeid prawns. The immigrant snapping shrimps *Alpheus inopinatus* and *A. edwardsi* are more common now in the rocky

littoral than the native *A. dentipes* (Lewinsohn and Galil, 1982). The decrease in the numbers of the previously prevalent indigenous jellyfish, *Rhizostoma pulmo*, has coincided with the massive presence of R. nomadica, and may also be a case of competitive displacement. The local red mullet, *Mullus barbatus*, and the native hake, *Merluccius merluccius*, were both displaced into deeper, cooler waters by their respective Red Sea competitors: *Upeneus moluccensis* and *Saurida undosquamis* (Oren, 1957).

However, the immigrants' ascendancy resulted not only in displacement of some native species but, increasingly, in displacement among the alien species themselves. *Trachypenaeus palaestinensis* was first recorded in the Mediterranean in the late twenties (Steinitz, 1929), already so abundant, it was sold on the Haifa fish market and was the most common penaeid on sandy-mud bottoms (Galil, 1986). In 1987 another alien, *Metapenaeopsis aegyptia*, joined it on the sandy-mud bottoms (Galil and Golani, 1990). By 1993 in samples collected along the central Israeli coast at depth of 35 m, *M. aegyptia* outnumbered *T. palaestinensis* 3 to 1, and by 1996 outnumbered it 25 to 1. That same year yet another migrant penaeid was recorded on the sandy-mud bottoms, *Metapenaeopsis moigensis consobrina* (Galil, 1997). *Charybdis longicollis* was first recorded in the Mediterranean in the mid 1950's (Holthuis, 1961), and has since dominated the macrobenthic fauna on silty-sand bottoms off the Israeli coast, forming up to 70% of the biomass at places (Galil, 1986). Of the thousands of specimens collected over three decades, none was parasitized till, in 1992, few prasitized crabs were collected, the parasite identified as a sacculinid rhizocephalan, *Heterosaccus dollfusi* - a Red Sea alien itself (Galil and Lutzen, 1995). Within three years it spread as far as the eastern Anatolian coast and infection rate at Haifa Bay rose to 77%. In the past year, we find, for the first time since the invasion of *Charybdis*, large numbers of the indigenous portunid crab *Liocarcinus vernalis*.The invasion of the Mediterranean by Red Sea fauna is a dynamic, ongoing, surprising process. The unique history of the easternmost Mediterranean, that left it warm, salty and impoverished, is at the base of a singular synergy between anthropogenic and natural environmental factors, past and present. And though the expected outcome of invasion is reduction in diversity, we witness an invasion that increases faunal diversity, and augments the local fisheries.

4.4 Geographical and environmental factors and the Levantine deep water fauna

Fish, molluscs, crustaceans and echinoderms collected at depths between 734 and 1558 m, during a series of cruises conducted between 1988 and 1999 off the coast of Israel, supplemented by a photographic survey carried out southwest of Cyprus, at depth of 2900 m, were analyzed. Considering the sampling effort, the diverse gear used and the extended period of

sampling, we may assume that the low number of species and specimens recorded actually reflects a low-diversity, low-density deep water fauna. The faunal scarcity may cause a different parceling of the populations that is reflected in bathymetric distributions that in many cases extend to greater depths than in the Western Mediterranean. The Levantine bathybenthos is composed of autochthonous, self-sustaining populations of opportunistic, eurybathic species that have settled there following the last sapropelic event.

The Mediterranean Pleistocene bathyal assemblages are more closely related to the Atlantic bathyal than to the present-day Mediterranean deep water fauna (Barrier et al., 1996). This disparity was attributed in part to the shallow Gibraltar sill that bars the deep water of the Atlantic Ocean from entering the Mediterranean, and the Mediterranean outflow that bars the entry of the deep water Atlantic fauna into the Mediterranean (Salas, 1996). The onset of the warm homothermy led to the demise of many cold stenothermic and stenohalinic species and the eventual impoverishment of the bathybenthos. In addition, the extreme oligotrophy of the Levantine Basin prevented settlement by members of the Atlantic bathyal that have been able to cross the shallow Gibraltar Straits and the Siculo-Tunisian sill (< 400 m) (Pérès, 1985). The recurring stagnant (dysoxic and anoxic) Quaternary episodes resulted in a reduction, or even extinction of deep bottom-living fauna unable to avoid annihilation by adapting to shallower depth: Van Harten (1987) reported that "Several species of deep-water ostracodes that are still common in the Western Mediterranean became extinct in the Eastern Mediterranean basin at the onset of early Holocene S1 sapropel deposition". Bacescu (1985) believed that the bathyal bottoms of the Levant are still "unfavourable", or even "azoic", after the last sapropelic event, dated between 9000 and 6000 years BP, and George and Menzies (1968) suggested "that sufficient time has not elapsed to allow colonization of the deep-sea floor".

The bathybenthic amphipods and cumaceans are indicative because the low mobility of their adults and their lack of a pelagic larval stage would restrict their dispersal into the Levantine Basin, effectively separated from the Atlantic Ocean by the Gibraltar and Siculo-Tunisian straits. Indeed, the common amphipods and cumaceans in depths greater than 1000 m off the Israeli coast are all eurybathic Atlanto-Mediterranean and Boreal species with an upper bathymetric range enabling them to overcome that barrier. None of the species with an upper bathymetric limit set at 400 m (Bellan-Santini, 1990), were collected during the study. This is the case for the molluscan fauna as well - *K. abyssicola, C. costellata, E. tetragona* and *B. pectunculoides* are eurybathic species with upper bathymetric range well within the circalittoral (> 150 m), whereas both the more stenobathic *B. macra* and *B. tenella* have epipelagic larvae (Bouchet and Warén, 1979), enabling them to overcome the barrier posed by the shallow sills. The evidence that the strictly epipelagic fauna is not impoverished in terms of species richness

underscores the importance of the sills and/or the Quaternary extinctions in determining the character of the deep bottom-living fauna.

Bouchet and Taviani (1992) suggested that much of the Mediterranean deep-sea fauna is made-up of non-reproducing pseudopopulations that have entered the Mediterranean as meroplankton with the Atlantic inflow at Gibraltar. However, the populations of the most common benthic molluscs in depths greater than 1000 m off the Israeli coast are composed of both adult and juvenile specimens, and one species, *Yoldia micrometrica*, the most common and abundant species in the Eastern Mediterranean, is unrecorded from the westernmost part of the sea (Salas, 1996). Moreover, gravid benthic decapod crustaceans and fish were collected from the depths of the Levantine Basin (Galil and Goren, 1994; Goren and Galil, 1997; Fishelson and Galil, 2001).

Though much reduced in diversity and richness compared with the deep sea fauna of the western and central basins of the Mediterranean, the Levantine bathybenthos is composed of autochthnous, self-sustaining populations of opportunistic, eurybathic species that have settled there following the last sapropelic event.

4.5 Population affecting the area

From the Neolithic Age, nearly 9000 years ago, until the late nineteenth century, the major population centers along the southeastern Levant were situated inland. However, the political realities that shaped the map of Israel forced a shift to the coastal plain, where the population expanded from 100,000 to 4 million within a century (out of a total of 5.8 million). Today, Israel is in a unique situation among the developed countries due to the combination of its high population density and high growth rate (Fig. 4). The population increase, due to high birth rate and massive immigration - 3/4 of a million in the early 1990's alone, subjects the coastal plain to increasing demands for housing, tourism, recreation, transportation, ports, energy and industrial facilities, sewer and effluent outlets, and marine farming.

These pressures led to examination of land reclamation schemes, either adjacent to the coastline or as offshore artificial islands, for housing, airports and various infrastructure facilities (e.g. gas terminals, seawater desalinization plants). Thus, the coastal strip, which constitute 5% of Israel's area, is and will be subjected to all those activities that may have a drastic short or long-term impact on the marine systems (Table 4-1).

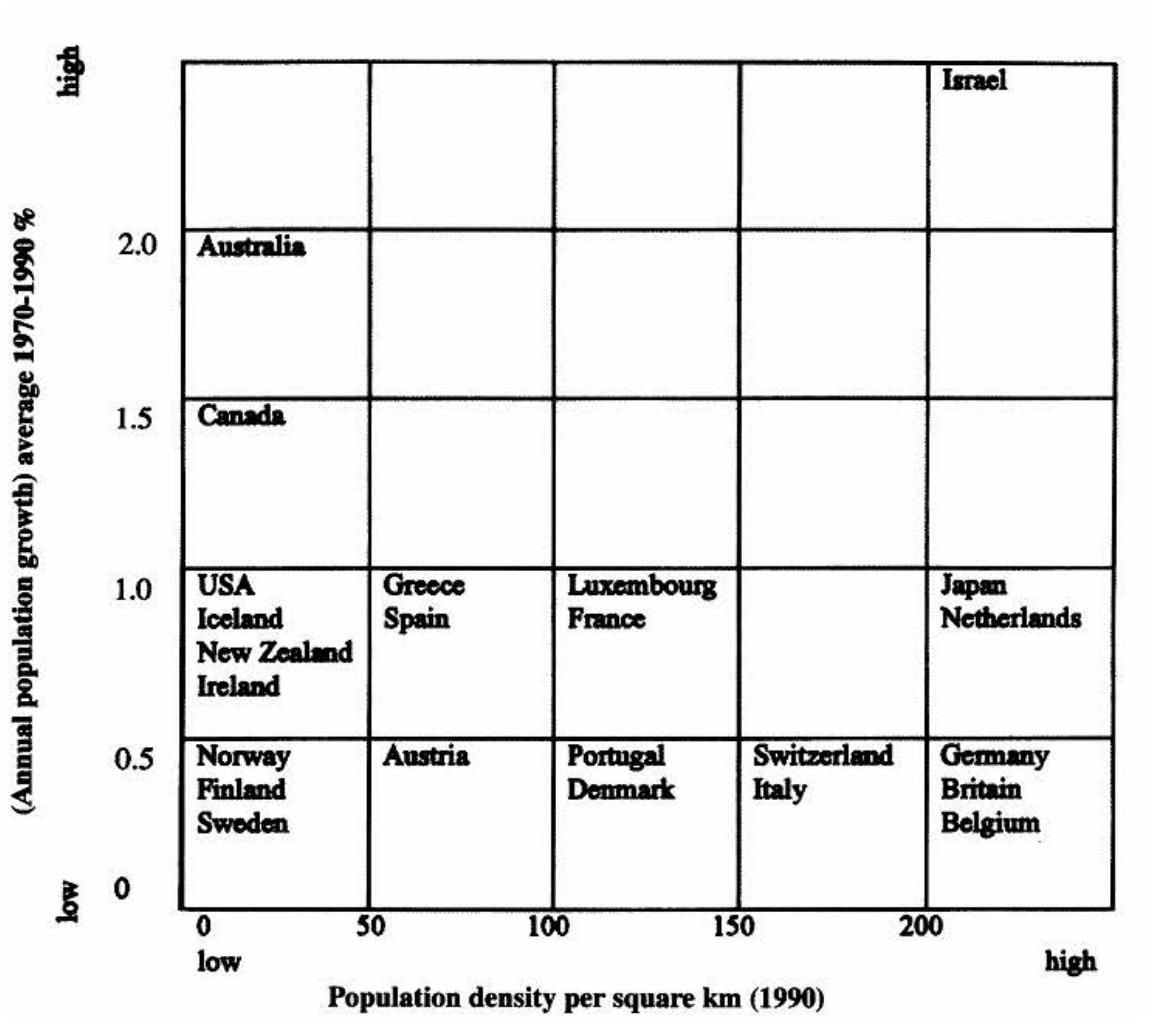

Fig. 4: The unique Israel situation with regard to population density and growth rate. Reprinted from Mazor (1993).

4.6 Effects of land-based pollution sources

The main pollution sources are connected to the intense coastal metropolis and industrial activities. More than 100 industries, cities and small settlements discharge wastes directly or via the coastal rivers into the sea. Since the early 1980's the overall pollution load into the coastal zone has declined due to the combination of the following factors: a) the increase of public awareness and governmental actions, b) the national commitment to implement international conventions on marine pollution prevention, and c) the progress and expansion of the National Sewage Project and sewage treatment. At present only two cities (Akko and Naharya) discharge raw sewage (after primary filtration) into the sea.

The three major classes of pollutants affecting the area are: nutrients, heavy metals and toxic organic compounds. Their introduction into the coastal zone is via point and non-point sources. The main point source inputs include direct pipeline discharges and riverine input, and the main diffused pathways are atmospheric deposition and runoff. No sufficient data is available to allow

a reliable estimation of the pollution inputs to the coastal zone. Table 4-2 presents a preliminary estimate of the pollution load entering the coastal zone, and its distribution among the main sources (Herut and Krom, 1996; UNEP, 1997; Herut, 1997; Herut et al., 1998). Nitrogen and phosphorous are introduced mainly through the Kishon River, Gush Dan outfall, and all other coastal streams, in approximately equal amounts. The atmospheric deposition is dominant in the open sea. The table probably represents minimal values as it does not include the input of agricultural runoff into the whole coastal zone area, and as the riverine input does not include the particulate nutrient loads (which are unknown). The main heavy metal and organic loads are industrial via the Kishon River and the Gush Dan outfall.

Since 1982 more than one million tons of coal fly ash (approximately 17% of the total amount generated) were dumped at a deep water site (1500 m, 200 km^2) located 70 km off the Israeli coast beyond the continental shelf (Kress et al., 1993). Industrial sludge was dumped as well at a nearby second deep-water site (Kress et al., in press). The Israeli government has agreed to the cessation of waste disposal in those sites.

4.6.1 Haifa Bay

Haifa Bay is exposed to the highest pollution load along the Israeli coast. Two rivers flow into the bay, the Naaman at its northern part, and the Kishon in the south. The latter is regarded as the most polluted river in Israel (Cohen et al., 1993; Herut et al., 1993; Herut and Kress, 1997). At the northern part of Haifa Bay anthropogenic mercury is introduced from a chlor-alkali plant (Hornung et al., 1984; Herut et al., 1996). High load of the heavy metals (Herut and Kress, 1997), nutrients (Kress and Herut, 1998) and organics (Cohen et al., 1993) are introduced via the Kishon River. Most anthropogenic heavy metals, nitrates and phosphates are discharged by acidic industrial effluents (about 90% of the total amount), while organic matter and ammonium originate mainly from the Haifa District sewage treatment plant effluents (about 90 and 70% of the total amount, respectively). Petroleum derived compounds are released mainly from the adjacent refineries.

Nutrients

In contrast to the oligotrophic open E Mediterranean waters, in Haifa Bay the dissolved nutrient and chl-a levels are high due to anthropogenic nutrient input through the Kishon River. The nutrient and chl-a concentrations decrease by more than an order of magnitude from the Kishon estuary towards the bay and the open sea (Fig. 5).

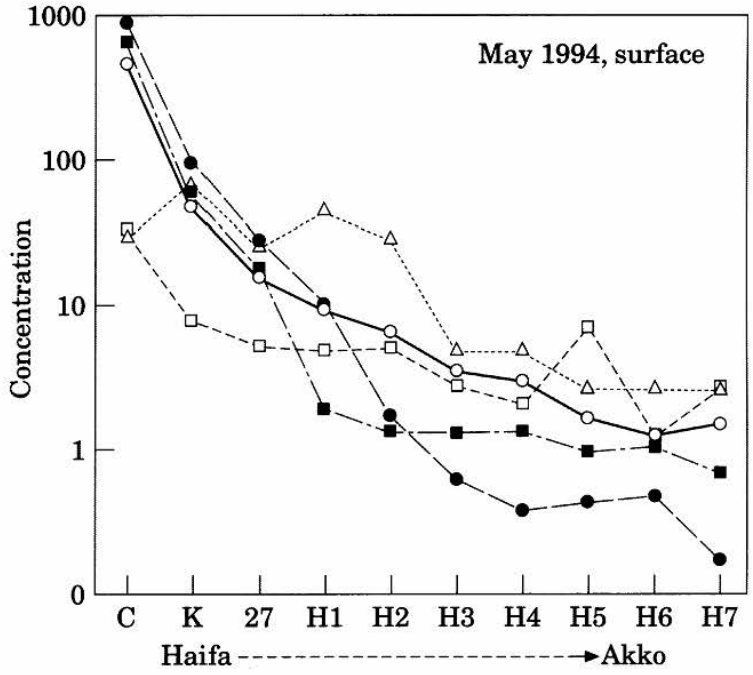

Fig. 5: The drastic decrease in the concentrations of some parameters in the surface waters along an S-N transect in Haifa Bay (from the Kishon estuary and Haifa port in the south to Akko at the north). Open circle – PO_4 (□M); open triangle – chlorophyll a (mg l^{-1}); filled square - NH_4 (□M); open square – suspended particulate matter (mg l^{-1}). Reprinted from Kress and Herut (1998).

The o-phosphate concentrations vary by more than two orders of magnitude. The chl-a concentrations in the bay are higher by a factor of about 4 than the maximal concentrations reported for the Israeli continental shelf (Berman et al., 1984). The bay ecosystem is N-limited in contrast to the P-limitation on the outer shelf and in the deep sea (Krom et al., 1991). The physical conditions (low currents, warm weather, high radiation, seasonal stratification) and nutrient overloading in Haifa Bay may easily lead to the development of potentially harmful algal blooms. Indeed, sporadic events of toxic plankton blooms (Kress et al., 1995; Kress and Herut, 1988; Kimor et al., 1996), unusual fish mortality and complaints on eye rashes by swimmers, were attributed to unusual high amounts of anthropogenic nutrients introduced via the Kishon River.

Toxic metal and organic pollutants

The sediments in Haifa Bay are contaminated by mercury from two sources, a chlor-alkali plant in the north and the Kishon River in the south, but the level of contamination is not high (Fig. 6). Most of the mercury in the sediments of the northern part of the bay accumulated prior to the introduction of waste treatment facilities by the chlor-alkali plant in 1976 (Fig. 7). Since the beginning of routine monitoring in the area, in the early 1980's, the amount of mercury in the

sediments decreased continuously, probably due to wave-induced resuspension of contaminated particles and their subsequent seaward transport (Fig. 7, Herut et al., 1996). The concentrations of mercury in benthic bivalves and fish sampled off the chlor-alkali plant and in the bay, respectively, also decreased during the same period (Fig. 7), and now approach background values. These data indicate that the bioavailable fraction of the mercury in the sediments of the northern bay is small, and therefore, that the remaining mercury reservoir in the sediments probably does not constitute a high ecological risk.

The sediments in the Kishon estuary are contaminated by several heavy metals. The degree of contamination in this area depends mainly on the hydrological conditions in the river and is maximal after heavy river floods (Herut and Kress, 1997). In recent years, mercury concentrations in the sediments of the Kishon estuary increased to higher levels than those found in the sediments of the northern part of the bay off the chlor-alkali plant. As of 1992, cadmium and mercury concentrations in the sediments are much higher than those found in previous years (Fig. 8). This is a result of a major flood in the Kishon in 1992 which carried a large volume of contaminated river sediments towards Haifa Bay, while usually the lower river system acts as a trap for contaminants discharged by the adjacent industries (Hornung et al., 1989; Cohen et al., 1993).

The suspended particulate matter (SPM) in Haifa Bay contains relatively high concentrations of mercury, cadmium, copper and zinc (Herut and Kress, 1997). The main source of mercury in surface water SPM is the chlor-alkali plant in the northern part of the bay. In near-bottom SPM the main source of mercury is the Kishon estuary. The Kishon is also the source of SPM contaminated by the other toxic metals (Herut and Kress, 1997).

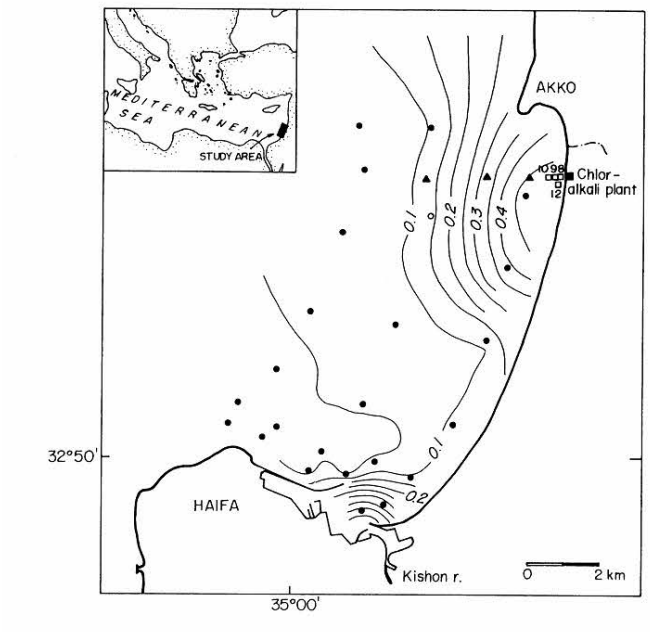

Fig. 6: Map of Haifa Bay showing the distribution of mercury concentrations (□g g^{-1} dry wt.) in the surficial sediments. From Herut et al. (1996).

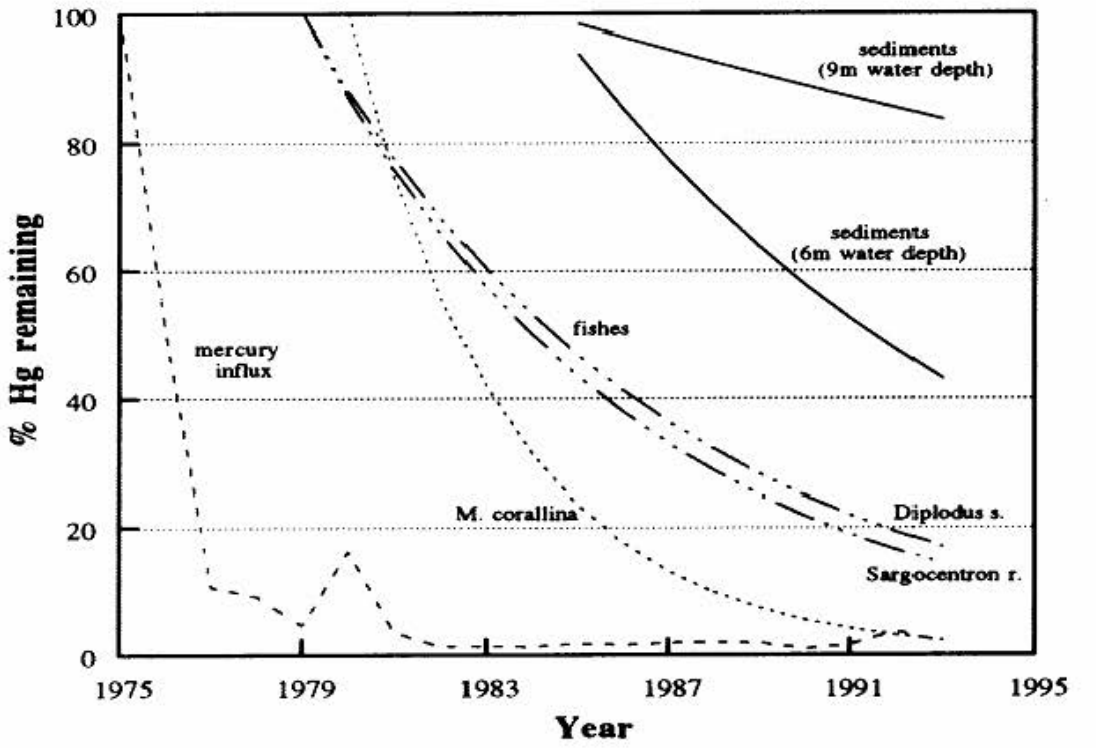

Fig. 7: The relationships between the reduction of mercury influx into northern Haifa Bay, the reduction in the amount of mercury in the top 50 cm of the sediments and the reduction of mercury concentrations in the biota (bivalves and fish) of Haifa Bay. Reprinted from Herut et al. (1996).

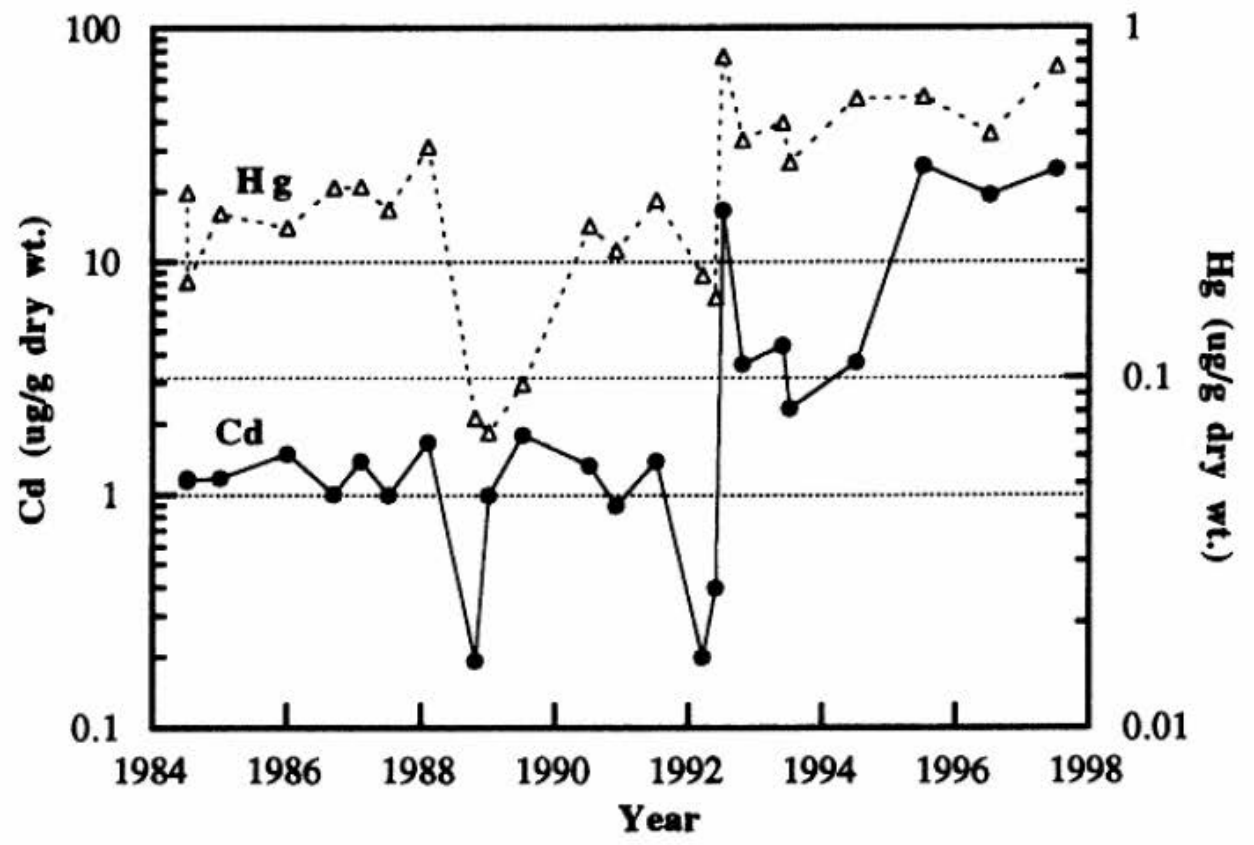

Fig. 8: Annual changes of cadmium and mercury concentrations (□g g^{-1} dry wt.) in surficial sediments from the Kishon estuary.

4.6.2 The coastal zone outside Haifa Bay

In general, with regard to the environmental levels of potentially toxic heavy metals and organic contaminants, the status of the coastal zone is quite satisfactory. Heavy metals and organics do not significantly contaminate the offshore sediments outside Haifa Bay. However, relatively high concentrations of some metals (5-7 times higher than "background" levels) are present near a sewage sludge outfall (Gush Dan) 5 km off central Israel. Very slight enrichment is also apparent near an industrial wastewater outfall off southern Israel (Ashdod), off the estuary of the Yarkon stream (Tel-Aviv area) and near a coal terminal off central Israel.

The sediments and SPM in some of the lower reaches of the coastal streams are enriched by mercury, cadmium, copper, zinc and lead indicating anthropogenic contamination but the degree of contamination is not high.

The mercury concentrations in commercial size specimens of fish caught off the Israeli coastline do not represent a risk to human health. In all fish examined, including those sampled in Haifa Bay, the mercury concentrations were well below the national safety limit for seafood. Other trace metal concentrations do not reveal any indication of contamination, and are below strict international sea-food standards.

In the offshore sediments, in benthic fauna and fish, there is no significant organic contamination. Recent screening of organic contaminants along the coastline revealed very low concentrations, and PCB's and dioxins could not be detected in the sediments (Herut et a., 1997).

The lower reaches of some coastal streams (Soreq, Poleg and Alexander) contain high nutrient concentrations (Herut et al., 1998). The high degree of contamination is attributed to the discharge of domestic and industrial wastes, and to agriculture runoff. The spatial and temporal variations of the nutrient and chl-a concentrations in the lower streams system and in the shallow water along the coast are poorly known. The phytoplankton species are poorly known as well, and a substantial effort to identify and quantify them is needed. The water quality is monitored for microbial indicators of fecal pathogens in authorized bathing beaches. Few beaches are occasionally closed due to a certain microbial contamination, but generally the status of the water quality is quite satisfactory. Other beaches, which are open to the public but are not declared as authorized bathing beaches, and extend over 100 km (out of 130 km of beaches), are not monitored at present.

4.7 Protective measures

At present, the marine environmental protective measures in Israel are encompassed within the framework of three main complementary legislative/administrative systems: the land use planning system, the system of marine and pollution control and the system for nature protection. Recently, a national plan for an integrated sustainable coastal zone management is halfway to be completed. It aims to guide the national coastal zone committee in a sustainable global planning policy including nature protection.

The land use planning (under the Planning and Building law from 1965) incorporates regulations for environmental protection both either in regional masterplans or specific projects. An environmental impact statement (EIS) is statutorily required since 1982 for development projects with anticipated significant environmental impacts. In 1983 a National Masterplan for the Mediterranean coast was affirmed. The plan includes regulations on the reservation and protection of the natural coastline and beaches, on the open view to the sea and on free public passage to the beach. Additional part of the program was submitted in 1991, and includes a more detailed land use assessment based on land and sea uses database prepared by a professional multidisciplinary team. This revised program is not yet affirmed.

The Ministry of Environment, and in a certain way also the Ministry of Transportation and the Ministry of Interior, are responsible for the legislation concerning marine pollution. This include the prohibition of oil discharge into the sea from ships and land-based marine installations, the regulation of dumping at sea, the regulation of waste discharges into the sea (directly and indirectly) from land-base sources and the maintenance of cleanliness in the public domain. Most of the related activities are financed by the "Sea Pollution Prevention Fund" which is based on taxes and penalization, and thus implements the "Polluter Pays" principle.
Israel is a party to the MARPOL 73/78 on prevention of pollution from ships. Israel is also a party to the 1976 Barcelona Convention and its protocols, and has accepted the changes made in 1996. The incorporation of the new Barcelona 1996 principals in the law is now under way.

The Israeli Nature Reserves and National Parks authority oversees 36 reserves and 14 coastal parks along the Mediterranean coast of Israel. There are four types of nature reserves: marine reserves (proposed and declared), coastal reserves (proposed and declared), islet reserves, and protected natural assets belts. Declared reserves have full legal protection, proposed reserves have a limited level of protection until the legally declared. All of the 14 proposed marine reserves (area 2500 ha, shoreline 45921m) come under the limited protection. Of the 20 coastal

reserves (area 3500 ha, shoreline 45732m), 4 are declared, and thus fully protected. The two islets reserves (33 ha), serving as important nesting sites, are fully protected too.

Several marine and coastal pollution-monitoring programs were undertaken in Israel since the 1970's (Fig. 9). Until the early 1970's only the monitoring of fecal pathogens in authorized bathing beaches was carried out. Since then other monitoring programs, as well as compliance monitoring programs in outfalls and dumping sites, were held. The "status and trends" type heavy metal monitoring, is carried out continuously since the early 1980's in Haifa Bay and from 1988 in the entire coastline, and constitutes a part of Israel's National Monitoring Program within the framework of MED POL (the international Mediterranean Pollution Research and Monitoring Program). In addition, several research projects aimed at understanding the pathways, fate and impact of anthropogenic metals in the marine environment were performed. The overall aim of the monitoring and related research activities is to provide a basis for decision-making on a variety of management issues such as marine waste disposal, pollution control and seafood safety. The specific objectives are to assess the status of the coastal zone with regard to pollutant contamination, to identify contamination sources and to detect early signs of potential health and ecological risks.

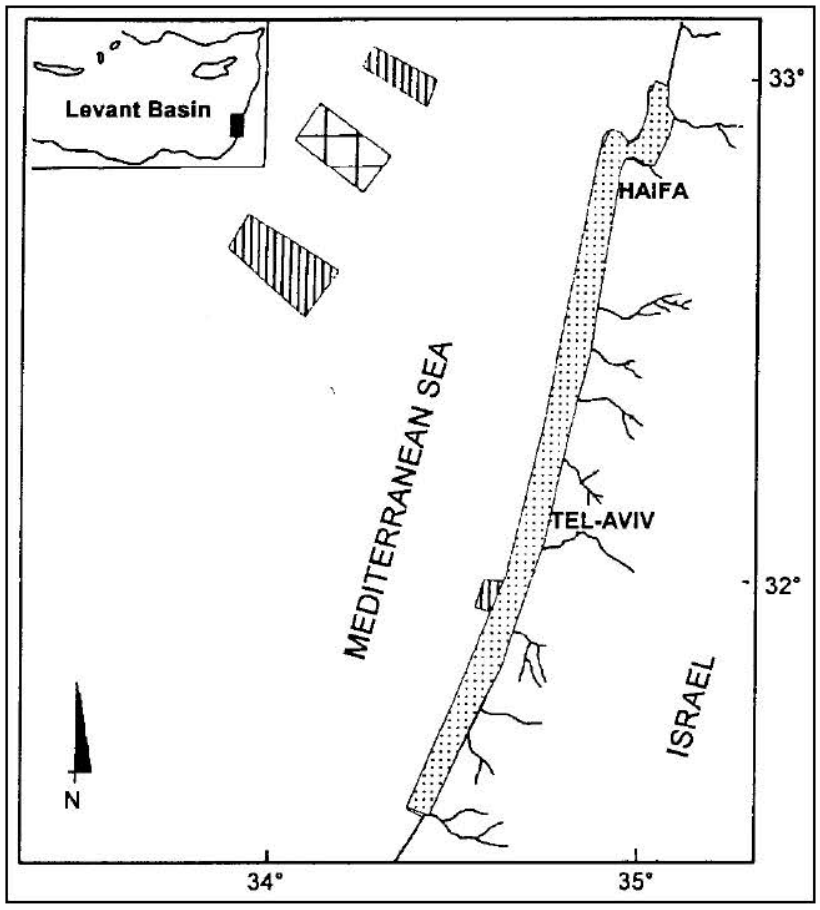

Fig. 9: Schematic map of sites monitored for heavy metal levels and biological structure at the Israeli Mediterranean continental margin. Dots: routine long-term monitoring activities; dark lines: waste disposal sites; squares: control site for deep sea monitoring.

The results of the monitoring are used as a basis for environmental decisions, control and abatement activities, as well as for the assessment of their effectiveness (Cohen, 1995). Such a contribution is demonstrated by the following two examples related to the presence of tar balls on the coastline and the bioaccumulation of mercury in fish from Haifa Bay (Cohen, 1995).

Monitoring of tar quantities on the beaches started in 1975 due to its heavy pollution on the beaches. The origin of this tar was unknown and among several speculations, the government agencies tend to believe it mainly originate from oil discharge into the sea far away west of Israel (500-1500 km). The analyses of vanadium, nickel and sulfur indicated that most of the tar balls were formed from oil transported to and from Israel and discharged into the sea less than 100 km from the coast (Shekel and Ravid, 1976). As a result the Ministry of Environment implemented a national program and new legislation for the prevention of oil pollution. Further monitoring confirmed the drastic decrease of the tar balls on the beaches (Fig. 10, Golik, 1982; Golik and Rosenberg, 1987).

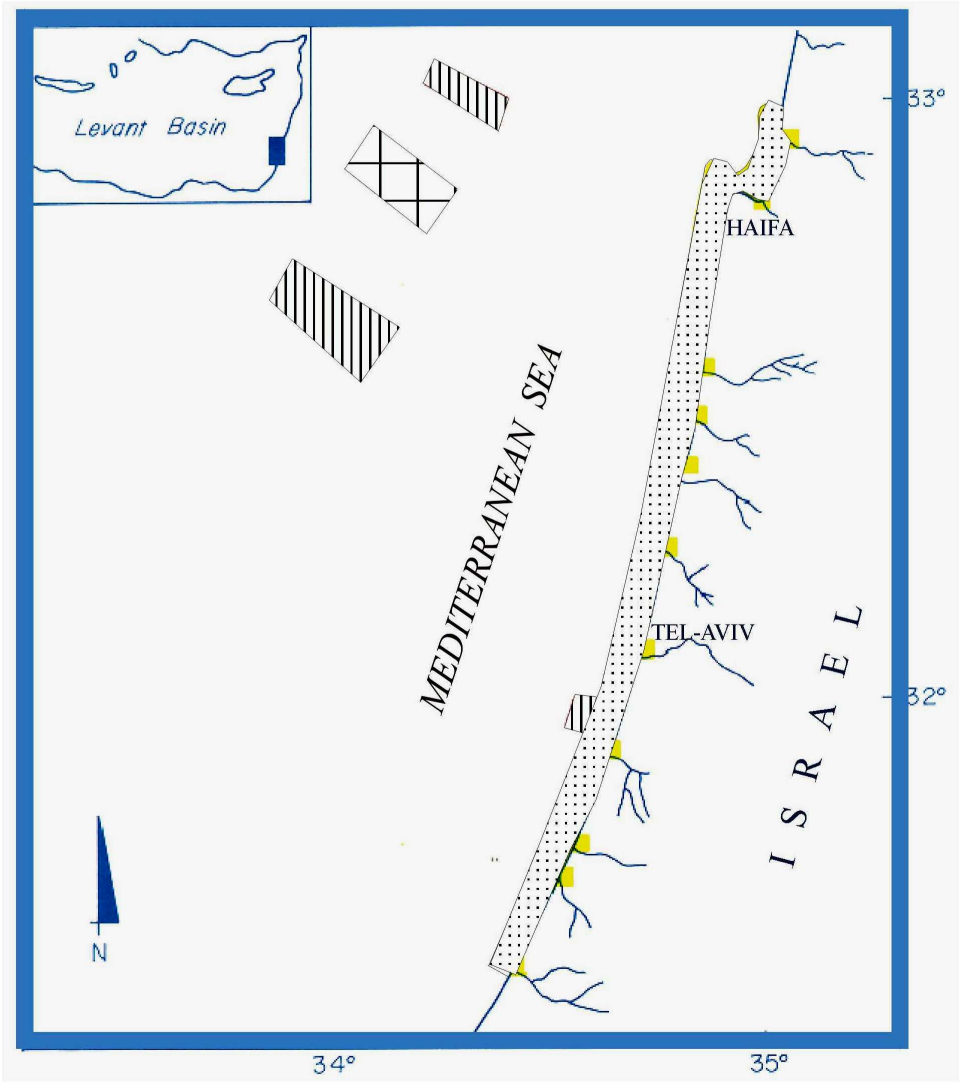

Fig. 10: Monitoring of tar quantity on the beach in the central coast of Israel (reprinted from Golik and Rosenberg, 1987).

Toward the late 1980's, in the frame of the toxic heavy metals monitoring in Haifa Bay, it was found that in large specimens of Diplodus sargus (an important commercially fish) the mercury concentrations exceeded the national safety limit (1 ppm, Hornung et al., 1984; Krom et al., 1990). The main source of anthropogenic mercury was a chlor-alkali plant that discharged mercury-containing effluents into the northern part of the bay since 1956. The drastic reduce (90%) of mercury discharge in 1976 due to the installation of treatment facilities in the plant was apparently not sufficient. As a result of the monitoring findings, the government prohibited the sale of D. sargus specimens of more than 100 g in size caught in Haifa Bay, and enforced the chlor-alkali plant management to further reduce its mercury discharge. A clear temporal decreasing trend of the mercury levels (below safety limit for all market sizes) was exhibited in further monitoring findings (Fig. 11, Herut et al., 1996; Herut et al., 1998). Thus, the long-term monitoring results contributed to the environmental management decisions and to verify the effectiveness of the correction actions.

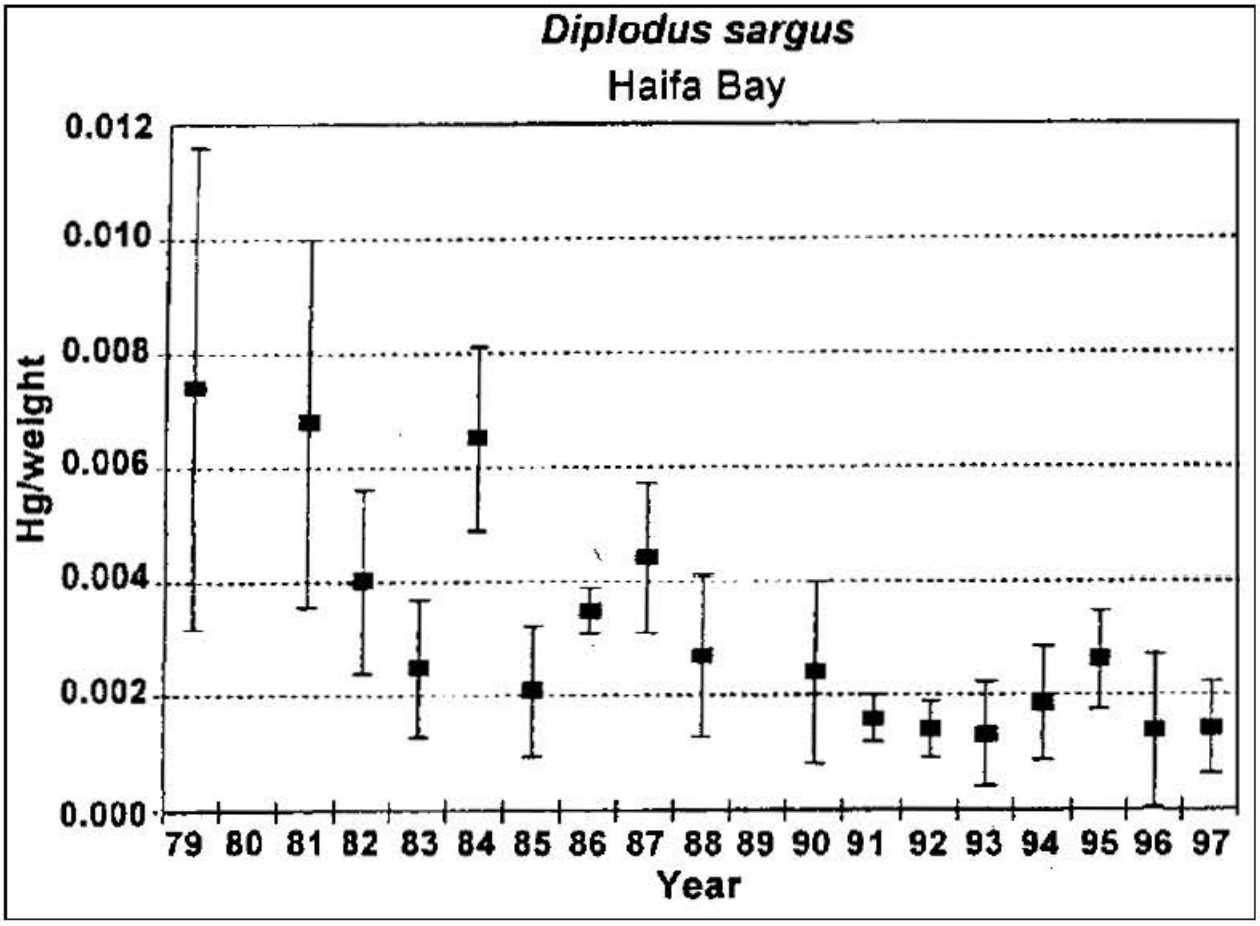

Fig. 11: Decrease of mercury concentration/body weight ratios (as a proxy to contamination level) in specimens of Diplodus sargus (annual average ± S.D.) from Haifa Bay.

4.8 Summary

Most of the Israeli population, industry and agriculture are concentrated along the narrow coastal plain. The past decade was of unprecedented growth, and the pressures to utilize coastal lands are increasing apace. Implementation of the present plans, many still mired in controversy, will dramatically change the coastline, in particular in and around the metropolitan areas. In addition propositions for marine constructions such as artificial islands for habitation, tourism or airfields, together with plans for a submarine gas pipeline, sand mining and marine farming. The planned enlargement of the Mediterranean ports and construction of additional marinas anticipate an increase in marine transport and leisure activities.

The National Plan has stated that marine and coastal resources should be utilized to the benefit of all citizens at present and in future despite pressures to accommodate special interests. As rapid development and population growth rate continue along the coastal plain, increasingly heavy demands will be placed on the remaining natural habitats. Protection of the marine environment depends on careful adherence to the principle of sustainable development that combines environmental commitments within the marine and coastal resource development and management policy.

4.9 References of Chapter 4

Achituv, Y., 1973. On the distribution and variability of the Indo-Pacific sea star *Asterina wega* (Echinodermata: Asteroidea) in the Mediterranean Sea. *Mar. Biol.*, **18**:333-336.

Bacescu, M. 1985. The effects of the geological and physiological factors on the distribution of marine plants and animals in the Mediterranean. In: M. Moraitou-Apostolopoulou, V. Kiortsis, (eds.), Mediterranean marine ecosystems, NATO Conference Series 1. Ecology, **8**: 195-212. New York, Plenum Press.

Barrier, P., I. Di Geronimo, Ch. Montenat, M. Roux, and H. Zibrowius. – 1989. Présence de faunes bathyales atlantiques dans le Pliocène et le Pleistocène de Méditerranée (détroit de Messine, Italie). *Bull. Soc. Géolog. France*, **4**: 787-796.

Bellan-Santini, D. – 1990. Mediterranean deep-sea amphipods: composition, structure and affinities of the fauna. *Prog. Oceanogr.*, **24**: 275-287, figs 1-10.

Ben Tuvia, A., 1973. Man-made changes in the eastern mediterranean sea and their effect on the fishery resources. *Mar. Biol.*, **19**, 197-203.

Ben Yami, M. and T. Glaser, 1974. The invasion of *Saurida undosquamis* (Richardson) into the Levant Basin - An example of biological effect of interoceanic canals. *Fishery Bull.*, **72**, 359-373.

Berman, T., Y. Azov, A. Schneller, P. Walline and D.W. Townsend. (1986). Extent, transparency and phytoplankton distribution of the neritic waters overlying the Israeli coastal shelf. *Oceanol. Acta*, 9, 439-447.

Berman, T., Townsend, D.W., El Sayed, S.Z., Trees, C.C. and Azov, Y. (1984). Optical transparancy, chlorophyll and primary productivity in the Eastern Mediterranean near the Israeli coast. *Oceanol. Acta*, 7, 367-372.

Bethoux, J.P., 1993. Mediterranean sapropel formation, dynamic and climatic viewpoints. *Oceanol. Acta.*, 16(2), 127-133.

Bouchet, P. and M. Taviani. – 1992. The Mediterranean deep-sea fauna: pseudopopulations of Atlantic species? *Deep Sea Res.*, 39(2): 169-184.

Bouchet, P. and A. Warén. – 1979. Planktotrophic larval development in deep-water gastropods. *Sarsia*, 64: 37-40.

Carmel, Z., Inman, D.L. and Golik, A. (1985). Directional wave measurements at Haifa, Israel, and sediment transport along the Nile littoral cell. *Coast. Eng.*, 9, 21-36.

Cohen, Y., Kress, N. and Hornung, H. (1993). Organic and trace metal pollution in the sediments of the Kishon river (Israel) and possible influence on the marine environment. *Wat. Sci. Tech.* **32**, 53-59.

Cohen Y. (1995). The Israeli experience of using marine and coastal pollution monitoring as a basis for environmental management. *Wat. Sci. Tech.* **27**, 439-447.

Emery, K.O. and Neev, D. (1960). Mediterranean beaches of Israel. Israel Geological Survey Bulletin, 26, 1-23.

Fishelson, L. and B. S. Galil. – 2001. Gonad structure and reproductive cycle in the deep-sea hermaphrodite tripodfish, *Bathypterois mediterraneaus* (Chlorophthalmidae, Teleostei). *Copeia* (2): 556-560.

Fredj, G. and L. Laubier, 1985. The deep Mediterranean benthos. In: Moraitou-Apostolopoulou, M. and V. Kiortsis (eds.), Mediterranan Marine Ecosystems. Plenum Press. pp. 109-145.

Galil, B. S. and M. Goren.–1994. The deep sea Levantine fauna – new records and rare occurrences. *Senckenberg. Marit.*, 25(1/3): 41-52.

Galil, B.S. and Ch. Lewinsohn, 1981. Macrobenthic communities of the Eastern Mediterranean continental shelf. PSZNI *Mar. Ecol.*, **2**, 343-352.

Galil, B.S., 1986. Red Sea decapods along the Mediterranean coast of Israel, ecology and distribution. In: Dubinsky Z. and Y. Steinberger (eds). Environmental Quality and Ecosystem stability, Vol. III/A, Bar Ilan Univ. Press: 179-183.

Galil, B.S. and D. Golani, 1990. Two new migrant decapods from the eastern Mediterranean. *Crustaceana* **58**(3), 229-236.

Galil, B.S., Spanier, E., Ferguson, W.W., 1990. The Scyphomedusae of the Mediterranean coast of Israel, including two lesepsian migrants new to the Mediterranean. *Zool. Meded.*, **64**,95-105.

Galil, B.S., 1993. Lessepsian migration: New findings on the foremost anthropogenic change in the Levant Basin fauna. In: Della Croce, N.F.R. (ed.), Symposium Mediterranean Seas 2000, pp. 307-318.

Galil, B.S. and M. Goren, 1994. The deep sea Levantine fauna - new records and rare occurrences. *Senckenbergiana marit.*, **25**(1/3), 41-52.

Galil, B.S. and J. Lutzen, 1995. Biological observations on Heterosaccus dolfusi Boschma (Cirripedia, Rhizocephala), a parasite of Charybdis longicollis Leene (Decapoda: Brachyura), a lessepsian migrant to the Mediterranean. *J. Crust. Biol.* **15**(4), 659-670.

Galil, B.S., 1997. Two Lessepsian migrant decapods new to the coast of Israel. *Crustaceana* **70**(1), 111-114.

Galil, B.S. and H. Zibrowius, 1998. First benthos samples from Eratosthenes Seamount, Eastern Mediterranean. *Senckenbergiana marit.*, **28**(4/6), 111-121.

George R.Y. and R.J. Menzies. – 1968. Additions to the Mediterranean deep-sea fauna. *Revue roum. Biol. (zool.)*, 13: 367-383.

GESAMP (1987) - IMO/FAO/UNESCO/WMO/WHO/IAEA/UN/UNEP. Joint group of experts on the scientific aspects of marine pollution. Land/sea boundary. Flux of contaminants. *Reports and studies GESAMP*, **32**, 172 pp.

GESAMP (1990) - IMO/FAO/UNESCO/WMO/WHO/IAEA/UN/UNEP. Joint group of experts on the scientific aspects of marine pollution. Review of potentially harmful substances, Nutrients. *Reports and studies GESAMP*, **34**, 40 pp.

Golik, A. (1982). The distribution and behavior of tar balls along the Israeli coast. Estuar. Coast. Shelf Sci., 15, 267-276.

Golik, A. and Rosenberg, N. (1987). Quantitative evaluation of beach-stranded tar balls by means of air photographs. *Mar. Poll. Bull.*, **18**, 289-298.

Golik A. (1993). Indirect evidence foor sediment transport on the continental shelf of Israel. Geo-Marine Letters, 13: 159-164.

Golik, A., Rosen, D.S., Golan, A. and Shoshany, M. (1996). The effect of Ashdod port on the surrounding seabed, shoreline and sediments. IOLR Report H/02/96, 66 pp.

Golik A. (1997). Dynamics and management of sand along the Israeli coastline. Bulletin de Institute Oceanographique, Monaco, n special 18, *Ciesm Science Series*, **3**, 97-110.

Goren, M. and B. S. Galil.– 1997. New records of deep-sea fishes from the Levant Basin and a note on the deep-sea fishes of the Mediterranean. *Israel J. Zool.*, 43: 197-203.

Goren, M. and B. S. Galil. – 2002. On the occurrence of *Cataetyx laticeps* Koefoed, 1927 and *Ophidion barbatum* Linnaeus, 1758 in the Levant Basin, Eastern Mediterranean, with a note on the deep sea fish community in this region. *Cybium*, 26(2): 150-152.

Hecht A., Pinardi N. and Robinson A.R. (1988). Currents, water masses, eddies and jets in the Mediterranean Levantine Basin. *J. Phys. Ocean.*, **18**, 1320-1353.

Herman, Y., 1989. Late Quaternary paleoceanography of the eastern Mediterranean: the deep-sea record. *Mar. Geol.*, **87**(1):1-4.

Hershkovitz, I. and Galili, E. (1990). 8000 year old human remains on the sea floor near Atlit, Israel. *J. of Human Evolution*, **5**, 319-358.

Herut B., Hornung H., Krom M.D., Kress N. and Cohen Y. (1993).Trace metals in shallow sediments from the Mediterranean coastal region of Israel. *Mar. Poll. Bull.*, **26**, 675-682.

Herut B., Hornung H. and Kress N. (1994). Mercury, lead, copper, zinc and iron in shallow sediments of Haifa Bay, Israel. *Fresenius Environ. Bull.*, **3**, 147-151.

Herut, B., Hornung, H., Kress, N., Krom, M.D. and Shirav, M. (1995). Trace metals in sediments at the lower reaches of Mediterranean coastal rivers, Israel. *Wat. Sci. Tech.* **32**, 239-246

Herut B., Hornung, H., Kress, N. and Cohen Y. (1996). Environmental relaxation in response to reduced contaminant input: The case of mercury pollution in Haifa bay, Israel. *Mar. Poll. Bull.* **32**, 366-373.

Herut, B., Hornung, H., and Kress, N. (1997). Lond-term record mercury decline in Haifa Bay (Israel) shallow sediments. *Fresenius Environ. Bull.*, **6**, 48-53.

Herut, B. and Kress, N. (1997). Particulate Metals Contamination in the Kishon River Estuary, Israel. *Mar. Poll. Bull.*, **34**, 706-711.

Herut, B., Hornung, H., and Kress, N. (1998). Monitoring of heavy metals along the Mediterranean coast of Israel in 1997. IOLR Rep. H18/98, 26 pp. (in Hebrew and executive summary in English).

Holthuis, L.B., 1961. Report on a collection of Crustacea Decapoda and Stomatopoda from Turkey and the Balkans. *Zool. Verh. Leiden*, **47**,1-67.

Holthuis, L.B. and E. Gottlieb, 1958. An annotated list of the decapod Crustacea of the Mediterranean coast of Israel, with an appendix listing the Decapoda of the Eastern Mediterranean. *Bull. Res. Coun. Israel*, **7B**, 1-126.

Hornung, H., Krumgalz, B. and Cohen, Y. (1984). Mercury pollution in sediments, benthic organisms and inshore fishes of Haifa Bay, Israel. *Mar. Environ. Res.*, **12**, 191-208.

Hornung, H., Krom, M. D. and Cohen, Y. (1989). Trace metal distribution in sediments and benthic fauna of Haifa Bay, Israel. *Estuar. Coast. Shelf Sci.*, **29**, 43-56.

Kideys, A.E. and A.C. Gucu, 1995. Rhopilema nomadica: a lessepsian schyphomedusan new to the Mediterranean coast of Turkey. *Isr. J. Zool.*, **41**, 615-617.

Kimor, B., Kress, N. and Herut, B. (1996). A short-lived toxic plankton bloom in Haifa Bay (Israel). ASLO Ocean Sciences Meeting, Feb. 12-16 1996, San Diego.

Kress, N., Golik, A., Galil, B. and Krom, M.D. (1993). Monitoring the disposal of coal fly ash at a deep water site in the eastern Mediterranean Sea. *Mar. Pollut. Bull.* **26**(8), 447-456.

Kress, N., Herut, H. and Angel, D.L. (1995). Environmental conditions of the water column in Haifa Bay, Israel, during September-October 1993. *Wat. Sci. Tech.* **32**, 57-64.

Kress, N. and Herut, B. (1998). Hypernutriphication in the oligotrophic Eastern Mediterranean. A study in Haifa Bay, Israel. *Estuar. Coast. and Shelf Sci.*, **46**, 645-646.

Krom M.D., Hornung, H. and Cohen, Y. (1990). Determination of the environmental capacity of Haifa Bay with respect to the input of mercury. *Mar. Poll. Bull.*, **21**, 349-354.

Krom M.D., N. Kress, S. Brenner and L.I. Gordon (1991). Phosphorus limitation of primary productivity in the Eastern Mediterranean Sea. *Limnol. Oceanogr.*, **36**, 424-432.

Lewinsohn, Ch. and B.S. Galil, 1982. Notes on species of Alpheus (Crustacea Decapoda) from the Mediterranean coast of Israel. *Quad. Lab. Tecno. Pesca, Ancona.* **3**(2-5), 207-210.

Linder, E. (1992). Ma'agan Michael ship wreck. Excavating an ancient merchanman. *Biblical Archeology Rev.*, **18**, 24-35.

Mazor, A. (1993). Israel 2020 – masterplan for Israel in the 21st century. Technion Research and Development Foundation. Haifa, Israel.

Muerdter, D.R., Kennett, J.P., Thunell, R.C., 1984. Late Quaternary sapropel sediments in the Eastern Mediterranean Sea: Faunal variatins and chronology. *Quat. Res.*, **21**, 1-69.

Nir, Y. (1982). Offshore artificial structures and their influence on the Israel and Sinai Mediterranean beaches. Proc. 18th Intern. Conf. On Coastal Eng., ASCE, 1837-1856.

NOAA (1996). NOAA's Estuarine Eutriphication Survey. Volume 1: South Atlantic Region. Silver Spring, MD. Office of Ocean Resources Conservation Assessment. 50 pp.

Oren, O.H., 1957. Changes in the temperature of the Eastern Mediterranean Sea in relation to the catch of the Israel trawl fishery during the years 1954/55 and 1955/56. *Bull. Inst. Oceanogr. Monaco*, **1102**, 1-12.

Pérès J. M. – 1985. History of the Mediterranean biota and the colonization of the depths. In Margalef, R (Ed): *Key Enviroments Western Mediterranean.* Oxford, New York, Pergamon Press: 198-232.

POEM Group (1992). General circulation of the eastern Mediterranean. *Earth Sci. Rev.*, **32**, 285-309.

Pomerancblum, M. (1966). The distribution of heavy minerals and their hydraulic equivalents in sediments of the Mediterranean continental shelf of Israel. *Jour. Sed. Pet.*, **36**, 161-174.

Por, F.D., 1978. Lessepsian Migration - The influx of Red Sea biota into the Mediterranean by way of the Suez Canal. Ecological Studies, 23. Springer-Verlag, 228 pp.

Por, F.D., (1989). The Legacy of Tethys - an aquatic biogeography of the Levant. Kluwer. Dordrecht.

Rosen D.S., (1998). Characterisation of mete-oceanographic climate in the study sector. IOLR Report H16/98.

Rosentraub Z., (1995). Circulation on the Mediterranean continental shelf and slope of Israel. IAEPSO 21 General Assembley, Honolulu, Hawaii, 5-12 August 1995.

Rossignol- Strick, M., (1985). Mediterranean Quaternary sapropels, an immediate response of the African monsoon to variation in insolation. *Palaeogeogr., Palaeoclimatol., Palaeoecol.*, **49**(3/4), 237-263.

Safriel, U.N., (1966). Recent vermetid formation on the Mediterranean shor of Israel. Proc. *Malacol. Soc. London*, **37**, 27-34.

Salas, C. – 1996. Marine bivalves from off the southern Iberian peninsula collected by The BALGIM and Fauna 1 Expeditions. *Haliotis*, 25: 33-100.

Shekel, Y. and Ravid, R. (1976). Sources of tar ball pollution on Israel's beaches. Tech. Rep., Israel Institute of Petroleum and Energy, 45 pp.

Steinitz, W., (1929). Die Wanderung indopazifischer Arten ins Mittelmeer seit Beginn der Quartarperiode. Inst. Rev. ges. Hydrobiol. Hydrog., 22:1-90.

Tom, M. and B.S. Galil, (1990). The macrobenthic associations of Haifa Bay, Mediterranean coast of Israel. PSZNI *Mar. Ecol.*, **12**(1), 75-86.

UNEP/UNESCO/FAO (1988). Eutriphication in the Mediterranean Sea. Receiving capacity and monitoring of long term effects. *MAP Technical Report Series*, **21**, UNEP, Athens.

Vergnaud-Grazzini, C., Ryan, W.B., Cita, M.B., 1977. Stable isotope fractionation, climate change and episodic stagnation in the Eastern Mediterranean during the Late Quaternary. Mar. *Micropaleont.*, **2**(4), 353-370.

Yacobi, Y., Zohari, T., Kress, N., Hecht, A., Robart, R.D, Wood, A.M. and Li, W.K.W. (1995). Chlorophyll distribution throughout the Southeastern Mediterranean in relation to the physical structure of the water mass. *J. Mar. Sys.*, **6**, 179-190.

Table 4-1: Existing and future planned coastal structures along the Mediterranean coast of Israel.

Marine structure	Present amount	Future development
Ports (Haifa and Ashdod)	2	large expansions of the existing ports and additi of a large port off Gaza
Marinas and small harbors	7	addition of at least one marina, expansion of harbors
Power plants + cooling basins	4	
Offshore unprotected coal unloading terminals	2	development of gas terminals
Breakwaters	at least 16	additions to protect beach and cliff erosion
Marine outfalls (excluding beach outfalls)	4	additional are planned
Mariculture farms	3	additional are planned
Artificial islands offshore	-	several are planned

Table 4-2: Estimated loading of pollutants to the coastal waters.

Parameter	Kishon river**	Coastal rivers	Gush Dan sewage sludge outfall	Ashdod outfall	Atmospheric input*
N *(t/y)*	3450	3670±2000	2900	600	1555
P *(t/y)*	2900	515±291	1200	7	62
Cd *(kg/y)*	2048	53	430	-	45
Cu *(kg/y)*	3194		19000	-	1672
Pb *(kg/y)*	810	3000	1670	-	9623
Hg *(kg/y)*	60 ?		60	-	-
Zn *(t/y)*	47.8		54	-	8029
BOD *(t/y)*	5371		13286	2630	-
COD *(t/y)*	6225		40665	12150	-
Oils *(t/y)*	25		-	11	-

* atmospheric input was calculated for area of 180 km length and 21.6 km width (12 miles) from shore. Nutrients load are wet deposition only.
** Only part of the load is transported into Haifa Bay.